UNIVERSITY OF MODENA AND REGGIO EMILIA

A dissertation submitted for the Degree of Doctor of Philosophy in

Molecular and Regenerative Medicine

Cycle XXVI

The role of p75NTR in progression and invasion of melanoma in 3D models

MENTOR:

Prof. Carlo Pincelli

CANDIDATE

Annalisa Saltari

PhD SCHOOL DIRECTOR:

Prof.ssa Rossella Tupler

Academic session 2013/2014

TABLE OF CONTENTS

CHAPTER 1: INTRODUCTION 6

- **Melanoma: Risk factors and genetic alterations** 7
- **Classification, Diagnosis and Treatment** 9
- **Melanoma progression and metastasis** 12
- **Melanoma chemoresistance** 16

- **Neurotrophins** 20
- **Neurotrophins and their receptors** 21
- **High affinity receptors Trks** 23
- **Low affinity receptor p75NTR** 25
- **P75NTR and skin** 27
- **P75NTR and melanoma** 28

- **Melanoma three-dimensional models** 30
- **Tumor multicellular spheroids** 30
- **Skin equivalents** 33

CHAPTER 2: MATHERIALS AND METHODS 35

- **Melanoma cells culture** 36
- **Human keratinocytes and fibroblast cell cultures** 36
- **Liquid overlay method** 37
- **MTT assay** 37
- **Treatment with cisplatin** 39
- **Collagen I invasion assay** 39
- **Facs analysis** 40
- **Extraction of cellular proteins** 41
- **Protein quantification with Bradford method** 42
- **Western Blotting:** 43
    - **Electrophoretic migration of proteins** 43
    - **Transfer of proteins from polyacrylamide gel to a nitrocellulose membrane** 46
    - **Incubation of the nitrocellulose membrane with primary and secondary antibody** 47
    - **Detection of target proteins with ECL chemoluminescent detection system** 48
- **Skin equivalents** 49
- **Hematoxylin and eosin staining** 52
- **Immunohistochemical detection in skin equivalents** 52

- **Confocal microscopy** **54**
- **Cell sorting** **55**
- **Melanoma cells transfection with siRNA p75NTR** **56**
- **Melanoma cells infection** **56**
- **Immunohistochemical staining of spheroids in collagen I** **57**
- **Analysis of spheroids with Image J software** **58**
- **Analysis of spheroids with Photoshop** **59**
- **Statistical analysis** **60**

CHAPTER 3: AIM OF RESEARCH **61**

CHAPTER 4: RESULTS **64**

- **3D multicellular melanoma spheroids recapitulate proliferative capacities of their original cell lines** **65**
- **3D multicellular melanoma spheroids recapitulate invasion abilities of their original cell lines** **68**
- **Spheroids derived from metastatic WM266-4 cells are more resistant to cisplatin induced apoptosis in comparison to primary WM115 cells** **70**
- **The invasion abilities after treatment with cisplatin are much more reduced in primary WM115 spheroids in comparison to metastatic WM266-4 spheroids** **73**

- **Evaluation of neurotrophins receptors expression in 2D and 3D melanoma models** **74**
- **P75NTR is differentially expressed in 2D and 3D melanoma models** **77**
- **P75NTR expression decreased with enhanced aggressiveness of melanoma multicellular spheroids** **79**
- **P75NTR expression decreased with enhanced aggressiveness of 3D melanoma skin equivalents** **81**
- **P75NTR expression is inversely correlated with enhanced predisposition to invade the microenvironment** **83**
- **SKMEL28 p75NTR dim spheroids proliferate more than SKMEL28 p75NTR bright spheroids** **85**
- **SKMEL28 p75NTR dim spheroids invade more than SKMEL28 p75NTR bright spheroids** **89**
- **WM115 acquire a more aggressive phenotype after p75NTR silencing** **91**
- **1205Lu p75NTR overexpressing spheroids decrease their size in comparison to mock spheroids** **95**

CHAPTER 5: DISCUSSION **98**

CHAPTER 6: REFERENCES **105**

CHAPTER 7: RINGRAZIAMENTI **129**

1. Introduction

Melanoma

Risk factors and genetic alterations

Cutaneous malignant melanoma (MM), represents the most common cause of death from skin cancer and, apart from female lung cancer, it is the tumor entity with the highest increase in incidence worldwide (Jemal A. et al,2010).

The incidence and mortality of cutaneous melanoma have increased substantially over the last fifty years among all Caucasian population. The higher rates (40 /100.000 population) were reported in Australia and New Zealand, probably due to the association of light skin phenotype of the population and a strong sun exposure (Marks, 2002).

When early diagnosed, primary melanomas can be treated by surgical resection. However, metastatic melanoma accounts for more than 80% of deaths by skin cancer, due to its aggressiveness and resistance to existing therapies (Gray-Schopfer et al., 2007a; Miller and Mihm, 2006). Therefore, new therapeutic approaches are urgently needed for this devastating disease.

Melanoma comes from alterations in melanocytes, pigment-producing cells that are responsible for the color of skin. Cutaneous melanocytes originate from highly motile neural-crest progenitors that migrate into the skin during embryonic development. They reside in the basal layer of the epidermis and in the hair follicles and their homeostasis is tightly regulated by epidermal keratinocytes (Slominski A, 2004).

In response to ultraviolet (UV) radiation, keratinocytes secrete factors able to regulate melanocytes survival, differentiation, proliferation and motility, stimulating the production of melanin and resulting in the tanning response. Thereby, melanocytes have a key role in protecting our skin from damage caused by UV radiation and in preventing the onset of skin cancers.

MM is characterized by a multi-factorial etiology. Sun exposure and genetic susceptibility have been proposed as major etiological and predisposing factors and may explain the reported increase of incidence to some degree (Lens MB, Dawes M., 2004).

Given melanoma heterogeneity and the difficulty in its classification and staging, the last decade has yielded a myriad of gene expression profile studies that intended to establish a molecular classification of melanoma. Those studies have confirmed the great heterogeneity of this disease and the key role that the tumour microenvironment has in determining melanoma gene expression programmes and progression to metastasis (Bittner et al., 2000; Hoek et al., 2006; Seftor et al., 2005).

A number of rare mutations, which often run in families, are known to greatly increase susceptibility to melanoma. Several genes have been identified as increasing the risk of developing melanoma. One class of mutations affects the gene CDKN2A leading to the destabilization of p53, an important transcription factor involved in apoptosis. Mutations that cause the skin condition xeroderma pigmentosum (XP) also seriously predispose to melanoma. Scattered throughout the genome, these mutations reduce a cell's ability to repair DNA. Both CDKN2A and XP mutations are highly penetrant.

Noteworthy, the Ras/Raf/MEK/ERK pathway is hyperactivated in 90% of human melanomas (Cohen et al., 2002). In fact, several second messengers of this pathway can be mutated. For example, it was seen that 15% -30% of melanomas present mutations in RAS gene, in particular in NRAS (Davies et al., 2002) while 50% -70% are BRAF mutated (Davies et al., 2002).

90% of the BRAF mutants have a glutamic acid for valine substitution at position 600 (V600EBRAF) (Davies et al., 2002) that is responsible for constitutive ERK signaling activation. These mutations also may contribute to angiogenesis by stimulating autocrine vascular endothelial growth factor (VEGF) secretion (Gray-Schopfer et al., 2005 & Sharma et al., 2005). Moreover, PI3 kinase pathway, which is normally involved into regulation of cells survival (Stahl et al., 2003), is hyperactivated and occurs in 3% of metastatic melanomas (Omholt et al., 2006).

The Wnt/β-catenin pathway is required for different cellular processes such as cell adhesion, proliferation, survival and migration. This pathway can be constitutively activated in melanoma due to mutations in β–catenin gene (Orgaz et al., 2013).

The Rho family of GTPases are involved in a wide variety of processes (Sahai and Marshall, 2002). In melanoma Rho GTPases control cell movement, melanoma invasion and metastatic dissemination. However, mutations in Rho proteins are relatively rare,

whereas their activities are frequently altered due of mutations in MAPK and PI3K pathways (Sahai and Marshall, 2002; Vega and Ridley, 2008).

Microphtalmia-associated transcription factor (MITF), responsible for melanoblasts survival, melanocytes lineage commitment and cells invasion (Levy et al., 2006), can be amplified in 10% of primary melanomas and in 21% of metastatic tumors (Garraway et al., 2005).

The activator of transcription-3 (STAT3) is an oncogene that inhibits apoptosis and promotes cell proliferation, angiogenesis, invasion and metastasis (Yu et al., 2009).

When STAT3 is constitutively expressed in melanoma (Yu et al., 2009) it can induce the expression of VEGF and of hypoxia-inducible factor 1-α (HIF1α), thereby promoting tumor angiogenesis (Kortylewski et al., 2005; Niu et al., 2002) and stimulating melanoma metastasis (Itoh et al., 2006).

Several genetic mutations can be associated with melanoma development. The majority of them lead to an alteration of apoptosis signaling such as overexpression of Bcl-2, NF-kB, Akt 3 and loss of PTEN (Gray-Schopfer et al., 2007a).

Classification, diagnosis and treatment

Melanoma is a very dangerous and deadly disease. For this reason, early diagnosis is of paramount importance to decrease its mortality (Carlson et al., 2003).

Visual diagnosis of melanomas is still the most common method employed by health professionals (Wurm EM, Soyer HP., 2010). A popular method to recognize signs and symptoms of melanoma is the mnemonic “ABCDE” method (Friedman et al., 1991; Thomas et al., 1998):

- **A**symmetrical skin lesion
- **B**order of the lesion is irregular
- **C**olor: melanomas usually have multiple colors
- **D**iameter: moles greater than 6 mm are more likely to be melanomas than smaller moles
- **E**nlarging: enlarging or evolving

Due to low level of accuracy and the limitations associated to the "ABCDE" diagnostic tool, new technologies have been developed.

Nowadays there isn't a reliable marker 100% sensitive and 100% specific for melanoma diagnosis that could replace routine histological examination and no test on tissue sections can predict the capacity of melanoma to metastatize. However one assay commonly used is the immunohystochemical detection of S100 protein on melanoma tissue sections (Quatresooz et al., 2009).

More accurate clinical diagnosis of melanoma is likely to improve patient management, reduce morbidity and mortality and generate considerable economic benefits. Recently, dermoscopy has improved the accuracy of the clinical diagnosis of skin tumors (Pascale G. et al, 2012). Studies investigating the role of reflectance confocal microscopy (RCM) in the clinical diagnosis of melanocytic tumors have shown that the identification of specific RCM features can improve the accuracy of diagnosis (Pellacani et al. 2005, 2007; Langley et al.,2007; Guitera et al., 2009).

Cutaneous melanoma is a very heterogeneous and complex disease. It can be classified into different types (James, William D., et al, 2006): 1) Superficial Spreading Melanoma, 2) Lentigo Melanoma, 3) Nodular Melanoma, 4) Mucosal Melanoma, 5) Polypoid Melanoma, 6) Acral Lentiginuous Malignant Melanoma, 7) Desmoplastic Melanoma and 8) Amelanotic Melanoma.

Superficial spreading melanoma is the most common type, it may develop on any part of the body and occurs at any age (Demitsu et al., 2000). Lentigo Melanoma, instead, develops on the sun-exposed skin and upper extremities of elderly patient (Cohen et al., 1995). Nodular, polypoid or occasionally peduncolated melanomas occurr anywhere on the body (Plotnick et al.,1990 & Kiene et al., 1995), while Acral Lentiginuous Malignant Melanoma (Reed, 1976) may develop on palmar, plantar, and subungual skin; in the oral cavity and other mucous surfaces, such as vagina, vulva, cervix and uteri (Ronan et al., 1990 & Batsakis et al., 2000). Furthermore there are several variants of malignant melanoma that do not show the typical histopathology classification, such as Desmoplastic Melanoma (Bandarchi et al., 2010).

Prognostic factors in melanoma can be classified in histological, pathological and clinical factors (Balch et al., 2000 & Lotze et al., 2001). Patient age, sex and tumor location, the

Clark level of invasion and Breslow's thickness measurements are the best known prognostic attributes for melanoma. The Clark level describes the involvement of the tumor within cutaneous and subcutaneous structures, whereas Breslow thickness is defined as the "total vertical height of the tumor measured from the top of the granular layer to the area of the deepest penetration into the skin" (DiChiara, 2013). Other prognostic factors are the mitotic rate, the number of mitoses/square millimeter (Zettersten et al., 2003),ulceration and the absence of intact epidermis overlying a significant portion of the primary tumor.

Unlike primary tumors, which can be surgically treated, metastatic melanoma is commonly resistant to conventional therapies such as chemotherapy, radiotherapy and immunotherapy. Moreover, the treatment options are still limited. The only chemotherapeutic drug approved by the FDA is the use of the alkylating agent Decarbazine (DTIC). Other chemotherapies that have been explored include Temozolomide, Fotemustine, Carmustine, Paclitaxel and Cisplatin. In addition, interferon (IFN)-α and interleukin (IL)-2 are used as adjuvant or in combination with chemotherapy (Tarhini et al., 2006).

Due to lack of effective therapies, the identification of the signaling pathways involved in melanoma initiation and progression represent a fundamental step to identify new therapeutic approaches. It could provide the opportunity to develop targeted therapies and tailor those treatments to patients according of specific genetic lesions (Gray-Schopfer et al., 2007a). For example, the discovery that 40-50% of melanomas harbor activating BRAF mutations (Davies et al, 2002) prompted the development of selective BRAF inhibitors. The first specific ones were the lead compound PLX4720 (Tsai J. et al., 2008) and the pharmacokinetically superior PLX4032/vemurafenib (Lee J.T et al., 2010).

Clearly, targeting one pathway is not enough to treat patients with advanced melanoma, but a combination of different agents, such as chemotherapy and targeted therapies, can improve the response to treatment.

Melanoma progression and metastasis

Melanoma development is considered a stepwise process that lead from benign to dysplastic nevi (characterized by a structural and architectural atypia), and progress toward radial growth phase (RGP) during which, malignant cells grow in an outward fashion spreading across the epidermis. After time, most melanomas progress to the vertical growth phase (VGP), more dangerous and aggressive, in which malignant cells invade the dermis and develop the ability to spread or metastasize (Meier et al., 1998).
In particular it's possible to distinguish five clinically and histomorphologically different steps in tumor progression: 1) congenital or acquired nevi, 2) the Dysplastic nevi, 3) the Radial Growth Phase, 4) Vertical-growth-phase tumor and 5) metastatic melanoma (Figure 1.1)**.**

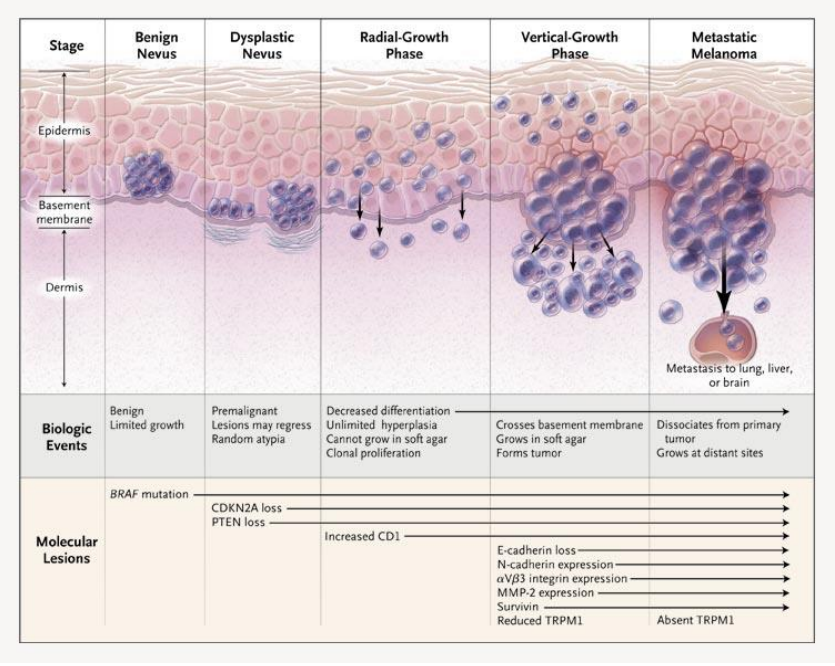

Figure 1.1 Representation of melanoma **progression**
It's possible to distinguish several steps in melanoma progression, each of which is characterized by the presence of a new clone of cells that acquires an advantage in growth compared to the surrounding tissue: 1) Benign nevus, 2) dysplastic nevus, 3) RPG melanoma, first stage malignant, which has no metastatic potential and remains confined to the epidermis, 4) VPG melanoma, the most advanced and aggressive stage, that has the ability to invade the underlying dermis and 6) Metastasis, the final step, with the dissemination of melanoma cells into the endothelial or lymphatic vessels

However, not all melanomas pass through each of these individual phases. RPG or VPG melanomas can both develop directly from isolated melanocytes or nevi, and both can progress directly to metastatic melanoma (Gray-Schopfer et.al., 2007).

Metastasis is the dissemination of cancer cells from the primary tumor and the subsequent formation of new tumor masses in peripheral tissues. The acquisition of an invasive behaviour is the key transition in the progression of benign melanocyte hyperplasia to life-threatening melanoma. Understanding this transition and the mechanisms of invasion are the key to understanding how to treat this neoplasia (Orgaz et al, 2013).

Underlying the invasive behaviour is increased cell motility caused by changes in cytoskeletal organization and altered contacts with the extracellular matrix (ECM) and the stroma. The second stage involves the dissemination of cancer cells away from the primary tumour either via lymph vessels or the vasculature in a process called intravasation (Bustelo, 2012). Circulating cancer cells then adhere to the microvasculature and move across the vascular endothelial cell layer and the ECM of the peripheral tissue in a process called extravasation. Finally, the extravasated cells colonize the new peripheral niche, a process called macrometastasis (Bustelo, 2012).

To efficiently metastasize and penetrate into blood or lymphatic vessels, invasive melanoma cells need to change their cytoskeletal organization and alter contacts with the ECM and the surrounding stromal cells.

Metastatic melanoma cells are highly plastic and accommodate their mode of invasion depending on the differing microenvironments they encounter during the metastatic cascade. In the last decades, much effort has been placed on identifying molecules and signaling pathways that are deregulated in melanoma cells and how these factors promote their invasive behaviour (Orgaz et al, 2013).

These subpopulations acquire a growth advantage in time on the primary site leading to the formation of a dominant proliferative population (Quatresooz and Pierard, 2011); this in turn undergo changes that provide tumor cells with the ability to overcome cell-cell adhesion and micro-environmental controls from the host, to invade surrounding tissues, and disseminate to distant sites (Li G et al., 2002).

Normal skin melanocytic homeostasis is maintained by dynamic interactions with keratinocytes, fibroblasts, endothelial cells, immunocompetent cells and the ECM.

Transformation of melanocytes into melanoma entails a number of genetic and environmental factors. Loss of adhesion receptors and mutation of growth regulatory genes enable melanocytes to escape from the regulation by keratinocytes. One key event that facilitates this escaping is the loss of E-cadherin and the gain of N-cadherin, which allows melanocytes to get away from the control of keratinocytes and start interacting with stromal cells from the dermis, such as fibroblasts and endothelial cells (Haass et al., 2004).

These events are crucial to allow melanoma cells to metastasize. These events promote inappropriate survival signals (Li et al., 2002), enhance the malignant phenotype (Hazan et al., 2000; Li et al., 2002) and provide a possible metastatic advantage to melanoma cells (Li et al., 2002). In addition, melanoma cells interact with each other and with stromal cells through other adhesion molecules, such as Mel-CAM/Mel-CAM ligand, L1-CAM/αvβ4 integrin, which are all involved in progression to malignancy and they are highly expressed in metastatic melanoma cells (Johnson et al., 1996; Thies et al., 2002b; Degen et al., 1998; Holzemann et al., 1998; Johnson et al., 1989) (figure 1.2).

While there are no strong genetic candidates to mediate the switch from RGP to VGP, microarray and immunohistochemistry analysis have identified numerous genes whose expression level is altered as melanoma becomes invasive (Alonso et al., 2004, 2007; Bittner et al., 2000; Clark et al., 2000; Gaggioli and Sahai, 2007; Gray-Schopfer et al., 2007a; Villanueva and Herlyn, 2009). The major mediators of cell–ECM interactions are integrins, which form heterodimeric complexes consisting of α and β subunits. Numerous groups have reported deregulated expression of integrins in invasive melanomas and shown the functional importance of integrins [(Melchiori et al., 1995; Seftor et al., 1999; Van Belle et al., 1999); reviewed in (Kuphal et al., 2005a)]. The main ECM components that integrins bind are collagen, laminin and fibronectin. In melanoma, the αvβ3 integrin appears to be important for the invasive potential of melanoma (Dang et al., 2006; Hsu et al., 1998; Van Belle et al., 1999). Peptides that block the ability of integrins to interact with laminin and fibronectin have been shown to reduce melanoma motility in vitro and metastatic spread in vivo (Kuratomi et al., 1999; Makabe et al.,

1990). Moreover, several studies have shown that high levels of β1, as well as the β3 integrins promote melanoma transition from RPG to VPG (Ramakrishnan et al., 2006; Seftor et al., 1998). Indeed, in melanoma, both αvβ3 and β1 integrins are highly expressed in invasive cells (Brooks et al., 1996; Hegerfeldt et al., 2002).

Angiogenesis, the formation of new vessels, is also a fundamental process for the amplification and progression of the tumor and provides a route for the migrating cells (Folkman, 2006; Wanebo et al., 2006). It is known that αvβ3 and αvβ5 integrins are involved in angiogenesis (Hynes et al., 2004), being upregulated in endothelial cells during tumor neovascularization (Eskens et al., 2003). Although these changes into adhesion molecules are very important, alone are not sufficient to induce active invasion and metastasis; additional genetic or environmental events, seem to be involved (Li et al., 2002).

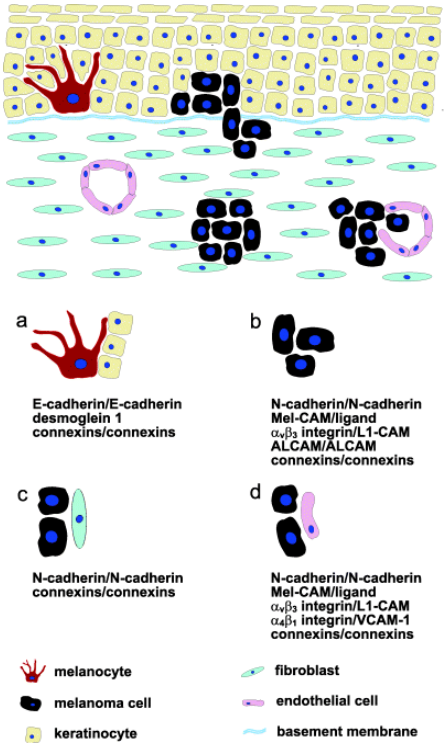

Figure 1.2: Cell–cell communication in melanoma. *Normal melanocytes interact with adjacent keratinocytes through E-cadherin, desmoglein 1, and connexins (a). A shift of the cadherin profile from E- to N-cadherin during melanoma development not only frees the cells from epidermal keratinocytes, but also confers new adhesive and communication properties. Melanoma cells interact with each other (b) through N-cadherin, Mel-CAM/Mel-CAM ligand, alphavbeta3 integrin/L1-CAM, ALCAM and connexins, with fibroblasts (c) through N-cadherin and connexins, and with endothelial cells (d) through N-cadherin, Mel-CAM/Mel-CAM ligand, alphavbeta3 integrin/L1-CAM, alpha4beta1 integrin/VCAM-1 and connexins.*

Melanoma chemoresistance

Metastasis is one of the main clinical parameters known to affect the prognosis of cancer patients, including melanoma, and it is associated with resistance to chemotherapeutic treatments, higher post-treatment recurrence rates and poor cancer patient survival rates (Valastyan and Weinberg, 2011).

A simple look at the wide range of antineoplastic treatments that are ineffective at killing melanoma cells implies that the resistance mechanisms in melanoma are complex. For decades, clinicians and basic scientists have been puzzled by the fact that melanoma cells simultaneously acquire the capability to escape immune surveillance mechanisms and evade the cytotoxic action of different cytotoxic insults, for example, DNA damage (e.g. by irradiation, alkylation, methylation or crosslinking), microtubule destabilization or topoisomerase inhibition. Complete treatment responses after chemotherapeutic regimens are rare (with benefits for 20% of the patients), and the term "remission" is rarely used for melanoma. Therefore, in this tumor, drug resistance is likely not a primary consequence of acquired genetic alterations selected during or after therapy, but rather inherent to the malignant behavior of melanoma cells at diagnosis.

Several functional and biochemical studies support the hypothesis that melanoma cells are 'born to survive'. Their aggressive behavior derives from intrinsic survival features of their paternal melanocytes nourished by additional alterations acquired during tumor progression. These inherent survival mechanisms may contribute to the poor treatment responses typically observed in clinical settings (Soegens and Lowe, 2003).

Some researcher postulated that melanoma chemoresistance could be due to the high motility and enhanced survival property of melanoma cells.

In addition, melanoma cells have low level of spontaneous apoptosis in vivo and are resistant to drug-induced apoptosis in vitro (Soengas and Lowe, 2003). Thus, an intense research for cell death factors altered during melanoma progression are necessary.

Some studies have lead to the identification of two groups of anti-apoptotic factors: apoptosis inhibitors (IAPs) and FLIPs (FLICE inhibitory proteins) that have been found overexpressed in multiple tumor types (Tschopp et al., 1998)

In melanoma, two members of the IAP family, survivin and ML-IAP, as well as FLIP

have been associated with tumor progression, as they are detectable in melanocytic nevi and overexpressed in invasive and metastatic melanomas (Grossman and Altieri, 2001). ML-IAP is upregulated in melanoma cells line, but is absent in normal melanocytes (Vucic et al., 2000).

Although the mechanisms of action of surviving in melanoma is unclear (Li et al., 1998), it seems to be related to the mithocondrial apoptotic pathway, where the proapoptotic factors Smac/Diablo, caspases 9 and 3 are inhibited (Vucic et al., 2002). The impact of FLIP in melanoma chemoresistance is controversial (Bullani et al., 2001), as the endogenous levels of FLIP is not necessarily correlated with drug response in patients (Ugurel et al., 1999).

Mutations in p53 protein seem to have a key role in melanoma chemoresistance. However, despite its extreme chemoresistance, melanoma displays a low frequency of p53 mutations (Soengas and Lowe, 2003). Probably the p53 function could be disabled by lesions that disrupt other components of the pathway. In fact, several studies have shown that the disruption of the upstream p53 regulator p14ARF, frequently mutated in melanoma, can lead to a loss of the p53 functionality (Chin et al., 2006; You et al., 2002). Moreover, the abnormal phosphorylation of p53 by Chk2 kinase may contribute to the resistance of melanoma cells to radiotherapy (Satyamoorthy et al., 2000a).

Thus, the disruption of the downstream p53-apoptosis signal may decrease drug sensitivity (Schmitt et al., 2002a, b).

In addition, in melanoma several survival pathways are constitutively activated, such as the Raf/MAPK, the PI3K/AKT/PTEN and the NK-kB pathway. All these pathways may contribute to melanoma resistance to treatments (Soengas and Lowe, 2003) (Figure 1.3).

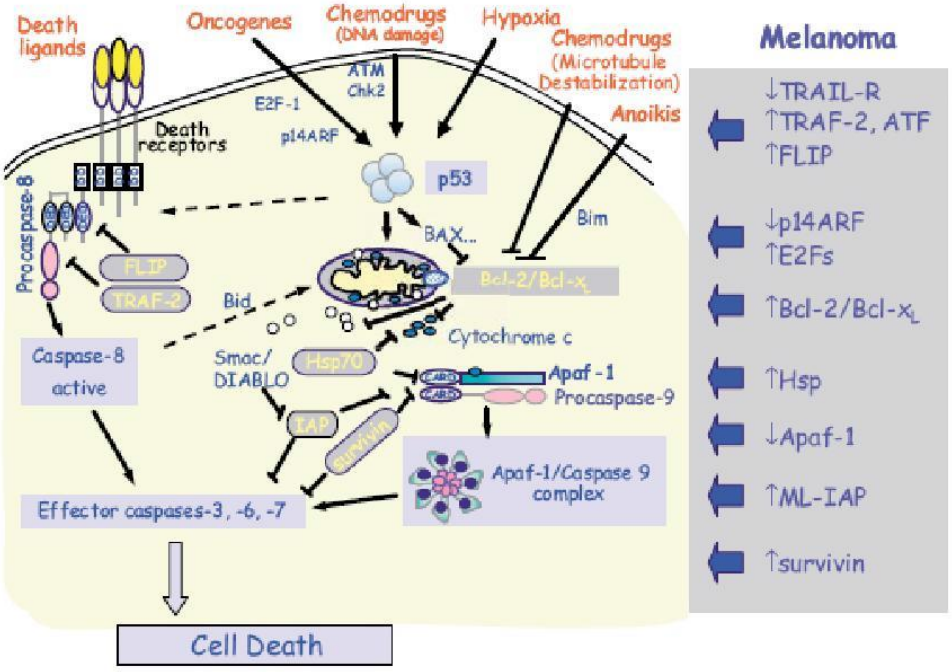

Figure 1.3: Apoptosis pathway and melanoma
Left pannel: Schematic representation of the apoptotic pathway. Right pannel: Examples of upregulated and downregulated apoptotic factors in melanoma (Soengens and Lowe, 2003).

Cancers are frequently composed of heterogeneous cell populations. It has been hypothesized that a cell subpopulation within a tumor is capable of tumor propagation (Clarke et al., 2006).

These cells, known as cancer stem cells (CSCs), seem to be responsible for generating and maintaining tumor heterogeneity (Clarke et al., 2006; Visvader et al., 2008). Several evidence support the idea that CSCs are involved in tumor initiation, progression, and in chemoresistance (Fang et al., 2005; Frank et al., 2005;).

Questions persist about the nature and number of cells with tumor-propagating capability in different types of cancer, including melanoma. In part, this is because identification and characterization of purified tumorigenic subsets of cancer cells has not been achieved to date.

This **“**CSC hypothesis**”** has been supported by numerous studies showing prospective purification of human cancer cell subsets that have the ability to give rise to tumorigenic and nontumorigenic progeny.

A major focus of melanoma stem cell research is the identification of markers for the cancer stem cell population.

The markers may not be unique to the cancer stem cells, being expressed in other cell types as well. Despite these caveats, some important insights have been obtained through the use of these markers and the identification of new potential markers may provide future therapeutic targets.

Stem and progenitor cell-associated proteins that have been proposed in melanoma are cancer testis antigens (Simpson et al., 2005), bone morphogenetic proteins (BMP) (Rothhammer et al., 2007), Notch receptors (Balint et al., 2005), Wnt proteins (Weeraratna et al., 2002), the ABCB5, CD20, CD133, CD166, CD34, nestin, or c-kit stem cell antigen (Frank et al., 2005, Hendrix et al., 2003; Klein et al., 2007; Van Kempen et al., 2000).

Neurotrophins

Neurotrophins (NTs) are a group of molecules that play a crucial role in neuronal cells, but also operate in skin where they take part in a complex network in which they stimulate proliferation, differentiation and apoptosis by autocrine or paracrine functions. (Chao et al, 2006). NTs were identified as promoters of neuronal survival, but it has been demonstrated that they regulate many aspects of neuronal development and function, including synapse formation and synaptic plasticity (Huang EJ & Reichardt LF 2003). The first neurotrophin, nerve growth factor (NGF), was discovered during a search for survival factors that could explain the deleterious effects of deletion of target tissues on the subsequent survival of motor and sensory neurons (Levi-Montalcini 1987).

Four neurotrophins are expressed in mammals: NGF, BDNF, neurotrophin-3 (NT-3) and neurotrophin-4 (NT-4).

The experiments leading to NTs discovery revealed the essential role of cellular interactions in controlling cell survival and differentiation (Jacobson MD *et al*. 1997). Preceding serious studies on membrane transport and endocytosis in other cells, neuroscientists have shown that NGF was internalized by receptor-dependent processes and transported along axons in membranous vesicles to the cell soma by cytoskeletal and energy dependent processes (Thoenen H & Barde Y 1980). Local signaling was shown to regulate growth cone motility, while signaling in the cell soma controlled cell survival and gene expression. Ligand turnover was shown to occur in lysosomes. It is clear that all cells use similar mechanisms to control ligand and receptor trafficking, signaling and degradation. Finally, neurotrophins activate receptor tyrosine kinases (Chao MV and Bothwell M 2002).

In addition, recent studies have revealed a diversity of roles for these factors outside the nervous system, most notably in cardiac development, neovascularization and immune system function (Donovan MJ *et al*. 2000; Lin MI *et al*. 2000; Coppola V *et al*. 2004).

Furthermore, several human genetics diseases have been associated with mutation in neurotrophins or their receptors, such as in congenital insensitivity to pain with anhydrosis (CIPA), severe hyperphagic obesity, severe impairments in nociception, learning and memory, impaired hippocampal functional and episodic memory (Indo,

2001; Yeo et al., 2004; Egan et al., 2003). Moreover, similarly to other growth factors, dysregulation of NTs signal transduction is found in a number of tumors where they contribute to malignant transformation.

Neurotrophins and their receptors

NTs effects are mediated by two classes of transmembrane receptors: 1) a family of tyrosine kinase receptors called Trks (Trk A, Trk B and TrkC) (Barbacid, 1994) and 2) p75 neurotrophine receptor (p75NTR) (Chao & Bothwell, 2002). While Trks receptors selectively bind specific neurotrophins, p75NTR is able to bind all neurotrophins with equal low affinity.

In particular, TrkA binds NGF and NT-3, TrkB binds BDNF, NT-3, NT-4, TrkC only binds NT-3, while p75NTR binds all NTs (Figure 1.4).

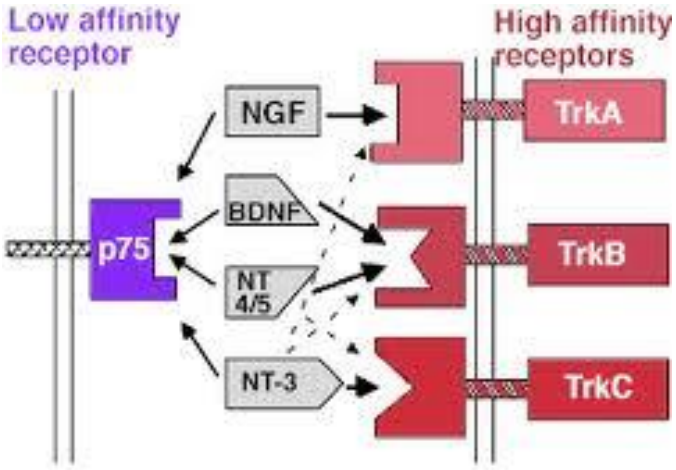

Figure 1.4: NTs and their receptors *NTs exert their actions by binding to two classes of receptors: the high affinity receptors Trks and the low affinity receptor p75 (p75NTR). Trks are divided in 3 classes: Trk A, that binds NGF and NT-3, Trk B, that binds BDNF; NT-3 and NT-4, and Trk C which only binds NT-3. P75NTR, binds all NTs, although with low affinity and specificity.*

Trks receptors promote mostly survival and differentiation, while the role of p75NTR is ambiguous, as it can either act as a co-receptor for Trks enhancing their ability to promote survival, or signal on its own by inducing apoptosis (Figure 1.5).

The biological effects induced by NTs strongly depend on the pattern of NT receptor/co-receptors expression in target cells as well as on the presence of intracellular adaptor molecules that link NT signalling to different biochemical pathways.

The propensity of NTs to produce diametrically opposing effects on cell survival has led to propose a "yin and yang" model of neurotrophin action, where the binary actions of NTs depend on both the form of the neurotrophin (pro- versus mature) and the class of receptor that is activated. Central to the proposed "yin- yang" model of NTs function is the observation that a mature NT binds preferentially to Trk receptors to enhance cell survival, whereas an unprocessed proNT binds to p75NTR to induce cell death (Lu et al., 2005).

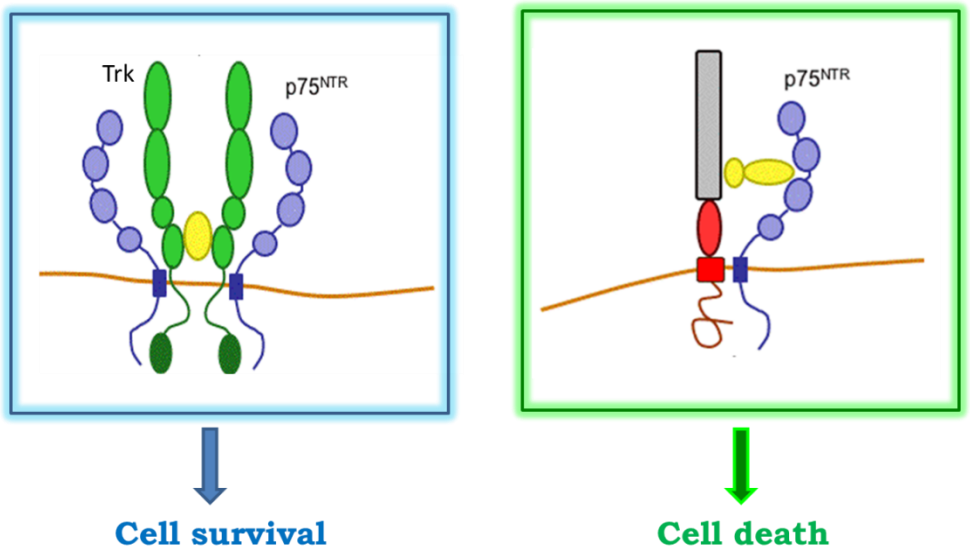

Figure 1.5 Trks and p75NTR functions
Trk receptors promote cell survival and differentiation (alone or in combination with p75NTR), while the role of p75NTR is ambiguos as it can either acts as a coreceptor for Trks, enhancing their ability to promote survival or signal on its own to induce apoptosis.

High affinity receptors Trks

The Trk (tropomycin receptor kinase) receptor was first identified as a colon-derived oncogene in which tropomyocin was fused to a tyrosine kinase domain. However, the normal cellular counterpart of this oncogene, namely Trk (lacking tropomycin), was found to be a transmembrane protein that is highly expressed in the developing and adult nervous system. To date, three Trk receptors have been identified: TrkA (or NTRK1), TrkB (or NTRK2) and TrkC (or NTRK3).

They are widely distributed in neuronal tissues and hematopoietic cells (Barbacid, 1993; Chao, 1992; Meakin and Shooter, 1992; Saltier and Decker, 1994).

NTs interact with Trk receptors at the membrane proximal immunoglobulin-like domain (Ultsch et al., 1999). The cytoplasmic domain, instead, consists of a tyrosine kinase domain surrounded by several tyrosines that serve as phosphorylationdependent docking sites for cytoplasmic adaptors and enzymes. The three dimensional structure of these domains in each of the Trk receptors have been solved (Ultsch et al., 1999) (Figure 1.6).

Thus, the activation of Trks occurs following the interaction with NTs, which allows the dimerization, autophosphorylation and the subsequent binding of adaptor molecules that lead to different intracellular signal transducing pathways (Reichardt, 2006). Expression of a specific Trk receptor confers responsiveness to the NT to which it binds.

Splicing, however, introduces some limitations to this generalization. For example, differential splicing affects ligand interactions of each of the Trk receptors through insertions of short amino acid sequences into the juxtamembrane regions of the extracellular domains of TrkA, TrkB and TrkC (Meakin SO *et al*. 1992; Clary DO & Reichardt LF 1994). For both TrkA and TrkB, the insertion of the sequence encoded by a small exon enhances the binding of the receptor to non-preferred ligands. TrkA and TrkB isoforms that lack these inserts are activated strongly only by NGF and BDNF, respectively. The isoform of TrkA including an insert is also activated by NT-3 in addition to NGF (Clary DO & Reichardt LF 1994), while the similar isoform of TrkB is activated by NT-3 and NT-4 in addition to BDNF (Strohmaier C *et al*. 1996). Thirty-six novel isoforms of TrkB proteins with unique properties have been described recently.

This suggest high complexity in the synthesis, regulation and function of this important NT receptor, emphasizing the need for further study of these novel TrkB variants.

TrkC has several characteristics of a tumor suppressor and its expression in tumors has often been associated with good prognosis (Luberg et al., 2010). TrkC was recently demonstrated to be a dependance receptor, transducing different positive signals in the presence of ligand but inducing apoptosis in the absence of ligand **(**Tauszig-Delamasure et al., 2007). Indeed, the TrkC ligand NT-3 is upregulated in a large fraction of aggressive human neuroblastomas (NB) and it blocks TrkC-induced apoptosis of human NB cell lines.

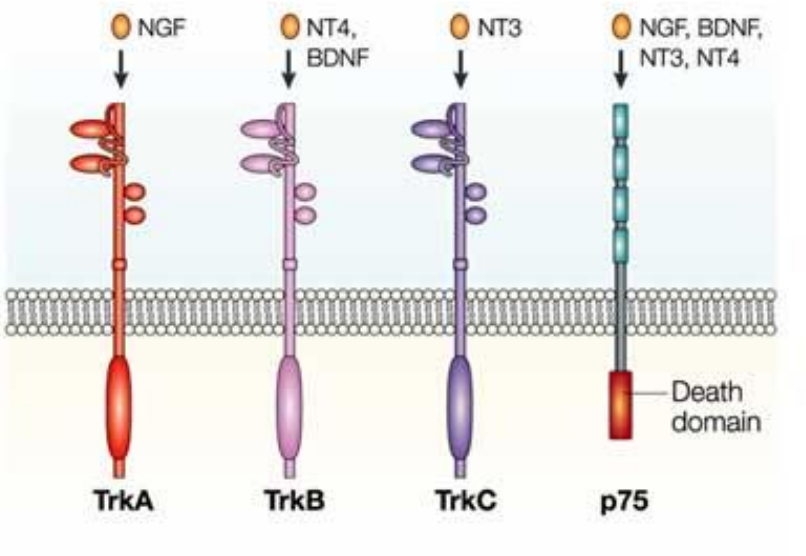

Figure 1.6: Schematic representation of neurotrophine receptors.
Trks consist of an membrane proximal immunoglobulin-like domain, that binds NT and of a cytoplasmic domain, which consists of a tyrosine kinase domain surrounded by several tyrosines that serve as phosphorylation-dependent docking sites for cytoplasmic adaptors and enzymes. Thus, the activation of Trks occur following the interaction with NTs, which allow the dimerization, autophosphorylation and the subsequent binding of adaptor molecules that lead to different intracellular signal trasducing pathways. P75NTR consists of an extra-cellular domain containing four cysteine-rich motifs, a single transmembrane domain and a cytoplasmic domain that includes a 'death' domain. Although this receptor does not contain a catalytic motif, it can interacts with several proteins that transmit crucial signals for regulating neuronal survival and differentiation as well as synaptic plasticity.

Low affinity receptor p75NTR

p75NTR was initially identified as a low-affinity NTs receptor for NGF, but it was subsequently shown to bind each of the neurotrophins with a similar affinity (Rodriguez-Tébar et al., 1990; Frade & Barde, 1998). It is composed of an extra-cellular domain containing four cysteine-rich motifs, a single transmembrane domain and a cytoplasmic domain which includes a "death domain" (He & Garcia, 2004). In fact p75NTR belongs to the tumor necrosis factor receptor superfamily.

Although this receptor does not contain a catalytic motif, it can interact with several proteins that transmit crucial signals for regulating neuronal survival and differentiation as well as synaptic plasticity (Reichardt et al., 2006). The three-dimensional structure of p75NTR extracellular domain in association with NGF dimer indicates that each of the four cysteine-rich repeats participates in binding to NGF (He & Garcia, 2004).

Apoptosis via p75NTR can be triggered by neurotrophins, proneurotrophins, and other ligands including aggregated amyloid and neurotoxic prion (review: Schor NF 2005). For instance, during the development of the chick eye, a subpopulation of the nascent retinal ganglion cells, which has weak TrkB expression and/or receives insufficient amounts of BDNF, can be driven to apoptosis by stimulation of p75NTR with NGF (Frade JM *et al*. 1999).

NGF/p75NTR-mediated apoptosis may also regulate cell numbers in the developing inner ear (Frago LM *et al*. 1998). Amyloid induced apoptosis in a neuroblastoma cell line is exclusively mediated by p75NTR (Tsukamoto E *et al*. 2003).

Several interaction partners of the intracellular domain of p75NTR have been linked to apoptosis. However, all pathways appear to converge on the activation of Jun kinase (JNK), p53, and certain caspases. The involvement of the tumor suppressor protein p53 raises the possibility that p75NTR-mediated apoptosis may use conflicting signals for cell division and growth arrest (Frade JM 1998). In sympathetic neurons, the neurotrophin receptor interacting factor (NRIF) and the factor p53 are required for p75/JNK-mediated apoptosis; conversely, overexpression of NRIF by transfection is sufficient to trigger p53-mediated apoptosis, suggesting that NRIF has also a function of its own that is not related to p75NTR (Linggi MS *et al*. 2005). Beside NRIF, another interaction partner of

p75NTR, TRAF6, is also required for p75NTR-mediated apoptosis (Yeiser EC *et al*. 2004).

There are further apoptotic factors interacting with p75NTR, including neurotrophin receptor interacting MAGE homolog (NRAGE) and p75NTR-associated cell death executor (NADE); both activate JNK like NRIF. NRAGE competes with TrkA for the same p75NTR binding site and may prevent the opposing influence of TrkA on apoptotic p75NTR signaling (Frade et. Al, 1998).

A gene related to p75NTR, named NRH-2, has recently been identified. The product of this gene lacks the extracellular cysteine-rich repeats present in p75NTR and fails to bind NGF, but it is able to interact and influence the ligand-binding properties of TrkA (Murray et al., 2004).

The role of p75NTR is still controversial and it may vary depend on the ligand or on the co-expression with Trk receptors: when p75NTR is expressed alone binds mature NTs that are capable of inducing apoptosis or promoting survival depending on the intracellular adaptor molecules present in target cells, by interacting with a mounting number of downstream molecules (Wang et al., 2000), while in presence of Trk receptors, p75NTR increases high affinity NT binding, enhances Trks ability to discriminate a preferred ligand from the other NTs, and promotes NTs survival effects (Teng & Hempstead, 2004). Recently, it has been shown that the proform of NT, proNGF, binds p75NTR in association with its co-receptor sortilin, but not Trk (Nykjaer et al., 2004). More specifically, sortilin, a member of the vps-10 protein family, binds the "pro" region of NGF, whereas p75NTR binds mature NGF. The p75NTR‑sortilin complex couples with proNGF to induce apoptosis (Kaplan & Miller, 2004).

p75NTR and skin

Work over the past 10 years has indicated that NTs possess a range of function outside the nervous system (Sariola, 2001). In the skin, a complex network exists in which various cells are either the target or the source of NTs, thus playing autocrine and paracrine functions (Marconi et al., 2003, 2006). Keratinocytes synthesize and secrete all NTs (Di Marco et al., 1993), in particular NGF, that acts as a growth factor for these cells (Pincelli et al., 1994) and induces their proliferation (Di Marco et al., 1993). Human keratinocytes express the high affinity receptors TrkA and TrkC, but not the functional form of the TrkB (Marconi et al., 2003). Endogenous NGF autocrinally sustains keratinocyte proliferation. Moreover, NTs modulate susceptibility to apoptosis in the epidermis. Autocrine NGF protects human keratinocytes from UVB-induced apoptosis, while UVB downregulates both NGF and TrkA expression in these cells (Marconi et al., 1999). Because in normal human keratinocytes TrkB lacks functional isoform, NTs may exert different functions by binding p75NTR alone. p75NTR acts as a proapoptotic receptor in human keratinocytes.

Indeed, p75NTR siRNA-transfected keratinocytes fail to undergo cell death after addition of NT-4 (Truzzi et al., 2011). p75NTR is mostly expressed in the differentiated transit amplifying (TA) cells, and it is barely detected in keratinocyte stem cells (KSC). TA cells have been shown to be more susceptible than KSC to apoptosis (Tiberio et al., 2002).

Therefore, the espression of p75NTR predominantly in TA cells seems to be consistent with the pro-apoptotic role of this receptor in human keratinocytes (Truzzi et al., 2011).

Melanocytes, which share with neurons the neuroectodermal origin, express all NTs and their receptors, except TrkC (Pincelli and Yaar, 1997; Marconi et al., 2006). NTs are important for melanocyte migration, viability and differentiation together with other paracrine signalling molecules (Pincelli et al., 1997). They also express p75NTR, which is upregulated by different stimuli, like UV radiation (Peacocke et al., 1988) or after phorbol 12-tetra decantate 13 acetate (TPA), a strong activator of protein kinase C treatment (Yaar et al., 1994).

p75NTR and melanoma

As for many other growth factors, dysregulation of NT signal trasduction is found in a number of tumors inside and outside the nervos system where they accompany or contribute to malignant trasformatiom (Kruttgen et al., 2006). Yet, the precise role of NTs and their receptors has to be clarified (Thiele et al., 2009; Papatsoris et al., 2009).

The role of p75NTR in melanoma is not yet entirely clear, and many publications are controversial. Iwamoto et al. have shown that p75NTR is not detectable in melanocytes of normal epidermis, whereas it is expressed in 13 of 14 benign nevi. Moreover, p75NTR was found to be weakly expressed in several types of melanoma, such as epithelioid, desmoplastic and spindle cell melanomas (Iwamoto et al., 2001). This was confirmed by others who showed p75NTR staining to be more diffuse and intense as compared with S100 (Kanik et al., 1996; Lazova et al., 2010). On the contrary, other authors have observed that only 33% of the desmoplastic melanoma contains p75NTR positive cells (Huttenbach et al., 2002).

Marchetti et al, by using melanoma cell lines, observed that NGF/p75NTR signalling promotes the survival of melanoma cells. They also observed the presence of NGF and NT-3 in tumor adjacent tissue at the invasive front of melanoma brain metastases, which might indicate a paracrine activation of p75NTR and TrkC in melanoma cells by NGF and NT-3 produced by nearby glial cells (Marchetti et al., 2003).

Besides promoting melanoma cell survival, NTs also induce the expression in melanoma cells of heparanase, an important enzyme for local invasion and metastasis, that cleaves heparan sulfate chains of proteoglycans, thus modifying the extracellular matrix of tumor cells (Walch et al., 1999). Moreover, Shonukan et al have shown that NTs are chemotactic for melanoma cells, and that the actin-bundling protein fascin co-immunoprecipitates with p75NTR in an NGF-dependent manner (Shonukan et al., 2003).

NTs appeared to be important for melanoma cell migration *in vitro*, with special respect for metastatic cell lines. The migratory phenotype is necessarily dependent on the presence of both the high- and low-affinity NTs receptors. Truzzi et al. have detected p75NTR in all melanoma cell lines and they have established that the autocrine action of NTs is responsible for melanoma cell proliferation and migration through the formation

of the p75NTR-Trk complex. Melanoma cells treated with p75NTR small interfering RNA (p75NTRsiRNA) fail to respond to NTs stimulation. In addition, they have shown that proNGF strongly stimulates melanoma cell migration, suggesting that p75NTR mediates melanoma invasiveness, most likely in combination with sortilin (Truzzi et al., 2008).

Other authors have reported that p75NTR is frequently overexpressed in aggressive melanoma (Brocker et al., 1991; Herraman et al., 1993; Mattei et al., 1994) and that it can play a direct and active role in NT signalling to promote invasion of melanoma cells (Marchetti et al., 1998). In addition, it was shown that the NT responsiveness, regulation of ECM degradative enzyme (Heparanase) and cell invasion correlated with augmented p75NTR levels in brian-colonizing melanoma cells (Marchetti et al., 1993; Marchetti and Nicolson, 2001) Futhermore, it was shown that p75NTR (CD271), previously identified as a marker of neural crest cells (Stemple, 1992), may be also a marker for the CSC in melanoma. Boiko and co-workers showed that p75NTR expression characterized a population of melanoma cells with tumor initiating proprietes (Boiko et al., 2010). However the number of cells capable of recapitulating the tumors *in vivo* may vary depending on the assay conditions (Quintana et al., 2008).

The use of sensitive mouse models, such as the NOD/SCID IL2R (null) mice, demostrated that cell isolation through p75NTR does not enrich melanoma CSC, and melanoma cells are able to metastasize independently from their expression pattern, being able to reverse their phenotype through clonal expansion (Quintana et al., 2010; Civenni et al., 2011).

Consistently, in another study CD34-neg/p75NTR-pos cells from mouse melanomas only rarely form tumors, while the p75NTR-negative counterpart frequently forms tumors, depending on CD34 expression (Held et al., 2010). This suggests that although some lines of evidence point to p75NTR as a good marker for the isolation of melanoma CSC, it may not be the right candidate. It is interesting to mention though that the frequency of p75NTR-positive cells in melanoma samples correlates with higher metastasis and worse patient prognosis (Civenni et al., 2011). Altogether, these results suggest that p75NTR-positive cells are not the CSC population in melanoma, but may retain characteristics of aggressiveness and susceptibility to metastasize.

Further characterization of these cells and evaluation of the role of p75NTR in melanoma stem cells is necessary. Since there are conflicting data regarding the role of p75 in melanoma, further studies are needed.

Melanoma three-dimensional models

Although melanoma is one of the most studied neoplasia, laboratory techniques used for the study of this tumor have not lead to satisfactory results. The use of clinical samples, for the extraction of cells, involves both ethical and practical problems. Biopsies, in addition to being difficult to find because they are principally used by pathologists, are often embedded in paraffin and this does not allow RNA and DNA studies.

In order to overcome this limitation, melanoma cell lines, from primary and metastatic tumors, were developed. These cells have permitted to obtain important informations regarding the progression of melanoma. Nonetheless, these cells grow in adhesion on the culture substrate which differs considerably from the morphology, cell-cell and cell-matrix interactions of the real tumor, Thus, it does not allow the study of the tumor in its real 3D architecture and in its microenvironment.

Animals, in particular mice, are often used for studying melanoma. In vivo models are fundamental because they allow to study the in vivo tumor development. Yet, these models are very expensive and may not adequately reproduce the features of the human tumors.

Thus, new models were developed that bridge the gap between traditional cell culture and animal models (Griffith and Swartz et al., 2006; Rangarajan et al., 2004). In detail, in vitro three-dimensional (3D) models permit to study the tumors in a micro-environment that is closer to the in vivo situation.

Tumor Multicellular spheroids

Multicellular spheroids are three dimensional in vitro microscale tissue analogs. Spheroids model reproduce physiologic parameters present in vivo, including complex multicellular architecture, barriers to mass transport, and extracellular matrix deposition.

Relative to two-dimensional cultures, spheroids also provide better target cells for drug testing and are appropriate in vitro models for studies of drug penetration (Geeta M et al, 2012).

Spheroids, which are microscale, spherical cell clusters formed by self-assembly, are one of the most common and versatile methods of culturing cells in 3-D (Ingram M et al, 1997). Spheroids with radii of 200 μm and larger will have zones of proliferating cells on the outside and quiescent cells on the inside due to nutrient and oxygen transport limitations. Significantly larger spheroids can also harbor necrotic cells at the center as can be observed in some cancers in vivo. Spheroids have been used as models for evaluations of drug sensitivity and resistance, and they are typically more resistant to chemo-and radiotherapies compared to cells cultured as 2-D monolayers (Torisawa Y.S et al, 2005). These models also allow analyses of different growth constraints such as oxygen tension and nutrient consumption, radiation effects, and angiogenesis (Olive P.L et al, 1992).

Spheroids present a more physiological platform for drug delivery testing due to the following reasons:

1) Spheroids model the 3-D architecture of tissues, including multicellular arrangement and extracellular matrix deposition, found in vivo. Such arrangements,which are absent in conventional culture formats, reproduce how drug delivery might occur in vivo.

2) Being closely packed 3-D structures; spheroids have sizeable cell–cell interactions, including tight junctions, comparable to those in in vivo tissues. These cell–cell contacts and ensuing communication have been found to influence response of cells to drugs (Oloumi A. et al, 2002).

3) Spheroids have diffusional limits to mass transport of drugs, nutrients and other factors, similar to in vivo tissues. Due to their mimicry of the physiological barriers to drug delivery in vivo, spheroids can serve as an improved assay format for testing efficacy.

4) Co-culture spheroids are formed with two or more cell types in varying ratios representing intercellular signaling and architecture seen in vivo. These co-culture spheroids can help decipher how multiple cell types found in tissues in vivo might impact drug delivery.

5) Rare cells such as cancer stem cells or primary stem cells may be incorporated and maintained in spheroids, which can facilitate targeting these specific cells with drugs. It is often difficult to maintain small numbers of such cells in conventional culture formats and to decode how these cells respond to the drug and delivery mechanism.

6) Spheroids are 3D models of in vivo solid tumors. Larger spheroids develop central necrosis and regions of hypoxia present in many cancers, which is critical for testing anti-cancer therapeutics. Cellular microenvironments such as hypoxia, which have been identified as one cause of drug resistance (Kim S.H et al, 2011; Shekhar M.P et al, 2001; Andre F et al, 2010), can be modeled and created within spheroids for accurate testing of drug efficacy.

Formation of spheroids occurs spontaneously, in environments where cell–cell interactions dominate over cell–substrate interactions. Conventional methods for spheroid generation include hanging drops, culture of cells on non-adherent surfaces, spinner flask cultures, and NASA rotary cell culture systems (Friedrich J. et al, 2007; Torisawa Y.S et al, 2007; Kelm J.M et al, 2010).

All molecular methods can be applied to study cells from spheroids at the cellular, protein, RNA and DNA level. Several papers have described the genomic stability of cells in multicellular spheroids, their gene expression profiles and function. Several comparative transcriptomics studies have shown that numerous genes associated with cell survival, proliferation, differentiation and resistance to therapy are differentially expressed in cells grown as multicellular spheroids versus 2D cultures. This was shown also for cell lines originating from epithelial ovarian cancer (Cody et al., 2008; Zietarska et al., 2007), hepatocellular carcinoma (Chang and Hughes-Fulford, 2009; Shimada et al., 2007; Yamashita et al., 2004) or colon cancer (Gaedtke et al., 2007; Timmins et al., 2004). The expression profiles more closely resemble the profiles of the respective tumor tissue in vivo (Hirschaeseuser et al, 2010).

The capacity for spheroid outgrowth in 3D matrices or on adherent, ECM coated or non-coated surfaces, has previously been described as an interesting parameter to study the migratory behavior of tumor spheroid cells (Hirschberg et al., 2006; Lambert et al., 2006). One method that can be utilized to assess the invasive capacity of the cells in spheroids is the “collagen invasion assay”, in which spheroids are immersed in a type I

collagen coat. The collagen I mimics the tumor environment that may promote cells invasion. Thus, spheroids offer the promise of improving clinical efficacy predictions. Indeed, the potential of sophisticated, 3D culture systems to be incorporated into mainstream development processes for new anti-cancer therapeutic strategies is increasingly recognized; it is thought to improve the pre-animal and pre-clinical selection of both the most promising drug candidates and novel, future-oriented treatment modalities (Abbott, 2003; Friedrich et al., 2007a, 2009; Kunz-Schughart et al., 2004; Mueller- Klieser, 2000).

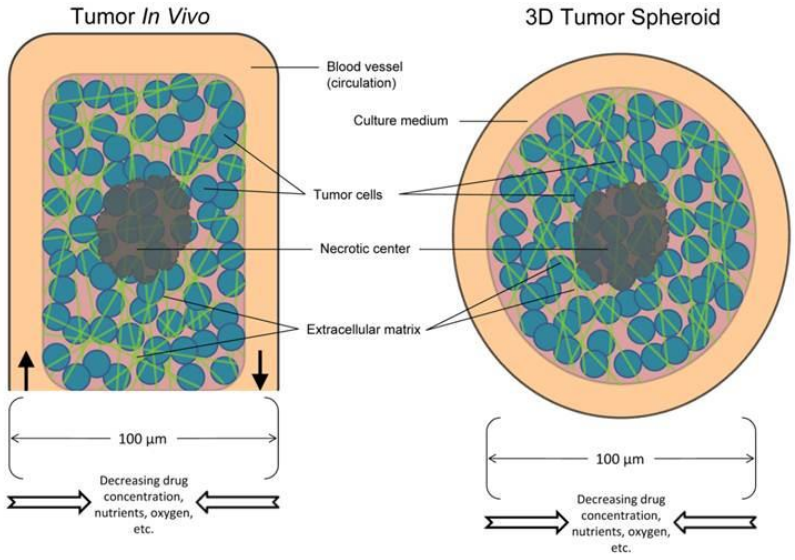

Figure 1.7: Schematic representation of the microenvironments inside a spheroids.
Tumor spheroids exhibits a concentrically layered structure consisting of a necrotic core, due to nutrient and oxygen transport limitations, surrounded by a viable layer of quiescent cells and an outer rim of proliferating cells.

Skin equivalents

Skin equivalent are advanced models, which permit to study melanocyte/keratinocyte interaction without culture artifacts. Skin equivalent comprise a stratified, terminally differentiated epidermal compartment and dermal compartment consisting of fibroblast embedded in collagen (Bilbo et al., 1993; Hsu et al., 1998) (Figure 1.8). Melanocytes are located in the basal layer in the engineered epidermis in close contact to keratinocytes. This in vitro reconstruction of the skin reproduces the *in vivo* situation (Valvy-Nagy et

al., 1990). These models can provide versatility and answers to physiological questions that cannot be solved solely in the context of monolayer tissue culture (Brohem et al., 2011). Skin equivalents has been used as an alternative to animal testing for studies of skin barrier function (Simonetti et al., 1995), skin irritation (Kuroyanagi et al., 1996; Ponec et al., 1995), wound healing (Jansson et al., 1996) and UV light-induced damage (Archambault et al., 1995; Nakazawa et al., 1997). Recently, this model has been used for treatment of burns (Rennekampff et al., 1996) and other wounds (Limat et al., 1996; Sabolinski et al., 1996). Skin equivalents can be used for studying cell-cell interactions and effects of the stromal environment in the regulation of melanogenesis, proliferation and differentiation of keratinocytes.Furthermore, human skin equivalents can easily be engineered with specific genetic alterations in either dermal or epidermal compartments to determine how the outcome of these modifications may be modulated by the stromal environment (Brohem et al., 2011).Likewise, melanoma cells can be incorporated into skin equivalents. It was established that melanoma cells show a striking similarity to the growth and invasion properties of the primary lesion from which they were taken (Meier et al., 2000). Invasion of melanoma cells into the dermis of the respective human skin equivalents model has been observed by several groups (Bechetoille et al., 2000). Melanoma-skin reconstructs is an invaluable tool for the investigation of tumor-stroma interaction, which have been increasingly recognized as essential for tumor cell survival, growth and invasion (Berking et al., 2001).

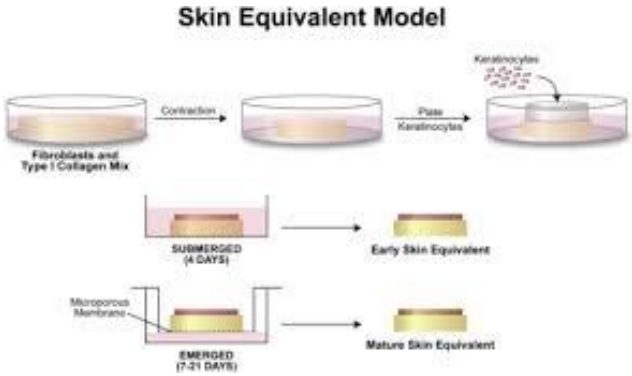

Figure 1.8: Schematic of the in vitro reconstruction of human skin *Collagen is layered into inserts followed by a layer of collagen with fibroblasts. After that collagen is contracted, keratinocytes with melanocytes or, eventually, melanoma cells are added into the developing nest, grown, initially, submerged in epidermal growth medium for 5 days, followed by air lifting from 7 up to 21 days.*

2. Material and methods

Melanoma cell culture

The experiments carried out in this work have been performed using five melanoma cell lines: WM115 and WM266-4, derived, respectively, from a primary and metastatic Radial Growth Phase (RGP) tumour of the same patient; SKMEL28, derived, from a very aggressive Vertical Growth Phase (VGP) primary tumour, and finally WM793-B and 1205Lu, derived from primary and metastatic Vertical Growth Phase-type tumours that are the most aggressive ones (American Type Culture Collection, Manassas, VA, USA).
WM115, WM266-4 and SKMEL28 lines were maintained in BME Melanoma Medium composed by: BME (Lonza), Fetal Bovine Serum (FBS) 10% (Lonza), Lglutammine 2 mM (Lonza), sodium pyruvate 1 mM (Lonza), non essential amminoacidis 0.1 mM (Lonza), penicillin/streptomycin 1% and sodium bicarbonate 1,5 g/L (Lonza) WM793-B and 1205Lu lines were cultured in Tumor Medium 2% containing: MCDB154CF medium (Gibco), sodium bicarbonate 1,5g/L (Lonza), Leibovitz L-15 medium (Cambrex), L-glutammine 2mM (Lonza), 2% FBS (Lonza), CaCl2 200mM (Lonza), insulin 5mg/ml and penicillin/streptomycin 1%.

Human keratinocytes and fibroblasts cell cultures

Keratinocyte cultures were prepared as described in Pincelli et al., 1997. Briefly, keratinocyte for primary culture were obtained from neonatal foreskin. Skin was minced and trypsinized (0.05% trypsin, 0,02 ethylenediammine tetraacetic acid - EDTA) at 37°C for 3 hours and keratinocytes were grown in 75-cm2 culture flask (Costar, Cambrdige, MA) with mytomicin (10 mg/ml)- treated 3T3 cells (Sigma, St. Louise, MO) for 2 hours at 37°C.
Cells were cultured Dulbelcco's modified Eagle's medium/Ham's F12 (DMEM/F12, 3:1) (Seromed-Biochrom, Berlin, Germany) containing insulin (5ug/ml, Sigma), transferrin (5ug/ml, Sigma), triiodotyronine (2nM, Sigma), hydrocortisone (0,4 ug/ml, Sigma), adenine (180mM, Sigma), mouse epidermal growth factors (10 nm/ml, Sigma), and 10% fetal calf serum (Seromed-Biochrom).

Human fibroblasts were obtained by explant culture from foreskin and grown in Dulbecco's modified Eagle's medium (DMEM) containing 5% fetal bovine serum.

Liquid overlay method

This culture method allows the growth of cells in suspension and the formation of multicellular spheroids. Usually melanoma cell lines grow as monolayer cultures and adhere to plastic flasks. The liquid overlay method prevents the adhesion of cells by using plates previously coated with a thin layer of agar where only cancer cells are able to grow and aggregate to form multicellular spheroids under non adhesion conditions.

The agar solution was prepared by diluting agarose (Sigma) at 1,5% in the appropriate base medium (without medium growth factors), and the solution was heated in the microwave to dissolve the agar. 100 ul/well of the solution were placed on a 96-well tissue culture plate. After agar polymerized at room temperature, the plate was placed under a source of UVB radiation for 30 minutes to sterilize the plate.

The cells were detached by using a solution of Trypsin 0.5 / EDTA 0,02 (Lonza) for 3 minutes in the incubator at 37°C with 5% CO2 . After that, trypsin digestive action was blocked with medium containing 10% of FBS.

Finally, 100 ul for well (containing 5000 cells) were seeded in the pre-coated 96-multiwell. 24 hour after plating multicellular spheroids were visible at the microscopy and they were monitored up to 168 hours later.

MTT Assay

MTT assay is a quantitative colorimetric assay for detection of mammalian cells survival and cells proliferation. This technique lets to evaluate the cell viability by quantifying the oxidative capacity of the cells with a spectrophotometric measurement.

The assay is based on the reduction of the yellow tetrazolium salt MTT (3-(4,5-dimethylthazol-2-yl)-2,5-diphenyl tetrazolium bromide), by the mitochondrial

dehydrogenase of viable cells, to purple formazan crystals, whose amount produced is proportional to the number of living cells present in culture (Figure 2.1).

The formazan crystals produced are insoluble in water but can be dissolved using a suitable solvent, for example isopropanol, DMSO, etc, and the resulting colored solution is quantified using a scanning multiwell spectrophotometer.

The sensitivity of MTT assay depends on the cell type, their average metabolic status, and the technique selected for solubilizing the formazan crystals. In this thesis project MTT assay is used to evaluate proliferation of all melanoma cell lines seeded using both in 2D and in 3D for a period of time from 24 hours up to 168 hours.

In a 96-multiwell plate 5.000 cells/well were seeded in 2D and in 3D. 20 ul of 0.5% MTT (Sigma-Aldrich) in PBS + with calcium were added, which was allowed to incubate (protected from light) for 4 hours at 37°C in the incubator. At the end of the incubation time, formazan salts were dissolved using 100 ul of a lysing solution, composed of Isopropanol with 0.04 NHCl, resuspending thoroughly to desegregate formazan salts and spheroids. Subsequently, only the spheroids cell suspension was transferred into empty wells; necessary step in order to avoid that the presence of agar could interfere with the spectrophotometric reading.

The formazan dye produced was evaluated by a multiwell scanning spectrophotometer at 560 nm and 650 nm for the background. The values obtained were subtracted from the values of the background.

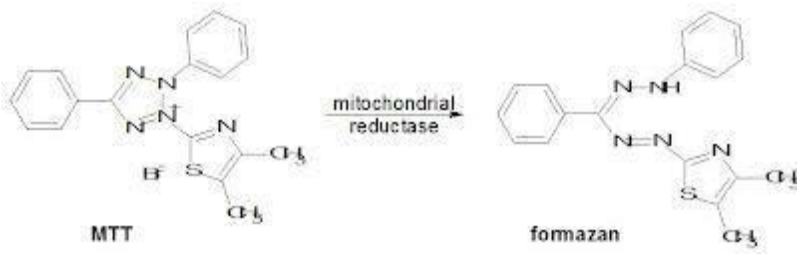

Figure 2.1: Reaction from Tetrazolium salt MTT to a formazan salt by viable cells
The mitochondrial dehydrogenase of viable cells perform the reaction that reduces the yellow tetrazolium salt MTT (3-(4,5-dimethylthazol-2-yl)-2,5-diphenyl tetrazolium bromide) to form purple formazan crystals

Treatment with cisplatin

5000 cells derived from WM115 and WM266-4 cell lines were seeded in 96-multiwell in 2d- and 3D cultures. 72 hours from seeding, cells were treated with the alkylating agent cisplatin. Cisplatin (Pronto Platamine, Pfizer 0,5 mg/ml) was used at the doses of 5 ul / ml and 20 ul/ml in physiological solution and 1N HCl (pH 3-4). As diluent was used the same saline solution adjusted to pH 3-4 with 1N HCl. Treated cell were used to assess viability, growth and invasion abilities.

Collagen invasion assay

Collagen invasion assay was used to assess the invasion ability of melanoma cells within a collagen matrix, which mimics the *in vivo* tumor ECM. The melanoma cell lines were seeded at a density of 5000 cells / well on agar (1.5%) in order to obtain 3D spheroids. After 72 hours from seeding the collagen solution was prepared, in ice, using: 1XDMEM, L-glutamine 200nM, 10% FBS, sodium bicarbonate 7,5%, collagen I (derived from rat tails) 1.5 mg / ml and penicillin/streptomycin 1%. 100 ul/well of collagen solution were placed into a 96 - multiwell and was allowed to polimeryzed for 30 minutes at room temperature. The spheroids were collected with a pipette tip from agar and were inserted within the collagen, trying not to make holes. Finally, 100ul of medium for melanoma were added in each well.

The growth and cell invasion was monitored for the next 24, 48, 72, 120 and 144h.

This experiment was performed for: all spheroid of melanoma cell lines (WM115, WM266, SKMEL-28, WM793 and 1205 Lu), SKMEL28 p75NTR dim and bright, WM115 spheroid trasfected with p75NTR siRNA.

FACS analysis

This analysis was performed to evaluate the expression of p75NTR in spheroids obtained with all melanoma cell lines. For this purpose, spheroids were stained with a monoclonal antibody anti-p75NTR, which allows to distinguish the cell populations expressing this receptor through the appropriate detection system. At the end of the experiment values express as percentage corresponde to the expression of p75NTR in the cell suspension analysed. MN Lx value, which corresponds to single cell expression intensity of the marker, was also considered.

WM115, WM266-4, SKMEL28, WM793-B and 1205Lu melanoma cell lines were seeded on top of 1.5% agar (previously dissolved in BME or MCDB154CF by using the base medium) in a 96-multiwell at the density of 5000 cells/well (see Liquid overlay method).

After 72 hours from seeding, spheroids were collected in a tube and, after washing them in PBS, they were incubated with 200 ul of Trypsin 0.05% / EDTA 0.02% for 2 minutes and, finally, mechanically disgregated to obtain a single cell suspension.

The resulting single cells suspension was counted (by using a Burker chamber) and about 500,000 cells were resuspended in 1 mL of PBS and centrifuged for 5 minutes at 1200 rpm. Subsequently, cells were incubated with primary antibody anti-p75NTR (Neomarker) diluted 1:50 in PBS- with 5% FBS (incubation at 4 ° C for 20 minutes). Then, after a wash in 1mL of PBS, cells were resuspended in 100 ul of secondary antibody anti-mouse IgG-FITC (dil 1:50 in PBS- with 5% FBS) (Alexa Fluor 488), and incubated in the dark for 20 minutes at 4°C.

Furthermore, two negative controls were used: in the first one, primary and secondary antibodies were not added, necessary step to verify if the cells had their intrinsic fluorescence; in the second control, instead, at the cell suspension only the secondary antibody was added, to make sure that the fluorescence detected was attributable only to the marker expression and not to the secondary antibody. At the end, after a further washing with PBS-, the cells were resuspended in 400ul of PBS- and the solution was read to the instrument Epics XL flow cytometer (Coulter Electronics Inc., Hialeah, FL, USA).

Extraction of cellular proteins

Melanoma cells were seeded on the agar coat to form spheroids and let to grow for at least 72 hours. Spheroids were, then, recovered in a tube, centrifuged at 1200 rpm for 5 minutes and the excess medium was eliminated.

After 2/3 washes in PBS, 500 μL of trypsin 0.05 % / EDTA 0.002 % solution was added and the cells were incubated for 3 minutes at 37°C in order to obtain a single cell suspension. After blocking trypsin action with medium containing 10% of FBS, cells were centrifuged for 5 minutes at 1200 rpm and the supernatant was discarded to obtain a dry pellet.

The cells were lysed, on ice, using a lysing solution consisting of: 425 μL lysis buffer (specific for p75NTR or b-actin) 75 μL of 1 mM protease inhibitors (Complete Mini, protease inhibitor cocktail tables, dissolved in water) and 1 μL (for p75NTR) or 20ul (for b-actin) of phenylmethylsulfonyl fluoride 1 mM; for a total volume of 500 μL.

The amount of lysing solution to use is chosen depending on the size of the pellet. In particular RIPA for p75NTR, (pH 7,5) is composed by : 150mM NaCl, 15mM $MgCl_2$, 1mM EGTA, 50mM Hepes, 10% glycerol, 1% Triton X-100; while for bactin a generic ripa buffer was used (Tris-HCl 50 mM - Sigma, NaCl 150 mM, Na deoxycholate 1%, Triton X-100 1%, SDS 0,1 %, NaN_3 0,2%).

The cells were left on ice for 25 minutes pipetting the lysate every 5-10 minutes to promote the action of the lysis solution. After 20-25 minutes, the cell suspension is passed through a syringe (insuline syringe-0,45 x 12,7 mm) to disrupt the cells. Finally a cycle of sonication and incubation on ice (10 seconds in the sonicator and 15 seconds in ice, repeated 3 times) was made.

The solution was centrifuged in a cold centrifuge (at 4°C) for 15 minutes at 13,000 rpm and, finally, the supernatant, which contains the cellular proteins, was recovered in an eppendorf and kept at -40°C.

Protein quantification with Bradford method

The amount of protein in a solution can be determined by colorimetric methods; in this case the Bradford method was used.

The Bradford assay is a protein determination method that involves the binding of Coomassie Brilliant Blue G-250 dye to proteins. The dye exists in three forms: cationic (red), neutral (green), and anionic (blue). Under acidic conditions, the dye is predominantly in the doubly protonated red cationic form (Amax = 470 nm).

However, when the dye binds to protein, it is converted to a stable unprotonated blue form (Amax = 595 nm). It is this blue protein-dye form that is detected at 595 nm in the assay using a spectrophotometer or microplate reader.

The comparison of the unknown protein sample with a standard curve (BSA protein standard, Bio-Rad) allows to calculate the concentration of the sample.

The solution Protein Assay Dye (Bio-Rad) was diluted 1:5 in water and then filtered with filter paper. The standard curve was prepared using different concentrations (20, 40, 80, 120, 140 mg / mL) of BSA (Bio-Rad protein standard) (see Table 2.2).

Thereafter, 250 uL of Dye and 5 uL of the standard protein diluition were placed in an eppendorf. This procedure was performed for each concentration of BSA.

Then, 200 uL of the solutions thus prepared were placed in a well of a 96-well microplate, and it was carried to the reading microplate reader at a wavelength of 595 nm. Finally, to measure the absorbance of the unknown sample, 5 uL of sample were added to 250 uL of Dye and 200 uL of this solution were put in a microplate and the reading was performed.

The O.D. values thus obtained were placed in a graph Excel in order to calculate the equation of the line to extrapolate the concentration of the samples.

BSA Concentration (mg/mL)	uL water	uL BSA
20	**47,86**	**7,14**
40	**35,72**	**14,28**
80	**21,44**	**28,56**
120	**7,2**	**42,8**
140	**/**	**5**

Tabel 2.2 : ***Amount of BSA and water to prepare the Standard curve*** **.**

Western Blotting

The western blotting is a rather sensitive method to detect expression levels of a specific protein. This method allows to identify proteins of interest based on the specific antigen-antibody recognition.

The procedure takes place in three steps: i) protein cell lysate solubilization and separation by electrophoresis on SDS-PAGE; ii) quantity and irreversible transfer to nitrocellulose membranes, ii) detection of the protein of interest immobilized by the use of a specific antibody.

Electrophoretic migration of protein

Proteins extracted from the cells and quantified are separated by gel electrophoresis of poliacrylamide. The separation takes place under the influence of an electric field and in the presence of Sodium Dodecyl Sulfate (SDS), which binds the proteins by giving them a negatively charge. All this must be performed in conditions in which the proteins are completely dissociated into their individual polypeptide subunits, as the SDS binds denatured proteins.

The amount of SDS bound is independent of the polypeptide sequence, so that the density of negative charge becomes almost constant; thus it is proportional to the molecular

weight of the polypeptide. The SDS-polypeptide complexes migrate thus through the polyacrylamide gel in function of their size, regardless of their charge.

The polyacrylamide is a matrix formed by the polymerization of acrylamide with a monomer cross-linker such as N-N'-metilenebisacrilammide. The range of separation of polyacrylamide gels depends on the percentage of Acrylamide-N-N'-metilenebisacrilammide. The reaction is triggered by the addition of two catalysts; ammonium persulfate (APS) and TEMED (N, N, N'N'-tetramethylethylenediamine), and it occurs through catalysis of free radicals: the TEMED catalyzes the decomposition of persulfate ions to generate a free radical. During this reaction molecules of bisacrylamide are also incorporated, which allow two polymers of acrylamide to bind between them. This process form bridges of Acrylamidebisacrylamide which give to the gel the rigidity and tensile strength and forms pores through which the SDS-polypeptide complexes can migrate. For the electrophoretic run, it is necessary to prepare two poliacrilamide gels, different for pH and ionic strength: the first one is used to separate proteins (*Gel Running*, pH 8.8) and it is prepared with a proportion of Acrylamide-N-N'-metylenebisacrilammide chosen in function of the molecular weight of the protein to be analysed (low percentage to protein with high PM, and vice versa), the second gel (*Stacking gel*, pH 6.8), placed above the first, allows to concentrate the proteins deposited in the well in such a way that they arrive at the running gel below as a linear front, and it is used as a mixture containing 3.5% of Acrylamide-N-N'-metilenebisacrilammide. The two gels were prepared following the Table 2.3 and Table 2.4; usually, the Running gel was used at percentage of 7,5 % or 10 % of Acrilammide (Bio-Rad). The two gels are prepared in two separate containers, without adding APS and TEMED. The Run chamber (Bio-Rad) is set up and then the two catalysts are added at to the Running gel. This is poured between the two glasses, leaving a space of about a centimetre in the upper part that will be filled with water to equalize the front of the gel, which will be removed once the polymerization of the gel has occured. When the Running gel has polymerized, the stacking gel is prepared and added in to the upper part of the gel. Than a pecten is added between two glasses which will be used to form the gel wells where the samples will be loaded.Once the gel is polymerized you can proceed with the preparation of samples or the gel may be kept for a night at 4°C.

Gel Percentage	**6,5%**	**7,0%**	**7,5%**	**10,00%**	**12,00%**
Acrylamide	4,6 mL	4,37 mL	4,7 mL	6,3 mL	7,5 mL
Tris HCl 1,5M pH 8,8	6,25 mL	6,25 mL	6,25 mL	6,25 mL	6,25 mL
Water deionized	14,32 mL	14 mL	13,68 mL	12,12 mL	10,9 mL
SDS 10%	250ul	250ul	250ul	250ul	250ul
APS	125ul	125ul	125ul	125ul	125ul
TEMED	12,5ul	12,5ul	12,5ul	12,5ul	12,5ul

Table 2.3: ***Amounts and reagent for the preparation of the Running Gel***

Acrylamide	1,25 mL
Tris HCl 0,5M pH6,8	3,15 mL
Water deionized	7,96 mL
SDS	125ul
APS	62,5ul
TEMED	12,5ul

Table 2.4 : ***Amounts and reagent for the preparation of the Stacking Gel***

Protein samples are thawed slowly, in ice, and aliquoted into eppendorf in order to achieve the desired concentration (e.g. 20ug): the final volume of the sample is chosen, so that the volume is equal for all. The volume of proteic lysate, which serve to obtain the concentration necessary for the preparation of the samples, are calculated and the final volume is reached by adding RIPA Buffer.

In addition, Loading Dye (6X) is added to the sample, which serves to precipitate the proteins, to help the loading and for follow the electrophoretic run. If the reducing conditions are required, the beta-mercapto-ethanol must also be added (2.5% of the final volume).

Once that the samples are prepared, these are placed in a thermal cycler at 98°C for 5 minutes and then immersed in ice; this process denatures the proteins. Finally, the samples are spinned down.

The running room (Bio-Rad) is filled with Running Buffer 1% (1L of Running buffer 10%: 30.3g Tris – Sigma, 144.2 g of glycine – Bio-Rad, 10.0 g of SDS- Bio-rad, all brought to volume with distilled water), which is important to allow the electrophoretic run. The samples are inserted in the corresponding well and, also, 3 uL of Marker (solution containing a mixture of polypeptides with known PM) (Bio-Rad) are loaded which will serve to estimate the molecular weight of the polypeptide chain of interest.
The electrophoretic run was performed at 100-120V using the Power Pac 3000 tool (Bio-Rad) as long as the proteins reach the bottom of the gel (usually an hour).

Transfer of proteins from polyacrylamide gel to a nitrocellulose membrane

At the end of the electrophoretic run, proteins which have been separated according to their molecular weight, are transferred from the gel onto a solid support, a nitrocellulose membrane.
The gel is placed in contact with three 3 sheets of paper soaked in Transfer Buffer (192 mM Glycine -Bio-Rad, 25 mM Trizma base - Sigma, 20% methanol and water).
Successively, the nitrocellulose membrane (Bio-Rad) is, also, soaked in Transfer buffer and placed over the gel and another 3 sheets of wet paper are added to the upper the membrane. The sandwich thus formed is closed between two porous sponges and tight in a plastic holder (Bio-Rad). The whole thing is placed in the transfer chamber having care that the gel containing the proteins negatively charged, is on the side of the cathode, while the membrane, portion toward which the protine must migrate, is facing towards the anode **(**Figure 2.5). The transfer chamber is filled with cold transfer buffer . The transfer can be done over-night at 4°C at 15V or overday in ice at 100V for 1h.

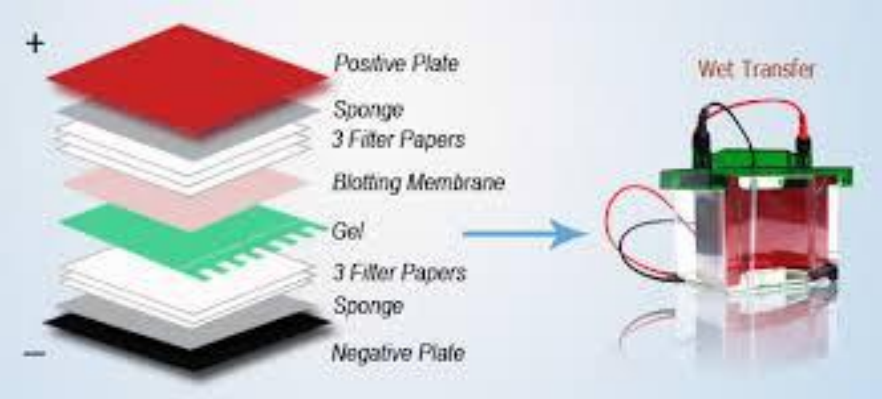

Figure 2.5: Preparation of the sandwich for transfer of proteins from gel to nitrocellulose membrane. *The sandwich was performed placing the gel in contact with three 3 sheets of paper, the nitrocellulose membrane and, above this, other 3 sheets of paper, each soaked in Transfer Buffer. This sandwich is closed between two porous sponges and tight in a plastic holder. The whole thing is placed in the transfer chamber having care that the gel containing the proteins negatively charged, is on the side of the tool cathode, while the membrane, portion toward which the proteins must migrate, is facing towards the anode. The transfer chamber is filled with cold transfer buffer and the transfer can be done over-night at 4°C at 15V or in ice at 100V for 1h.*

Incubation of the nitrocellulose membrane with primary antibody and secondary antibody

Once the transfer is finished, the sandwich is disassembled and the nitrocellulose membrane is immersed in a solution of Red Ponceau (0.2 g Red Ponceau in 100 mL of trichlor acetic acid 7.5%). The Red Ponceau solution is able to color temporarily attached proteins on the membrane. This step is useful for checking whether the transfer has occurred in an appropriate manner.

Subsequently, the membrane is incubated with a Blocking Solution (Blotting Grade Blocker Milk - Bio Rad) to 5% in a solution of PBS-Tween (Tween 0,05%, PBS 1X) for 2 hours under stirring. This step serves to block nonspecific antibody binding sites present on the nitrocellulose membrane.

After that, the membranes are incubated overnight at 4°C with primary antibody: human mAb anti-p75NTR (1:1.000; Upstate, Lake Placid, NY) and human mAb anti-b-actin (1:5,000; Sigma-Aldrich).

After having washed the membrane in PBS-Tween (Tween 0,05%, PBS 1X) (15 minutes wash followed by three subsequent washes of 5 minutes each), the membranes are incubated for 45 minutes at room temperature with the following peroxidase-conjugated secondary antibodies goat anti-mouse (1: 3,000; Bio-Rad, Hercules, CA).

Detection of target proteins with ECL chemoluminescent detection system

Membranes are washed in PBS-Tween (20 minutes wash, followed by four subsequent washes of 5 minutes each) and developed using the ECL chemiluminescent detection system (Amersham Biosciences UK Limited, Little Chalfont, Buckinghamshire, England) in obscure room.

This method of detection provides a high sensitivity for chemiluminescent detection of immobilized specific antigens conjugated to Horseradish Peroxidase (HRP) labeled antibodies. Chemiluminescence is defined as light emission produced in a multi-step reaction whereby peroxidase catalyzes the oxidation of luminol.

In the presence of chemical enhancers and catalysts, the light intensity and the duration of light emission is greatly increased in a process known as enhanced chemiluminescence (ECL). ECL based on horseradish peroxidase (HRP)- conjugated secondary antibodies is a sensitive detection method where the light emission is proportional to protein quantity (Figure 2.6).

The membranes were covered with ECL solution, obtained by mixing the solution A and the solution B of the Amersham Biosciences kit (GE Healthcare Bio-Science AB, Sweden), and were incubated for 5 minutes. Subsequently on each membrane was placed a photographic plate in the dark.

The proteins of interest (linked to primary antibody and secondary antibody conjugated with peroxidase) are detectable because of an emission of signal that is impressed on the plate. After an exposure time, which varies depending on the protein to be detected, the photographic plate is developed using a developing solution (Kodak - dil 1:5 in water) and a fixative solution (Kodak -dil 1: in water).

The marker is taken as reference to obtain the molecular weight of the protein detected.

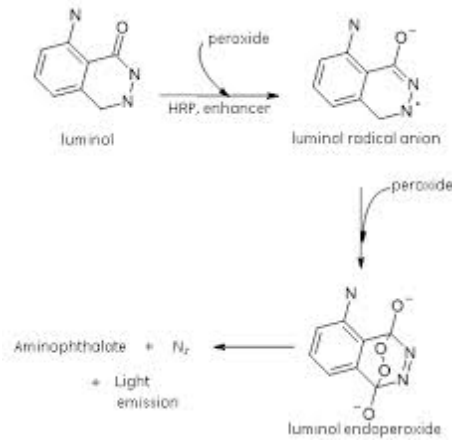

Figure 2.6: Multi-step reaction performed by peroxidase enzyme in the Enhanced Chemimuminescence (ECL) method. The ECL solution is composed by horseradish peroxidase (HRP)-conjugated secondary antibodies. The peroxidase catalyzes the oxidation of luminol which emits light.

Skin equivalents

Skin equivalents are a model used to study the interactions between melanocytes-keratinocytes and melanoma cells. This three-dimensional reconstruction of the skin is a tool which allows to evaluate the behaviour of the tumor in an environment that most closely approximates the in vivo situation.

The skin equivalent was been made using the tissue culture inserts namely Corning Costar Transwell Supports (Biocompare, South San Francisco, CA, USA) on which are inserted a cell-free solution and, subsequently, a cell solution; together these will constitute the dermis. Furthermore, a solution consisting of keratinocytes and melanoma cells is added, which will constitute the epidermis with melanoma.

The Corning Costar Transwell Supports were first made equilibrate with HBSS or DMEM (Lonza) at 37°C 5% CO2 for 30 minutes. Meanwhile, the cell-free solution was prepared; for 6 skin equivalent were used (working in ice): 0,3 ml of DMEM 10X, 25 ul of L-Glutamine 200 nM, 0,3ml of FBS 10%, 60 ul sodium bicarbonate 7,5%, 2,3 ml of

type I rat collagen (was extracted following the protocol from Rajan et al., 2006) and penicillin / streptomycin 1%.

Then, the medium from transwell was aspirated and 0.5 mL of cell-free solution is added on each support. This solution was allowed to polimeryzed at room temperature for at least 30 minutes: the solution should turn from straw-yellow to pink.

Subsequently, the cell solution was prepared: fibroblasts (obtained from human skin biopsies; passage P6 or P7) were detached with trypsin 0,5 / EDTA 0,02 and were counted with a Burker chamber. About 150.000 fibroblasts/skin equivalent were re-suspended in 0.5 mL of medium (DMEM with 10% FBS and 1% penicillin / streptomycin). In a tube were added (on ice) 0,55 ml of DMEM 10X, 50 ul L-glutamine 200nM, 0,616 ml of FBS 10%, 0,116 of sodium bicarbonate 7,5%, 4,6 ml of collagen I and the cell suspension of fibroblasts.

This solution was well resuspended without forming bubbles and 1mL of this solution was added to each filter. Everything is allowed to polimeryze at 37°C 5% CO2 for 45 minutes (the solution should turn from straw-yellow to pink).

Finally, the medium (DMEM with 10% FBS and 1% penicillin /streptomicin) is added both above and below dermis and left at 37°C 5% CO2 for 4 days.

After that time, the medium present above and below dermis is deleted, and 2 mL of HBSS (Lonza) are added and left for 1 hour at 37 ⁻C 5% CO2.

Meanwhile, the epidermis solutions with melanoma cells was prepared: the keratinocytes are detached with trypsin 0.5 / EDTA 0.02 and were re-suspended at a concentration of 350,000 cells for skin equivalent in Medium I (for 100 m : 72,5 mL DMEM, 24 mL of HAM'S F12, 2mL of L-Glutamine 200nM, 200ul Hydrocortisone 269g/ml (Sigma), 200 ul of ITES 500X, 200 ul of Ophosphotylethanolammina 0.05 M, 200 ul of adenine 90mm, 200 ul of progesterone 2nm, 1,2 ml of CaCl2 200 nM, 200 ul of Triiodrithyronine 10 nM, 100 ul of chelexed newborncalf serum and 1% P/ S).

Subsequently melanoma cells were tryspinized (0.5 trypsin / EDTA 0.002) and about 100,000 cell / skin (at ratio of 1 melanoma cell to 3.5 keratinocytes) were re-suspended in medium I. The washing medium over the dermis is deleted. Keratinocytes and melanoma cells are combined and resuspended in a volume of 50ul / skin. This solution is then added above the dermis and the plate was left for 10 minutes at room temperature and,

after, the plate is placed at 37 ⁻C 5% CO2 for 30 minutes. Finally, the Medium I is added above and below the filters and it was left in the incubator for 2 days. After 2 days, the medium was replaced with Medium II (for 100 mL: 72,5 ml of DMEM 10X, 24 ml of HAM'S F12, 2 ml of L-Glutamine 200 nM, 200 ul of Hydrocortisone 296g/ml, 200 ul ITES 500X, 200 ul of Ophosphotyethanolamina 0.05 M, 200 ul of adenine 90mm, 200 ul of progesterone 2nm, 1,2 ml of CaCl2, 200 nM, 200 ul of Triidothyronine 10 nM, 100 ul of newborn serum self an 1% P / S) for another 2 days.

After this period, the medium II is discarted and the Medium III (for 100 ml: 47,5 ml of DMEM, 47,5 ml of HAM'S F12, 2 ml of L-Glutamine 200 nM, 200 ul of Hydrocortisone 296g/ml, 200 ul of ITES 500X, 320 ul of adenine 90mm, 1,2 ml of CaCl2 200 nM, 200 ul of Triidothyronine 10 nM , 2 ml of newborn serum self and P / S 1%) is added below the dermis and changed every 2-3 days. After 6 days skin equivalent were paraffin embedded to obtain tissue slices.

After 6 or 12 days, the medium under the filters is removed. Skin equivalents were fixed with 1 mL of 4% buffered formalin (4% in PBS), under a chemical hood, 1 mL of 4% buffered formalin for 2 hours and then washed with HBSS.

One proceeds with the dehydration of the skin equivalent. In this process the alcohol replaces the water present in the piece of tissue. It is performed through a series of incubations with a concentrations decreasing solutions of ethanol (EtOH: 35%, 50%, 70%, 95%, each for 10 minutes) and, finally, with 100% ethanol for 20 minutes.

Subsequently, the skin equivalent is placed in Xylene for about 15 minutes to clarify the skin (it must be transparent). After that, the skin is put in liquid paraffin (1 hour for two times) and, finally, the skin is placed on a support in a vertical position and the liquid paraffin is poured and it allowed to solidify at room temperature.

In this study, skin equivalents were used to assess the spread of different melanoma cell lines within the layers of the skin after 6 days. Furthermore, we evaluated the expression of S-100 protein and p75NTR through a immunohistochemical detection.

Hematoxylin and eosin staining

Hematoxylin and Eosin (H&E) is performed to have an overview of the success of the skin equivalent. In this precedure, cells nuclei and cytoplasm are stained. The slice is deparaffinized and rehydrated: an incubation at room temperature with Histoclear for 5 minutes (for 3 times) and one incubations with alcohol in descending concentration (100%, 70%) for 1 minute (for 3 times), and finally the slide is placed in water for 1 minute. Subsequently, the slice is immersed in a solution of hematoxylin for 1 minute, after that the slide is washed thoroughly with running water until all residues of hematoxylin have been removed.

Two other incubations in alcohol are performed (alcohol 75% and 95% for 1 minute each), and the slide is immersed in a solution of alcoholic eosin (Eosin Y, 20 mL distilled water, alcohol, 95 % alcohol and glacial acetic acid) for one minute.

Finally, some incubations in a solution of ethanol at increasing concentration are performed (75% for 20 second, 95% for 30 second and absolute for 1 minute) and the slide is left to air dry and it is sealed with cover glass using Eukitt (Bio- Optica).

Immunohistochemical detection in skin equivalents

Once the skin equivalents were prepared and they were embedded in paraffin, these should be cut with the microtome to observe under the microscope the behaviour of melanoma within the reconstructed skin and to detect the marker of interest.

3 consecutive slices of skin equivalent are cut with the microtome with a thickness of 4 um and each slice is placed on a slide and allowed to dry at 37°C over-night. The first one was used to perform H&E while the others were used for immunohistochemical detection of S-100 melanoma marker (HRP / AEC) and p75NTR (Fast Red) respectively.

For this aim, the slices must be deparaffinized, rehydrated, and unmasked. The deparaffinization and rehydration were performed with an incubation, in Histoclear for 10 minutes and a subsequently incubation, each for 10 minutes, in a series of alcohol a

decreasing concentrations (100%, 90%, 80%, 70%, 50%) and in distilled water for 20 minutes. The unmasking, which serves to release the epitopes to allow binding of the primary antibody, was performed with 1X citrate buffer for 20 minutes in a water bath heated to 98 °C and 20 minutes at room temperature.

The immunohistochemical detection for S100 was performed using the HRP kit UltraVision Plus Detection System Anti-Polyvalent, HRP / AEC (Thermo Fisher scientific Anatomical Pathology), which is constituted by a labeled streptavidin-biotin immunoenzymatic antigen system.

This technique involves, initially, several steps where the kit reagents are used in order to block non-specific sites. Later, an incubation with unconjugated primary antibody specific for the protein of interest is performed (we have used the anti- S100 dil 1:400; Dako). Subsequently other kit reagent were added: a biotinylated polyvalent secondary antibody, which reacts with the primary antibody, an enzyme-labeled streptavidin, which binds to biotin present on the secondary antibody, and the enzyme substrate (AEC).

The reaction between enzyme and its substrate form a cromogen which can be viewed under a microscopy (the time of incubation are reported on the datasheet of the kit). The detection of p75NTR was performed using the Fast Red kit UltraVision LP Detection System AP Polymer & Fast Red Chromogen (Thermo Fisher scientific Anatomical Pathology), which detects a specific mouse IgG or rabbit IgG antibody linked to an antigen present in tissue sections.

Later to several steps where the kit reagents are used in order to block non-specific sites, an incubation with unconjugated primary antibody specific for the protein of interest is performed (anti-p75NTR, diluited 1:100, Neomarker). Subsequently, to detect the primary antibody bound at protein of interest, a secondary antibody conjugated to an enzyme-labeled polymer that recognize mouse and rabbit immunoglobulins, provided by the kit, is added. The polymer complex bound to p75NTR is then visualized at the optical microscopy with adding an appropriate substrate / chromogen (Fast Red tablet in Naphthol Phosphate Substrate), which is content in the kit. Both reactions are blocked in distilled water and counterstained with H&E. Finally, the slides are sealed with covers-lips using buffered glycerol and must be kept at 4°.

Confocal microscopy

The evaluation of protein-expression or membrane receptors within the multicellular spheroids with methods of immunohistochemistry, FC on individual cells or cytospin lack of comprehensive information due to the failure of the antibodies to penetrate completely inside the compact cancer spheres. These methods only allow a detection of the superficial cells of the spheroid unless it is made a serial sectioning in time.

Confocal microscopy allows to dissect the spheroids entire structure and also evaluate the inner levels. On each section is evaluated the expression of the protein of interest (in this case p75NTR) thanks to the use of fluorescent antibodies.

The spheroids in suspension were fixed with 4% PFA in PBS for 3 hours at 4°C and permeabilized in Triton X-100.

After 3 washing in PBS, the spheroids were dehydrated according to an ascending scale of methanol at 4°C in PBS (25%, 50%, 85% and 100% for 30 minutes to 5 hours). The spheroids were rehydrated using the same scale of methanol but in inverted order.

After 3 washings in PBS for ten minute each, the spheroids were blocked in PBS-tween (0.1% triton X-100 in PBS) plus 3% BSA at 4°C under agitation.

After 2 washing in PBS tween of 15 minutes each, the spheroids were incubated with primary antibody (anti-p75NTR, Neomarker 1:50 in PBST) and placed on a rotor at 4°C for 48h. Subsequently, spheroids were washed four times with PBS-tween (30 minutes each) and then incubated with fluorescent secondary antibody (Alexa Fluor 488) diluted in PBS-Triton on the rotor at 4°C for 24h. Finally, the nuclei were counter-stained with DAPI (4',6-diamidino-2-phenylindole) for 40 minutes at room temperature.

To mount the coverslip, the spheroids were resuspended in 15 ul of PBS and they were allowed to adhere on a glass slide. Subsequently, the excess PBS was removed and 15ul of glycerol at 90% were added. Finally, the coverslip was added using adhesive tape to create the space between the slide and the coverslip. Glass were stored at -20oC until microscopy analysis.

Cell sorting

The FACS ARIA III cell sorter was used to separate the cells subpopolations based on the expression of p75NTR in SKMEL28 cell line. In this way two different populations of cells were obtained: p75NTR bright and p75NTR dim.

SKMEL28 cells, cultured in 2D, were detached with trypsin 0.5 / EDTA 0.02 and counted with a Burker chamber. To perform the experiment we started from about 7,000,000 cells: 500,000 cells were used as a negative control in which no antibodies were added, 500,000 cells were used as a second negative control in which was added only secondary antibody, and the remaining 6,000,000 were divided into 3 samples from 2,000,000 cells each.

Cells were washed with PBS, centrifuged at 1200 rpm for 10 minutes and then re-suspended 500.000 cells in 100 ul of Blocking Buffer (1ml NaN3 0.1 M), 50ml DMEM 10% FBS, human gamma globulin 2g SIGMA G4386). They were incubated for 15 minutes at room temperature and, subsequently, the cells were washed with 1 ml of PBS- for 3 times and centrifuged at 1200 rpm for 5 minutes.

Then the cells were incubated with 100ul of sterile primary antibody antip75NTR (Dil. 1:50, Neomarker) in PBS / BSA 0.5% and they were left for 15 minutes at room temperature. After this time the cell suspension was washed with 1 ml of PBS, and centrifuged at 1200 rpm for 5 minutes. We then added 100ul of secondary antibody anti-mouse IgG - FITC (Alexa Fluor 488) (Dil. 1:50) in PBS / 0.5% BSA for 15 minutes at room temperature, in the dark.

Cells were washed in PBS, centrifuged at 1200rpm for 5 minutes, and 1 mL melanoma base medium was added. After that cells were filtered (70um) and the cell suspension was then centrifuged at 1200rpm for 5 minutes and 20 ul of 7AAD (7-Aminoactinomycin D), which serves to stain the DNA, were added on the dry pellet and they left to incubate for 15 minutes at room temperature, in the dark. The complete BME melanoma medium was added at the density of 1mL/106 cells and the whole was transferred to FACS tubes.

Finally the cells were sorted at the instrument FACS ARIA III and they were divided into two tubes: p75NTR negative cells and positive p75NTR cells.

The cells thus obtained were used for further experiments, such as: collagen invasion assay and MTT assay.

Melanoma cells transfection with siRNA

WM115 cells were transfected with siRNA p75NTR to assess whether the suppression of this receptor change the behaviour of the cells in terms of proliferation and invasion abilities.

Approximately 500,000 cells were seeded in two flask (control and treated) in BME medium (see above) without penicillin / streptomicin. 24 hours later, the cells were transfected with 100nM p75NTR siRNA (Dharmacon) for treated cells and scramble siRNA for control. In particular p75NTRsiRNA or scramble siRNA were combined to Lipofectamin 2000, diluited in Opti-MEM (both from Invitrogen Corporation, Carlsbad, CA), as suggested by datasheet. p75NTRsiRNA or scramble siRNA were added to cells in combination of BME melanoma medium without nor antibiotics and FBS, but with 0.1% BSA (BSA 5% without antibiotics). After one night the trasfection was repeated.

To verify that the trasfection was successful, WM115 melanoma cells transfected were lysed 48 hour later for detected analyzing p75NTR protein level by western blotting as described above. These cells were also used to form multicellular spheroids in order to verify their invasion and proliferation ability with a collagen invasion assay.

Melanoma cells infection

1205 Lu cells were infected with a vector containing p75NTR gene in order to assess whether the over-expression of this receptor change the behaviour of these cells in terms of proliferation and invasion abilities.

For this aim two packaging cell lines, LNSN mock (empty vector) and LNSN p75NTR, are used to recover the supernatants containing the viral vector.

Packaging cells were maintained in a medium composed by: DMEM, FBS 10%, L-glutamine 2% , penicillin/streptomicin 1%. In order to recover the supernatants to perform the infection, the medium of packaging cells was replaced with TU2% medium. After 4 hour the supernatans was recovered and filtered (0.45 um of diameter) and stored at -80°C.

Approximately 500,000 of 1205 Lu cells were seeded in two dish (control and infected) in TU 2% medium. 24 hours later, the medium are replaced with 3 ml of packaging cells supernatans, mock or p75NTR, with polybrene 4ug/ml. After one night the infection was repeated.

To verify that the infection was successful, 1205 Lu cells infected were lysed for detected analyzing p75NTR protein level by western blotting.

These cells were used to form multicellular spheroids in order to verify their proliferation ability with ImageJ analysis.

Immunohistochemical staining of spheroids in collagen I

The immunohistochemical detection on spheroids immersed in a matrix of collagen I was performed to detect p75NTR expression in order to characterized the invasive cells in spheroids composed by all melanoma cell lines.

Melanoma cells were seeded at density of 5000 cells / well in a 96-multiwell on coat of 1.5% agar to allow the formation of spheroids. After 72h the spheroids were placed in a matrix of type I collagen and were monitored over time.

At 48 h and 72 h, the collagen spheres were fixed in 4% buffered formalin for 30 minutes.

ubsequently, the button of collagen was removed from the wells, washed in PBS- and the immunohistochemical detection of p75NTR was performed (primary antibody anti-p75NTR dil 1:100 in PBS - Neomarker) with the Fast Red kit UltraVision LP Detection System AP Polymer & Fast Red Chromogen.

Subsequently, all p75NTR positive cells were counted by ImageJ program distinguishing between invasive and not invasive.

Analysis of spheroids with Image J software

In this project the area occupied by the spheroids of melanoma and the invasive capacity of cells was evaluated for all five melanoma cell lines and other melanoma cells subjected a different treatments. To this aim, cells were seeded on agar to form spheroids and subsequently they were inserted in a matrix of collagen type I. In order to analysing multicellular spheroids, calculating the area occupied and the invasive capacity of the cells, they were photographed with an optical microscope at different times (24, 48, 72, 120, 144 hours) both in suspension in agar and immersed in collagen. Subsequently, each image was analyzed with Image J program. To obtain an optimal analysis of the spheroids were defined specific culture conditions, of microscopic observation and image capturing.

To calculate total area and the area of invasion for each spheroids, the digital image was processed with Photoshop, brought to a resolution of 300 pixels / inch and converted to TIFF format. Thus, the image was opened with Image J program and it was converted to 8 bits in order to obtain it in black and white.

Subsequently, it was adjusted the application “threshold” which allows to obtain the area of interest such as a saturated zone of black in a uniform manner, in order to calculate both the total area and the area of invasion using the application “Analyze particle”.

To calculate the factor shape and the percentace of fragmentation were used, respectively, the following formulas: (perimeter) $2/4\pi$ (area) and (invasion area/ total area)*100.

For counting of invasive cells, instead, the image was opened with Photoshop and set with resolution to 500, 1000 and +30 contrast . With the tool "brush" the edge of the spheroid (the portion that appeared be more compact) was designed leaving outside the cells that invade the collagen. Subsequently, the image was analyzed with Image J and the invasive cells were counted using the command "Cell Counter" (Figure 2.7).

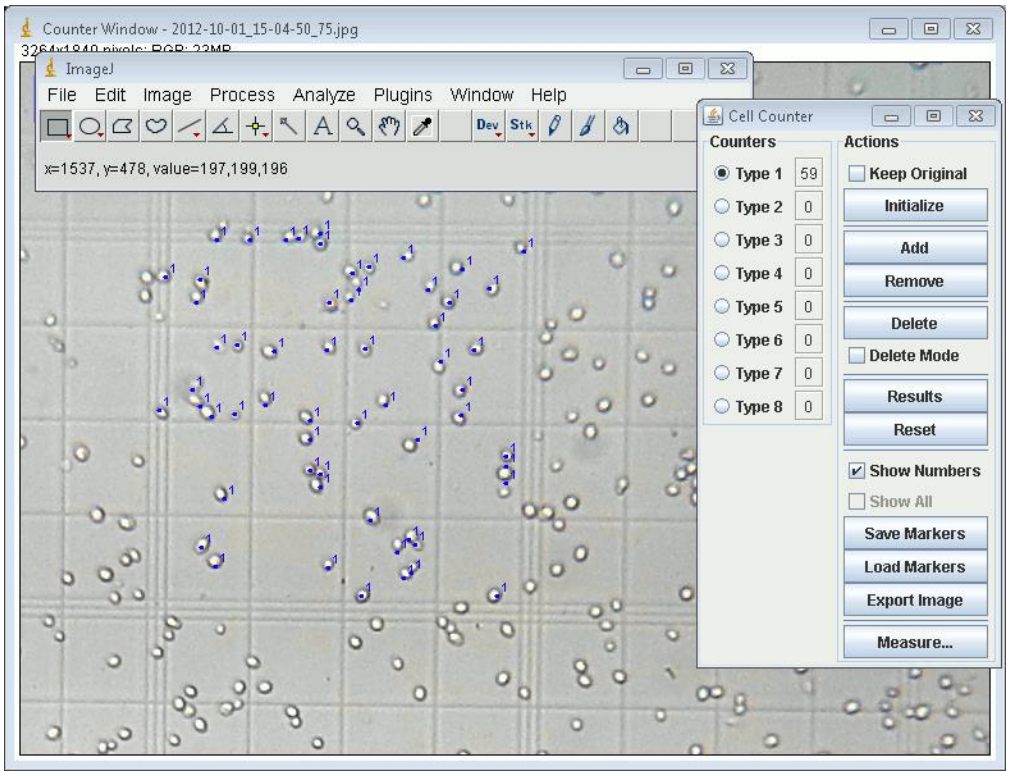

Figure 2.7: Representation of the screen ImageJ using the "Cell Counter"
The image was adjusted with Photoshop and set with resolution to 500, 1000 and +30 contrast and, with the tool "brush", the edge of the spheroid was designed. Subsequently, the image was opened with ImageJ in order to count invasive cells: selecting commands Plugin - Analyse - Cell counter, the application allows to select only one cell type and to be able to count the cells using the "click" of the mouse. The final number of cells counted there is shown in the working window.

Analysis of spheroids with Photoshop

This analysis was performed in order to detect the distance reached by cells migrated in type I collagen, by using all photos previously analyzed with Image J.

First, the measurement scale 1pixel = 50 microns was set. Then the image was opened with the Photoshop program and, with the instrument "Ruler", four measurements of the distance were made from the edge of the spheroid in the four directions, taking as reference the cell that in this area was longer far from the spheroid core (Figure 2.8).

From four values obtained for each image was made an average, which indicates the average distance reached by the cells in that picture.

This analysis was performed to evaluate invasion ability of all melanoma cell lines multicellular spheroids, SKMEL28 sorted cells and WM155 spheroids transfected with siRNA p75NTR.

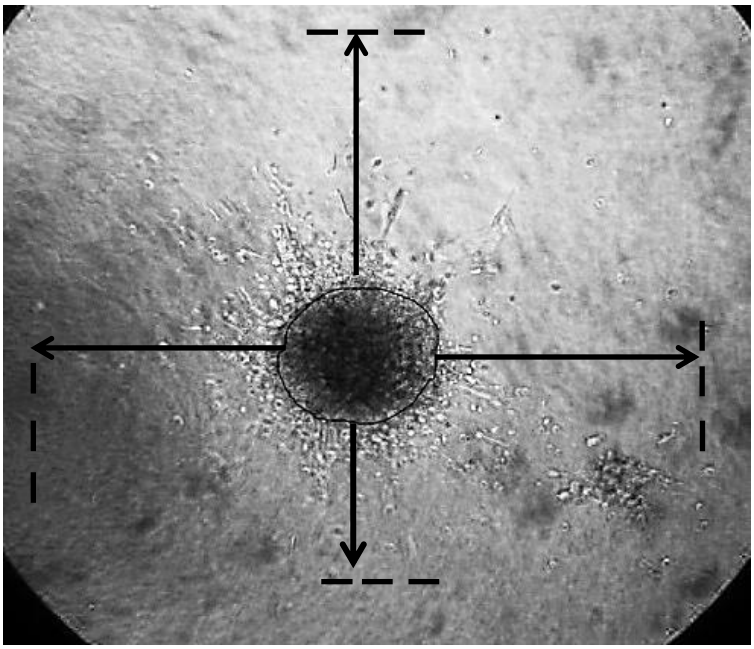

Figure 2.8 : Representation of the method utilized for the calculation of the distance of invasion of the cells from the spheroids in collagen type I. Four measurements of the distance were performed from the edge of the spheroidin the four directions, taking as reference the cell that in this area was longer far from the spheroid core. From four values obtained for each image was made an average, which indicates the average distance reached by the cells in that picture.

Statistical analysis

The results are calculated as the mean ± SD of three different experiments. Finally, a statistical analysis is performed with Student's T-test and are considered significant averages end with $p < 0.05$ or $p < 0.01$.

3. Aim of research

Melanoma, a malignant tumor of the pigment-producing melanocytes, is one of the most aggressive types of skin cancer. While cutaneous melanoma is curable with surgical excision in its earliest stages, metastatic melanomas are generally fatal due to their marked metastatic potential and resistance to current treatments. Hence, understanding the mechanisms behind the progression of melanoma is of extreme importance in order to find new therapies.

Neurotrophins (NTs) are a group of molecules that play a crucial role in neuronal cells, but also operate in skin where they take part in a complex network in which they stimulate both proliferation and apoptosis. The NT family exert their activities through two classes of transmembrane receptors: the high-affinity tyrosine kinase receptor Trks and the low-affinity neurotrophin receptor p75NTR. While Trks receptors promote mostly survival and differentiation, the role of p75NTR is ambiguous, as it can either act as a co-receptor for Trks enhancing their ability to promote survival, or signal on its own by inducing apoptosis.

Similarly to other growth factors, dysregulation of NTs signal transduction is found in a number of tumors where they contribute to malignant transformation. It has been shown from literature that NTs and their receptors appear to be important for melanoma cell migration, with special respect for metastatic cell lines. However, the role of p57NTR in melanoma is not yet entirely understood.

In professor Pincelli's laboratory it was previously established that the autocrine action of the neurotrophins is responsible of melanoma cells proliferation and migration (Truzzi et al., 2008). However, these experiments were carried out using the standard 2D monolayer cell cultures, which do not reflect the correct tumor micro-environment.

In the last few years, it has become increasingly apparent that cell survival and apoptosis, strongly depend on cell adhesion and the extracellular matrix.

In addition, it has also become clear that three-dimensional tumor models are able to mimic more closely the behavior of solid tumors in vivo representing a realistic experimental model to investigate many aspects of tumor biology such as drug resistance, growth and invasion abilities.

The aim of this research is to study p75NTR in melanoma, to investigate its role in progression and aggressiveness of the tumor using 3D models (multicellular spheroids and skin equivalent) that better reflect the tumor behavior and its microenvironment. For this purpose, we have optimized and validated 3D models in term of growth and invasion abilities using cell lines at different stage of progression. Secondly, we have studied the expression of p75NTR in this model and we have investigated the its role in melanoma progression and invasion.

4. Results

3D multicellular melanoma spheroids recapitulate proliferative capacities of their original cell lines

A fundamental aspect of a melanoma model is its ability to reproduce tumor growth in vitro. A good model for the study of melanoma progression should maintain peculiar features of primary and metastatic tumors (Kimberley AB et al., 2014). To evaluate whether the multicellular tumor spheroid (MCTS) model is able to reflect the growth properties of melanomas, we analyzed proliferation of spheroids obtained from five melanoma cell lines representing different stages of progression. Unlike the 2D cultures, in which all cells display similar morphologies, 3D spheroids show well distinct features (Figure 4.1A).

MCTS from primary (WM115) and metastatic (WM266-4) radial growth phase (RGP) melanomas show a circular and regular shape and present a more compact structure already to 24hours. On the contrary, the most aggressive primary (SKMEL28, WM793B) and metastatic (1205Lu) vertical growth phase (VGP) tumors are characterized by a less defined sphere denoting an ability of cells in remaining more independent from each other. This additional aspect could be related to a reduced cell-cell adhesion that could explain the increased susceptibility of the vertical growth phase cells to invade the dermis. Furthermore, VGP spheroids and WM266-4 spheroids show an increased size over time, while WM115 spheroids side was constant from 72hours onwards (Figure 4.1A). Peculiar trends of growth, reflecting the progression stage of the different tumor cell lines were also observed by MTT assay, while these differences were flattened in 2D model. In detail, WM115 spheroids don't proliferate in time, while the metastatic WM266-4 proliferate significantly more than its primary counterpart. SKMEL28, a high aggressive primary VGP tumor, show greater proliferative capacity in comparison to RGP spheroids. Finally, the most aggressive cell line 1205Lu, proliferated significantly more than its primary WM793-B counterpart and all other cell lines (Figure 4.1B).

The analysis of the cell cycle by flow-citometry allowed to calculate the proliferative peak of melanoma cells and revealed that, unlike 2D cultures, 3D spheroids reproduce the growth behavior of the tumor in vivo. As shown in Figure 4.1C, it's not visible a

proliferative peak in WM115 spheroids (as expected from a RGP primary tumor), while it is appreciable at 96 hours under adherent conditions. On the other hand, the other melanoma spheroids display a proliferative peak mostly to 48hours. On the contrary, SKMEL28 and WM793 don't show a proliferative peak in 2D model while it was observed at 72 hours for 1205Lu. The differences between the two models support the idea that multicellular spheroids better reproduce the behavior of melanoma in vivo, as they better reflect cells growth abilities in comparison to 2D cultures. Pictures of spheroids were taken up to 264 hours and they were analyzed by using Image J software (Figure 4.1D). We then calculated the area occupied by spheroids in time, expressed as number of pixel, thus allowing a quantification of their growth ability. The analysis revealed that the less aggressive cell lines failed to grow (WM115) or slightly grow (WM266 and WM793), while for the most aggressive ones (SKMel28 and 1205Lu) proliferation increased in a time-dependent manner ($p<0,01$), as shown in Figure 4.1E.

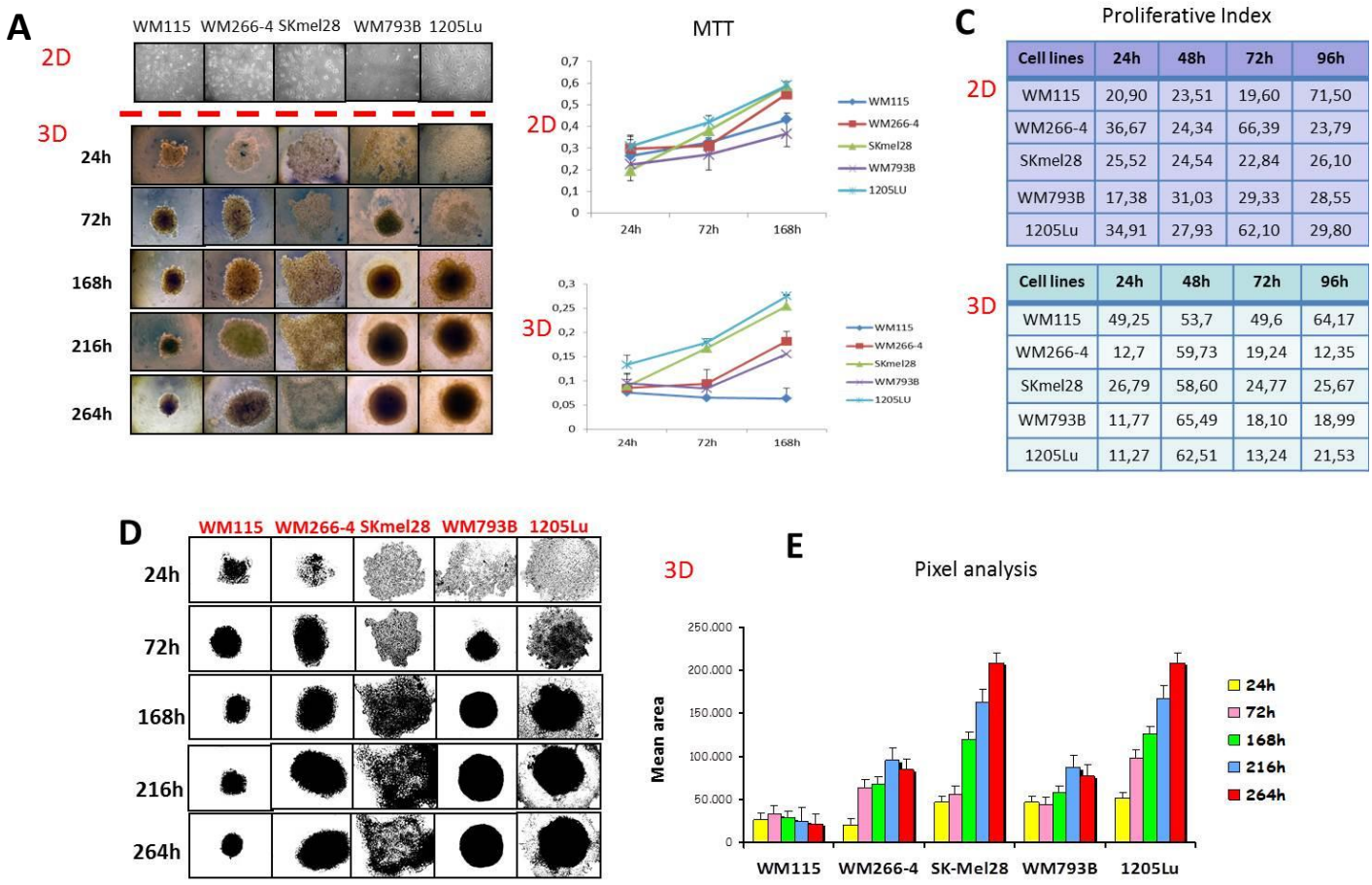

Cell lines	24h	48h	72h	96h
WM115	20,90	23,51	19,60	71,50
WM266-4	36,67	24,34	66,39	23,79
SKmel28	25,52	24,54	22,84	26,10
WM793B	17,38	31,03	29,33	28,55
1205Lu	34,91	27,93	62,10	29,80

Cell lines	24h	48h	72h	96h
WM115	49,25	53,7	49,6	64,17
WM266-4	12,7	59,73	19,24	12,35
SKmel28	26,79	58,60	24,77	25,67
WM793B	11,77	65,49	18,10	18,99
1205Lu	11,27	62,51	13,24	21,53

Figure 4.1 Evaluation of melanoma cell proliferation in 2D- and 3D-models.
Proliferative capacity of five melanoma cell lines was evaluated comparing 2D and 3D models. (A) Cells were cultured under adhesion conditions as 2D cultures (up), or in suspension as spheroids (down), as indicated in M&M. Pictures of 3D spheroids were taken at different time points (24, 72, 168, 216 and 264 hours). The proliferative capacity of cells cultured in 2D and in 3D (B) was evaluated by MTT assay. The values obtained were subtracted from the values of the background. The proliferative index was calculated in both 2D and 3D (C) through the analysis of different phases of cell cycle . D) Pictures of melanoma multicellular spheroids were taken at different times up to 120 hours after seeding and they were analyzed with Image J software; E) The area occupied by spheroids was calculated converting the pixels analysis of the pictures performed with Image J. Data represent the mean ± S.D. of triplicate determinations and T-Student was used for statistical analysis.

3D multicellular melanoma spheroids recapitulate invasion abilities of their original cell lines

The abilities of malignant tumor cells to bind and migrate through basement membranes are important steps in invasion and metastasis (Shoukat Dedhar and Ronald Saulnier, 1990). To study the invasive capacity of melanoma, multicellular spheroids were implanted, 72 hours after formation, into a matrix of collagen I which mimics the tumor microenvironment.

As shown in Figure 4.2A, all melanoma cells migrate from the central body of the sphere and the extent of invasion appear to correlate with the tumor stage.

Image J software was used to calculate: the total area occupied by spheroids and their invading cells, the factor shape and the percentage of fragmentation. The analysis of the area (Figure 4.2B) revealed that VGP cell lines (SKMEL28, WM793B and 1205Lu) invade collagen to a larger extent than the RGP spheroids (WM115 and WM266-4). Moreover, within the same tumor, metastatic cell lines (WM266-4 and 1205Lu) invade significantly more than their primary counterparts (WM115 and WM793B, respectively). In particular, the 1205Lu was the most invasive cell line, while WM115 showed the least invasive behavior ($p<0,01$).

Calculation of factor shape and percentage of fragmentation complete the analysis.

Factor shape is related to the shape of spheroids. It is close to 1 when the spheroid is a perfect circle while its value increases when cells begin to invade the microenvironment and the sphere lose the circular shape. The percentage of fragmentation is calculated as the percentage of cells released from the total spheroids area. High values of this parameter are then correlated with greater invasive capacities. In detail, for all time points analyzed, WM115 displayed the lowest values while 1205Lu the highest ones with a maximum value of 210,98 to 72 hours (Figure 4.2C).

The number of invading cells (Figure 4.2D) was significantly higher in 1205Lu than in WM115 cells ($p<0,01$) confirming previous results.

Finally, by using Photoshop, we calculated the average distance reached by the invasive cells considering the cells migrated in the directions of the 4 cardinal points (figure 4.2

E). 1205Lu cells were able to reach greater invasion distances if compared to the other melanoma cell lines ($p<0,01$).

From this first set of experiments we concluded that in terms of growth and invasion, the 3D spheroids reflect the behavior of the tumor from which are derived.

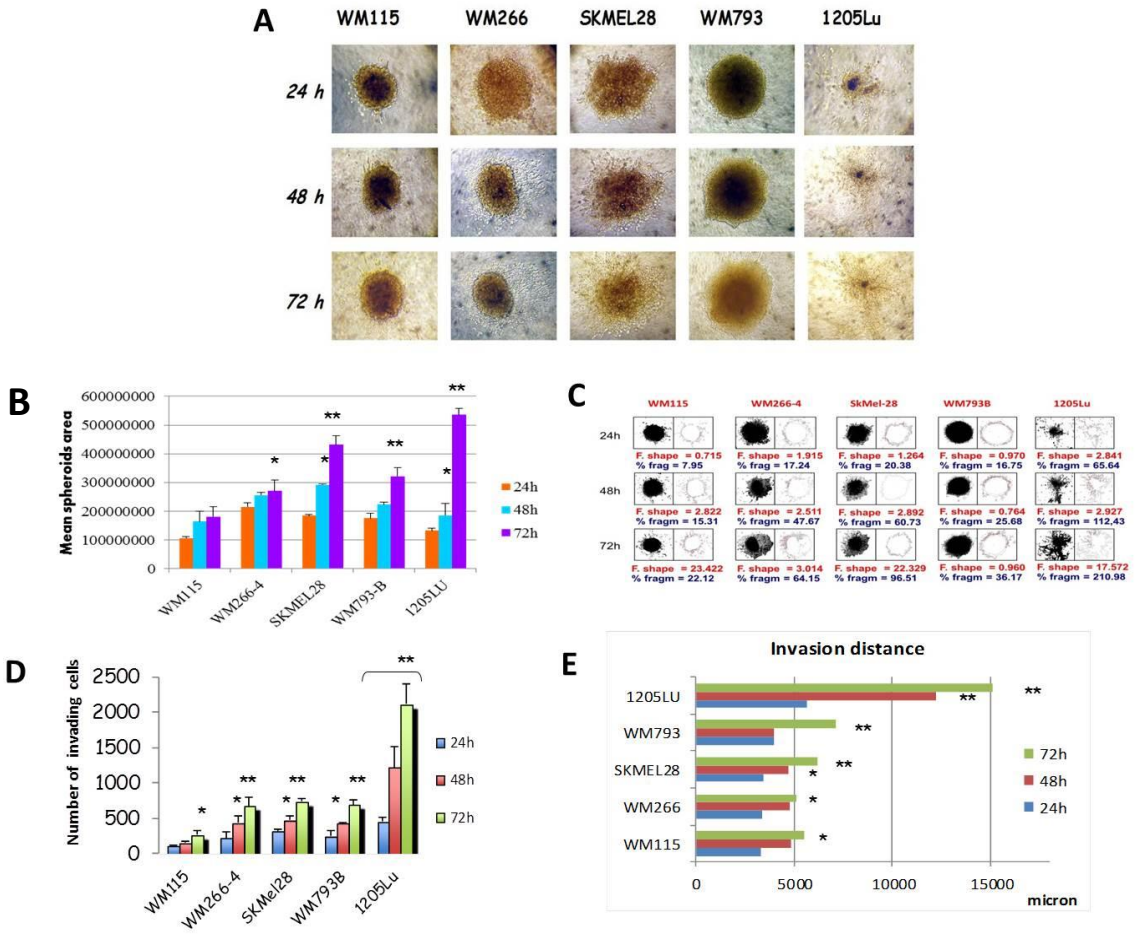

Figure 4.2 Analysis of multicellular spheroids invasive abilities in collagen I matrix
A) Spheroids derived from all melanoma cell lines were implanted into a matrix of collagen I and they were followed and photographed up to 72 hours. B) Pixel analysis of the pictures was performed with ImageJ, as described in M&M section and total area occupied was calculated. C) The factor shape (in red) and the percentage of fragmentation (in blue) were calculate, as described in M&M. In figure this value and the pictures processed by ImageJ program are reported. D) Total number of invading cells were counted by using "Cell Counter" application (ImageJ). E) The distances reached by the cells in collagen I was evaluated by Photoshop considering the cells migrated in the directions of the four cardinal points, as described in M&M section. The average distance was calculated and the number of pixel were converted into micron. All data represent the mean ± S.D. of triplicate determinations and T-Student was used for statistical analysis.

Spheroids derived from metastatic WM266-4 cells are more resistant to cisplatin induced apoptosis in comparison to primary WM115 cells

The potential of spheroids to contribute to either the elimination of poor drug candidates at the pre-animal and pre-clinical state or the identification of promising drug that would fail in classical 2D cell assays is increasingly recognized (Franziska Hirschhaeuser et al., 2010). After the validation of the 3D spheroid model in normal conditions, we chose two melanoma cell lines (of primary and metastatic origin), to assess whether this model was able to reproduce the behavior of melanoma following treatment with standard chemotherapy. To assess the pharmacological response we compared the behavior of 3D spheroids with the well-known 2D cultures (Figure 4.3A).

The proliferative capacity in the presence or absence of cisplatin was evaluated by MTT assay (Figure 4.3B). A proliferative block induced by treatment with cisplatin was observed in both primary WM115 and metastatic WM266-4 cell lines. No difference was found between 2D and 3D models. However, comparing the curves of "3D diluent" and "2D diluent" in both cell lines, we observe a decrease in proliferation after treatment much more pronounced and irregular in 2D compared to those observed in 3D. We hypothesized that in the initial stages the treatment is less effective in arresting proliferation of cells in the 3D model. We also calculated the area occupied by spheroids in time, expressed as number of pixel and we observed a reduction in the area occupied by the spheres after treatment in both cell lines (Figures 4.3C and 4.3D).

The analysis of the cell cycle by flow-citometry (Figure 4.3 E) revealed an increased apoptosis following treatment in WM115 spheroids especially at 96 hours, while the 2D model instead, despite having a strong block in proliferation, is less susceptible to apoptosis (p value $< 0,01$). The same assay performed in the metastatic WM266 cell line demonstrated that 2D cultures undergo apoptosis at 96 hours from treatment (p value $< 0,01$) while 3D spheroids are more resistant. The analysis shows that in 3D model the primary tumor respond to treatment with a significant increase in apoptosis while the metastatic counterpart is more resistant. In 2D model the opposite occurs, with a significant increase of apoptosis in the metastatic cell line and no effects in the primary

tumor. Since it is known from literature that metastatic melanomas are more aggressive and resistant to chemotherapy in comparison to their primary tumors, we concluded that the 3D model better reflects the pharmacological response to treatment.

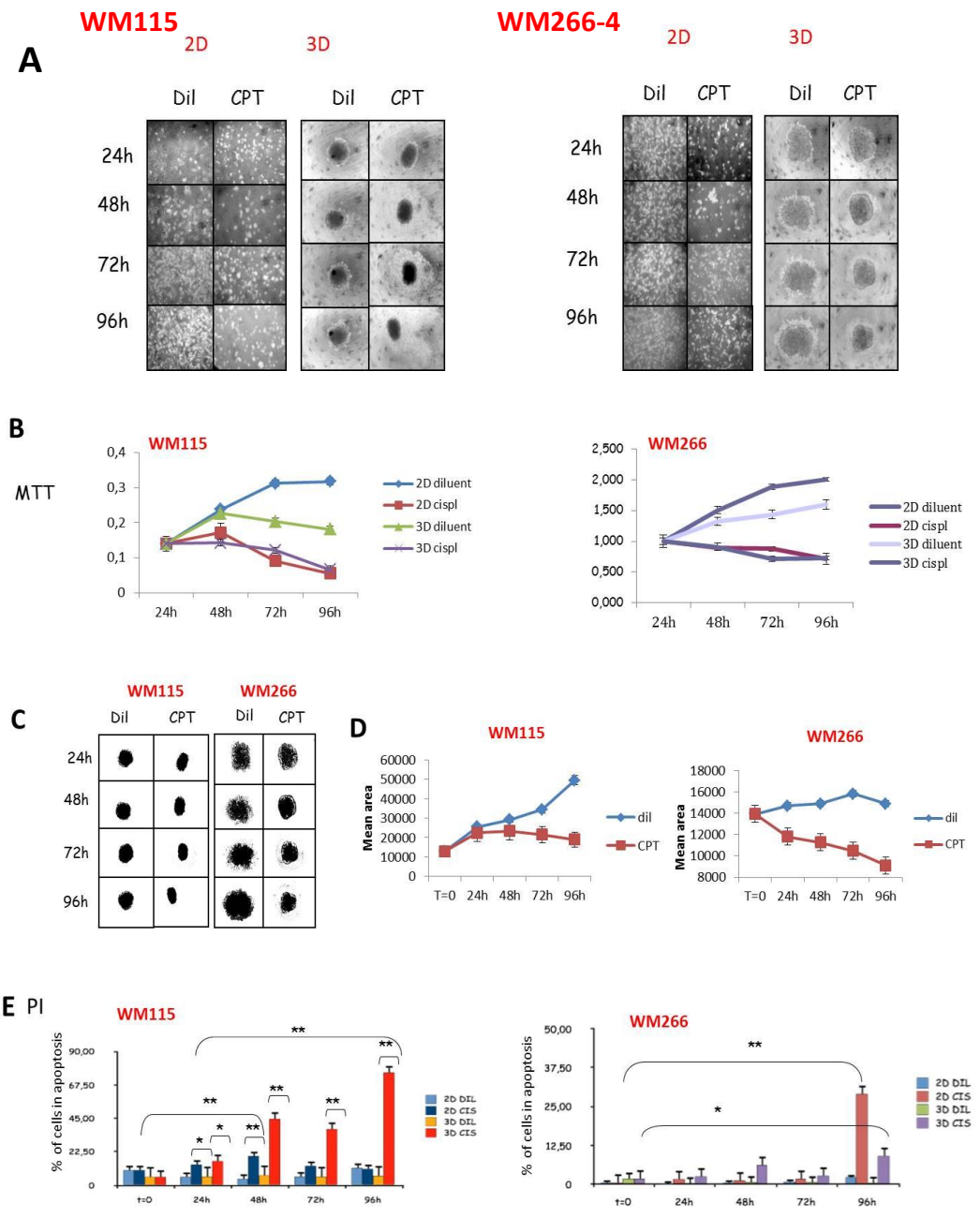

Figure 4.3Effect of Cisplatin on the aggressiveness of the melanoma cell lines

(A) 5000 cells derived from WM115 and WM266 -4 cell lines were seeded in 2D and 3D model in 96-well multiwell . B) To assess cell proliferation MTT assay was performed in both models at 24, 48 and 72 hours from treatment, C) 3D spheroids derived from both cell lines were photographed at different time points (24, 48 , 72 and 96 hours from treatment) and the total area was calculated by using Image J (D). E) Different phases of the cell cycle were evaluated by FACS 72 hours after treatment .

The invasion abilities after treatment with cisplatin are much more reduced in WM115 spheroids in comparison to metastatic WM266-4 spheroids

3D melanoma spheroids implanted into a collagen gel matrix mirror the in vivo tumor architecture and microenvironment more closely than adherent cell culture. Thus, this model can be utilized to study both drug efficacy and bioavailability (Franziska Hirschhaeuser et al., 2010)

After evaluating the proliferative response of melanoma 3D spheroids to cisplatin , we treated cells to evaluate if the drug could also affect their invasion ability.

Analysis of the pixels with Image J software (Figures 4.4A and 4.4B) revealed a reduction, with both doses of drug, in the invasion area of WM115 and WM266-4 spheroids especially at 72 hours (Figures 4.4C and 4.4D).

We also observed a significantly reduction of the factor shape after treatment with cisplatin in WM115 spheroids (Figure 4.4E), which is indicative of a reduced release of cells from the central body of the sphere (p value < 0,01).

The same was observed for the metastatic WM266 cell line with a lowering in the factor shape, although less evident than its primary counterpart, indicating a greater resistance to chemotherapy (Figure 4.4F). From our results we concluded that 3D spheroid model reflect the response to drugs of the in vivo tumors.

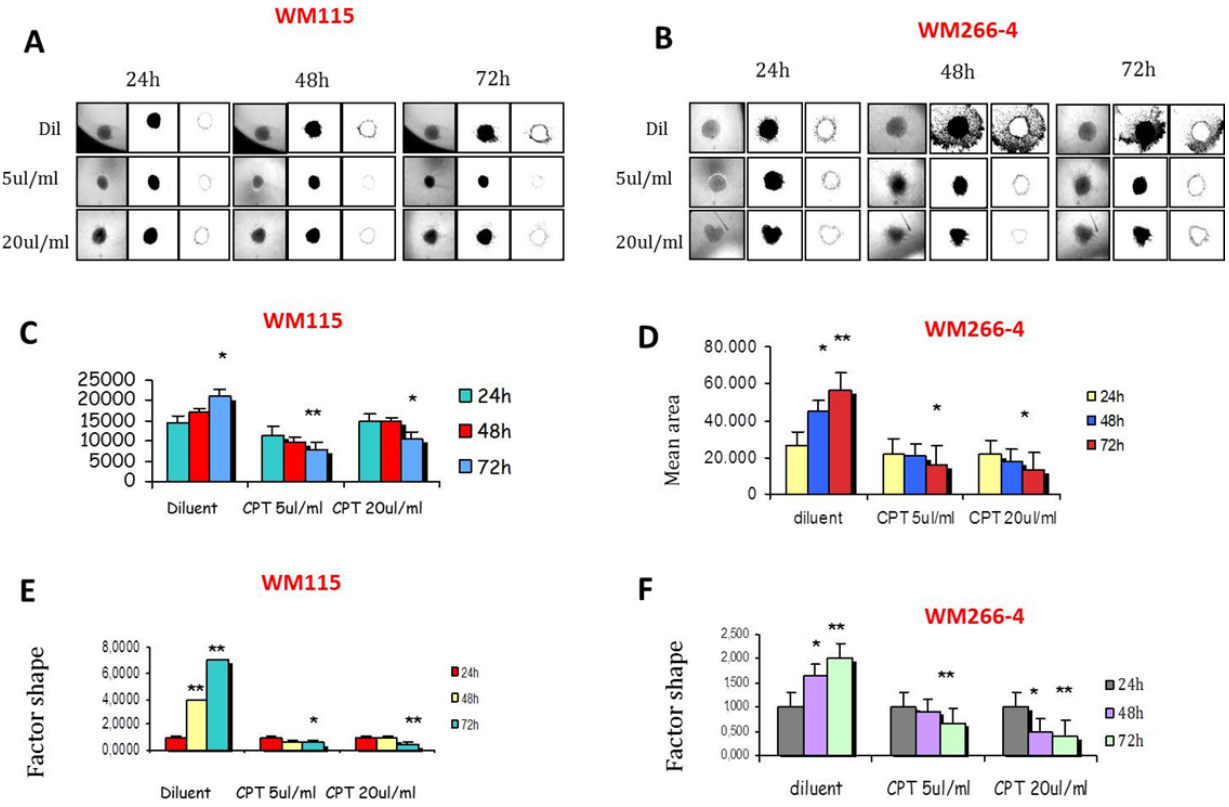

Figure 4.4: Evaluation of cisplatin effects on melanoma invasiveness

Spheroids obtained from WM115 and WM266-4 cell lines were transferred into a matrix of collagen I and were treated with two different doses of cisplatin (5ul/ml, 20ul/ml). (A, B) Spheroids were photographed 24, 48 and 72 hours from treatment and the total area occupied (C, D) and the factor shape (E, F) were calculated by using Image J.

Evaluation of neurotrophins receptors expression in 2D and 3D melanoma models

In our lab, we have previously demonstrated that melanoma cell lines synthesize and secrete all neurotrophins (NTs) and express both receptor's classes. Moreover, autocrine NTs are responsible for proliferation of melanoma cells (Truzzi et al, 2008). These results suggest that NTs and their receptors play a critical role in the progression of melanoma. However, melanoma cell lines used in this study, have been maintained as standard two-dimensional monolayer cultures.

For this reason, after having validated the 3D spheroid model in terms of proliferation, invasion and drug response we evaluated the expression of NTs receptors. As preliminary study, we analyzed over time the modulation of p75NTR and Trks receptors by Western Blotting comparing 2D- and 3D-cultures (Figure 4.5). As a first observation we noticed several differences , within the same cell line, in the expression level of neurotrophin receptors between 2D and 3D models. For example p75NTR was highly expressed in WM266-4 cultured under adherent conditions, while tended to disappear when cells were maintained as 3D spheroids.

Since we didn't observe significant differences within the five melanoma cell lines in Trks expression and given the emerging role of p75NTR in some tumors, we decided to focus on p75NTR.

Moreover, in our lab previously studies performed on paraffin section of melanoma biopsies revealed p75NTR was more expressed in poorly aggressive tumors (manuscript in preparation). Little is known about the role of p75NTR in melanoma. For this reason we proposed to study p75NTR function in melanoma progression.

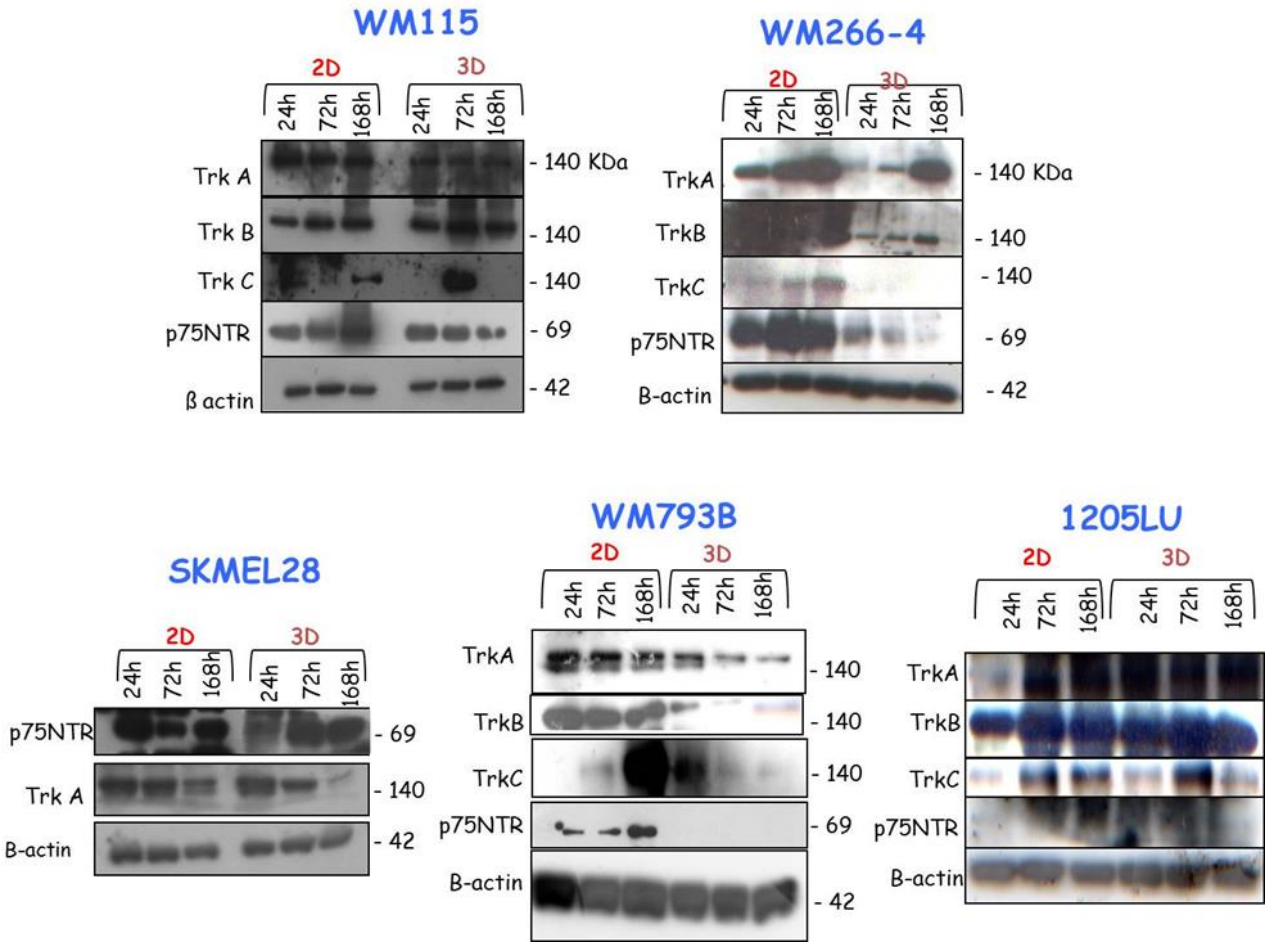

Figure 4.5 : Evaluation of p75NTR and Trk receptors in 2D and 3D melanoma models

P75NTR and Trk receptor expression level was evaluated by Western Blotting in all melanoma cell lines comparing 2D and 3D models. In particular proteins were studied at different time points (24h, 72h and 168h)

P75NTR is differentially expressed in 2D and 3D melanoma models

We evaluated the expression of p75NTR by FACS analysis in all melanoma cell lines in 2D and 3D cultures (Figure 4.6A). Discrepancies between the 2 models were detected, indicating that p75NTR expression is influenced by the culture method.

In detail, differences in p75NTR levels were flattened in 2D models with a similar expression in WM115 (89,97%), WM266-4 (99,67%), SKMEL28 (91,77%), and WM793B (98,22%) and a reduced expression in 1205Lu (21,33%) cell lines.

On the contrary, it was differentially expressed within the five melanoma cell lines in 3D model (Figure 4.6A): interestingly, p75NTR was found inversely correlated with progression of the tumor cell lines. In particular the advanced metastatic 1205Lu spheroids expressed the lowest level (47,99%), while primary RGP WM115 spheroids the highest one (97,3%).

To confirm the results obtained and understand whether p75NTR expression was influenced by the culture method, we repeated FACS analysis evaluating its expression in 2D, 3D and in cells obtained after having reseeded spheroids in a 2D system (Figure 4.6B). Differences in the expression of p75NTR were detected at 72hours in 2D and 3D models for all melanoma cell lines confirming the previous data. However, when spheroids were reeseded in a 2D system, the expression of p75NTR changed, getting closer to that observed in 2D cultures.

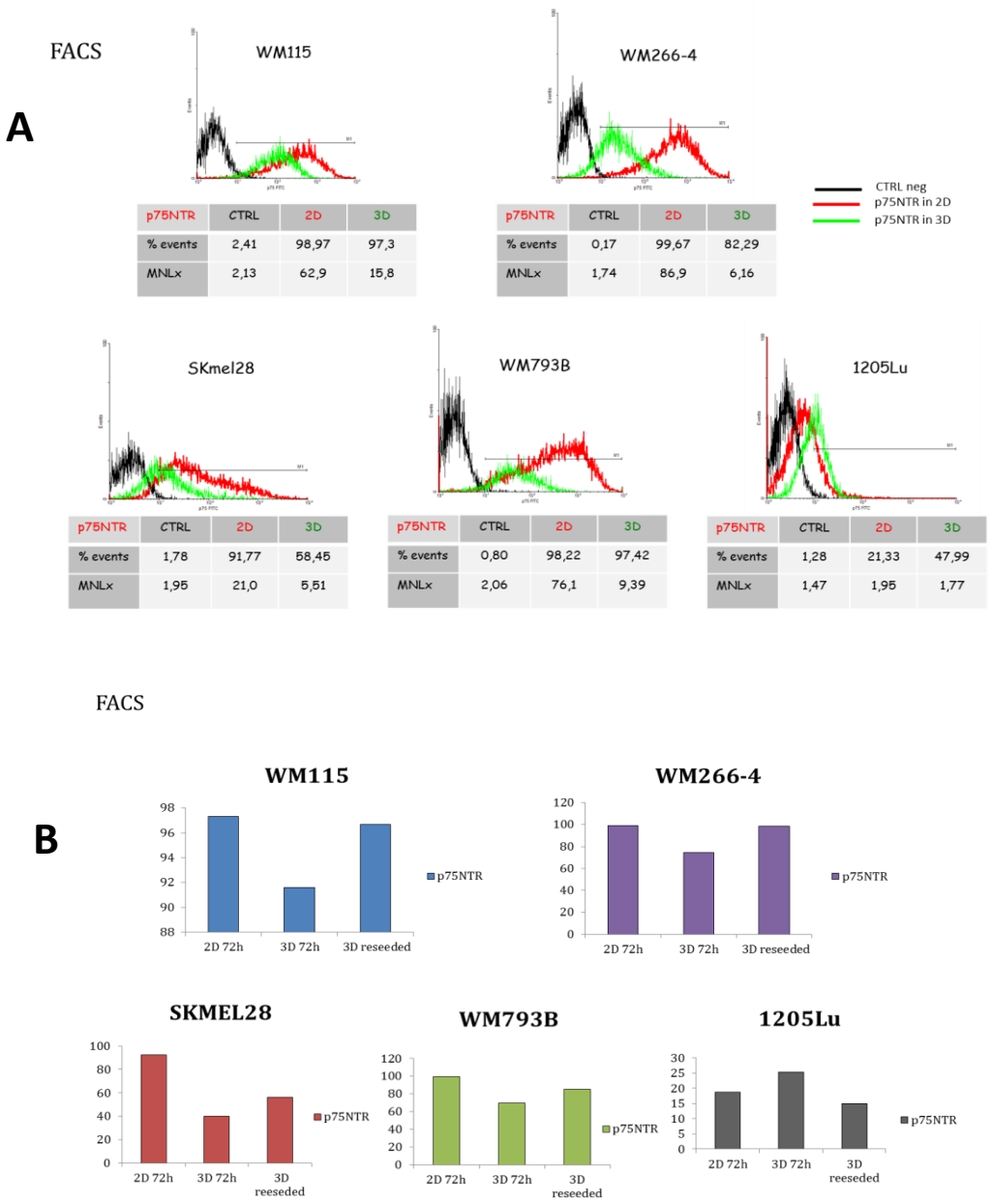

p75NTR	CTRL	2D	3D
% events	2,41	98,97	97,3
MNLx	2,13	62,9	15,8

p75NTR	CTRL	2D	3D
% events	0,17	99,67	82,29
MNLx	1,74	86,9	6,16

p75NTR	CTRL	2D	3D
% events	1,78	91,77	58,45
MNLx	1,95	21,0	5,51

p75NTR	CTRL	2D	3D
% events	0,80	98,22	97,42
MNLx	2,06	76,1	9,39

p75NTR	CTRL	2D	3D
% events	1,28	21,33	47,99
MNLx	1,47	1,95	1,77

Figure 4.6: P75NTR expression in melanoma cell lines

Melanoma cell lines were maintained in 2D and 3D cultures. A) 72 hours after seeding, the cells were labeled with primary antibody anti-p75NTR and its expression was evaluated by flow-cytometry, as described in the Materials and Methods. The results are shown on the y axis as% of positive cells p75NTR. .B) To demonstrate that p75NTR expression is influenced by the culture method, we repeated the analysis and we studied its expression even after having re-seeded 3D spheroids in a 2D model.

P75NTR expression decreases with enhanced aggressivenss of melanoma multicellular spheroids

Since the 3D model better reproduces the behavior of the tumors in vivo, by this time we conducted the experiments only by using 3D cultures. Firstly we confirmed by Western Blotting, Flow citometry and confocal microscopy that p75NTR expression inversely correlates with the progression stage of the tumor.

Flow citometry revealed that p75NTR expression decreases with enhanced aggressiveness of the tumor cell line and tends to disappear with the tumor progression (Figure 4.7A). In detail the most aggressive cell lines such as primary SKMEL28 and metastatic 1205Lu expressed the lowest level of p75NTR (45,5 and 27,0% respectively), while the least aggressive WM115 the highest level (82,3%). In addition, the MN Lx values detected were 5,51 (SKMEL28), 1,7 (1205Lu) and 14,1 (WM115).

This data were also confirmed by Western blotting (Figure 4.7 B). In fact p75NTR was higher in WM115 and WM266-4 RGP cell lines and decreased or was no detectable in the most aggressive SKMEL28 and 1205Lu VGP melanomas.

Finally, p75NTR expression was also evaluated by 3D confocal microscopy (Figure 4.7C). This protocol allows to dissect the spheroid entire structure in order to evaluate protein expression into the inner levels. Immunofluorescence confirmed previous results.

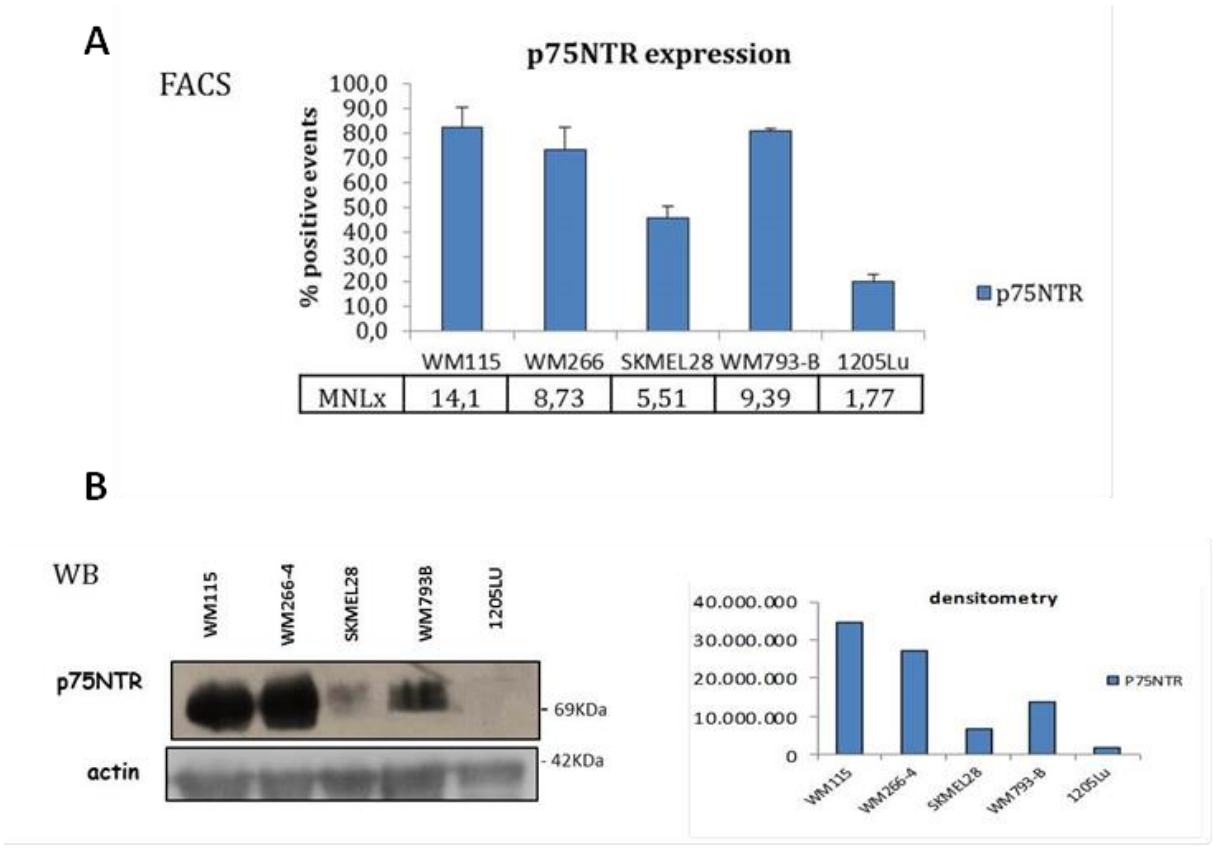

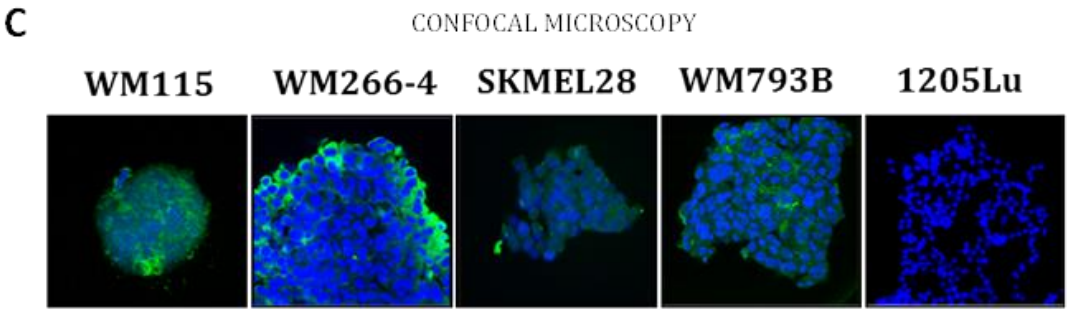

Figure 4.7 Evaluation of p75NTR expression in 3D models.
A) Melanoma cells were seeded in a 96multiwell (previously coated with 1,5% of agar) in order to obtain spheroids. FACS analysis was performed 72 hours after spheroids formation, as described in M&M. The percentage of p75NTR positivity is shown in the graph. MN Lx values are indicated in the table under the graph. B) Spheroids were collected 72 hours from cell seeding and Western Blotting for p75NTR was performed, as indicated in M&M. Beta-actin was used as internal control. C) Densitometric analysis of Western Blotting was calculated by using ImageJ. D) 40 spheroids for each cell line were used to evaluate p75NTR expression by 3D immunofluorescence with Confocal microscopy, as described in M&M (In green = p75NTR posivity; in blue=Dapi)

P75NTR expression decreases with enhanced aggressiveness of 3D melanoma skin equivalents

While RGP melanomas are confined to epidermis, VPG tumors invade the dermis, acquiring the ability to metastasize. In the last few years, in our laboratory has been optimized the 3D model of melanoma skin equivalent. Since skin equivalents reproduce the three dimensional structure of human skin, tumor cells should have a different behavior, depending on the progression stage of the melanoma cell line.

Melanoma and keratinocytes cells were seeded on preformed dermis equivalent and after 6 and 12 days of submerged condition, morphology of skin equivalents was studied by Hematoxylin and Eosin (H&E). Subsequently, melanoma cells were detected by immunohistochemical staining of S100, a recognized diagnostic marker for melanoma (Figure 4.8A).

As expected, melanoma cells displayed different locations in skin equivalents, depending on the stage of the original tumor. In detail we observed to 6 days that WM115 cells were confined to the epidermis, as expected from a primary RGP tumor, while WM266-4, SKMEL28, WM793-B and 1205Lu melanoma cells were at the dermal-epidermal junction. Moreover, in skin equivalents obtained from WM793B and 1205Lu, S100 positive cells invade the dermis to 12 days forming melanoma niches,as expected from VGP tumors.After having validated the skin reconstructs obtained from all melanoma cell lines, we evaluated the expression of p75NTR by immunohystochemical staining. The amount of p75NTR positive cells detected in melanoma skin equivalents confirmed earlier results obtained in 3D spheroids (Figure 4.8B). In particular P75NTR staining was high in reconstructs derived from WM115 cell line, it decreased or was almost absent in the most aggressive SKMEL28 and 1205Lu skin equivalents.

From the observations that p75NTR expression decreases with enhanced aggressiveness of the tumor in both 3D spheroids and skin equivalent, we postulated that it could have a crucial role in the progression of melanoma.

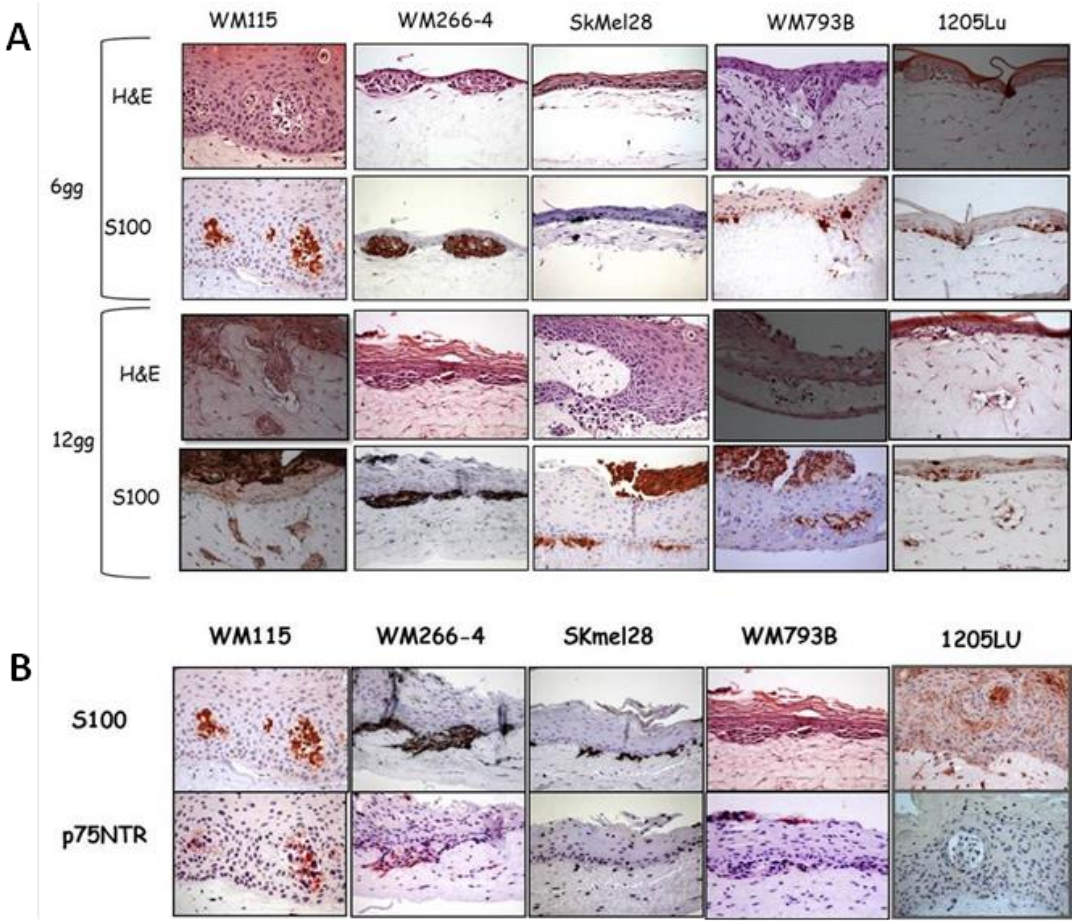

Figure 4.8 s100 and p75NTR immunohystochemical detection in melanoma skin equivalents.
A) Melanoma skin equivalents were performed, as described in M&M section and they were embedded in paraffin after 6 and 12 days of submersion. H&E was performed for morphological analysis (up),while S100 staining with HRP as cromogen (down) was employed for the detection of melanoma cells (in brown). B) Immunohistochemistry was performed at 12 days to evaluate p75NTR expression (Fast Red was used as cromogen). S100 (HRP as cromogen) was used as positive control, to stain melanoma cells

P75NTR expression is inversely correlated with enhanced predisposition to invade the microenvironment

To better understand the role of p75NTR, multicellular spheroids were transferred into a matrix of collagen I and its expression was evaluated 72 hours later by immunohistochemistry. P75NTR stained cells were then counted by Image J Cell Counter distinguishing between invasive and non- invasive cells, as shown in Figure 4.9A.

Consistent with our previous results, the total number of p75NTR positive cells was higher in poorly aggressive cell line (WM115), while it was significantly reduced ($p<0,01$) in the most aggressive spheroids (SKMEL28 and 1205Lu), as shown in Figure 9 C (green Bars).

Considering the total number of invading cells (Figure 4.9B), we observed that most were p75NTR - indicating a more aggressive behavior and a greater predisposition to invade the microenvironment and metastasize.

Considering the total number of p75NTR positive cells instead (Figure 4.9C), the majority were non-invasive cells (blue bars) to further confirm that the expression of this receptor is inversely related to the enhanced predisposition to invade the microenvironment . In fact, p75NTR positive cells were mostly confined to the central body of the sphere.

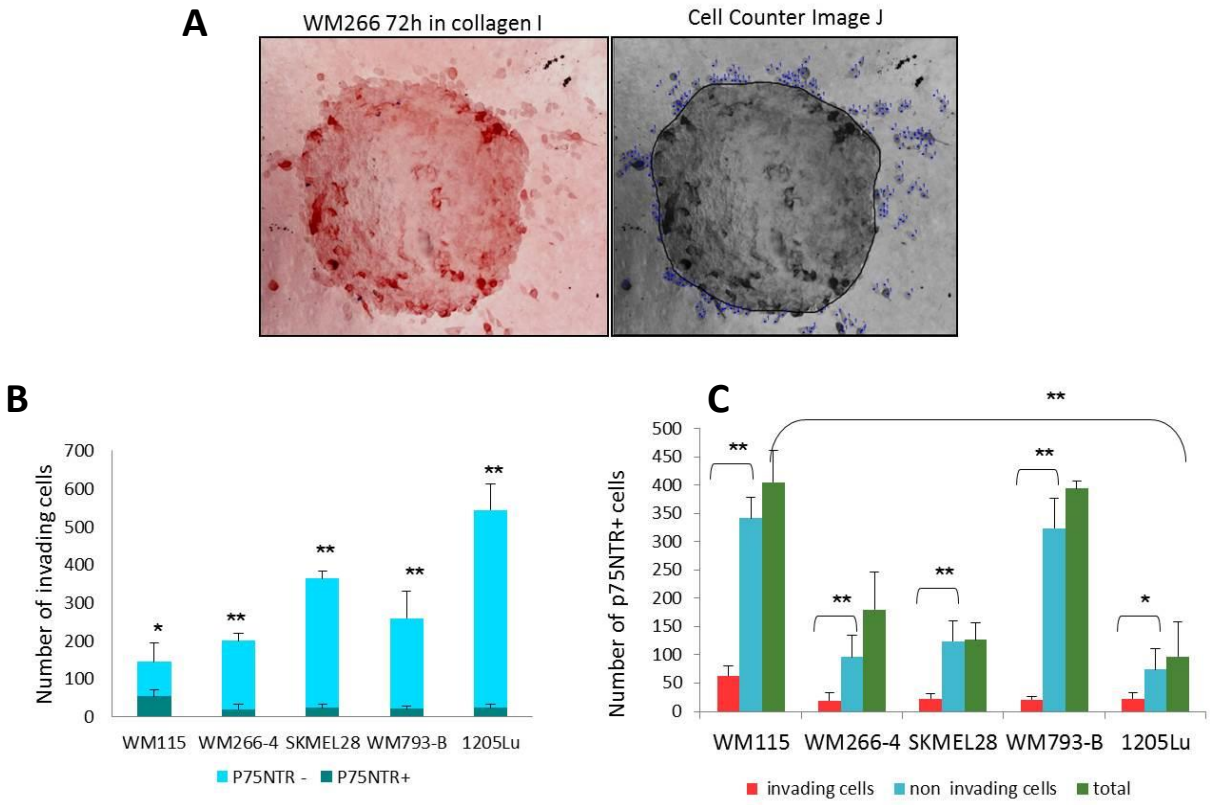

Figure 4.9 ***p75NTR expression in collageneI implanted spheroids***
Spheroids were implanted in collagen I, as described in M&M and fixed 72 hours. Later an immunoistochemical detection of p75NTR was performed and Fast Red was used as cromogen. Pictures were used to count the cell number. ***A****) From left to right: image of one spheroid spotted for p75NTR (positive cells are red) and the same image processed by "Cell Counter" application.* ***B****) The total number of p75NTR positive cells, distinguishing the invasive or not invasive ones.* ***C****) The total number of invasive cells, comparing p75NTR positive and negative ones. All data represent the mean ± S.D. of triplicate determinations and T-Student was used for statistacal analysis.*

SKMEL28 p75NTR dim spheroids proliferate more than SKMEL28 p75NTR bright spheroids

To better understand the role of p75NTR in melanoma progression, we decided to isolate p75NTR- (dim) and p75NTR+ (bright) subpopulations from melanoma cell lines and subsequently study their behavior in terms of growth and invasion abilities.
Flow citometry was used to evaluate which cell line was the best candidate to be sorted for p75NTR expression. FACS analysis revealed that only for WM266 and SKMEL28 was possible to isolate p75NTR bright and p75NTR dim subpopulations.

We decided to perform cell sorting for SKMEL28 cell line because it was possible to isolate two well distinct subpopulations (Figure 4.10A). In addition, being SKMEL28 a high aggressive primary cell line, we thought it was a most appropriate candidate to study tumor progression compared to the poorly aggressive metastatic WM266-4 cell line.

SKMEL28 cell line was sorted and purity control of the two subpopulations was evaluated (Figures 4.10 B and 4.10C) demonstrating that p75NTR bright cells were mostly p75NTR positive (83,9%), while in p75NTR dim subpopulation only 0.4% positivity was detected. These subpopulations were then used to perform functional studies. SKMEL28 p75NTR bright and SKMEL28 p75NTR dim subpopulations were isolated and multicellular spheroids were obtained (Figure 4.11A).

The proliferative capacity of sorted SKMEL28 p75NTR dim and bright spheroids was evaluated by MTT assay at 24, 72 and 168 hours after seeding and it was compared with the growth ability of the same subpopulations in 2D cultures to highlight differences between the two models (Figure 4.11B). As expected, 2D- and 3D-models presented a different behavior. In detail, SKMEL28 p75NTR bright spheroids showed reduced growth abilities in comparison to p75NTRdim spheroids demonstrating that the lack of p75NTR expression correlates with a greater proliferative capacity. In fact it can be appreciated, already at 72 hours, a significant difference in growth capacities between the two subpopulations (p value $< 0,01$). However, this difference was not relevant in 2D-

model. Total SKMEL28 spheroids were used as control and showed a proliferation curve intermediate between the two subpopulation.

The area occupied by spheroids was calculated by using Image J at different time points (24, 48, 72, 144, 168, 192, 216 hours) (Figure 4.11C). The analysis confirmed MTT results showing a significant increase in time of the areas only for p75NTR dim spheroids(p value < 0,01**)**. On the contrary, the area occupied by the p75NTR bright spheroids didn't increase over time (Figure 4.11D). In addition, we noticed that p75NTR dim spheroids were characterized by broader and less compact structures than those of p75NTR bright spheroids.

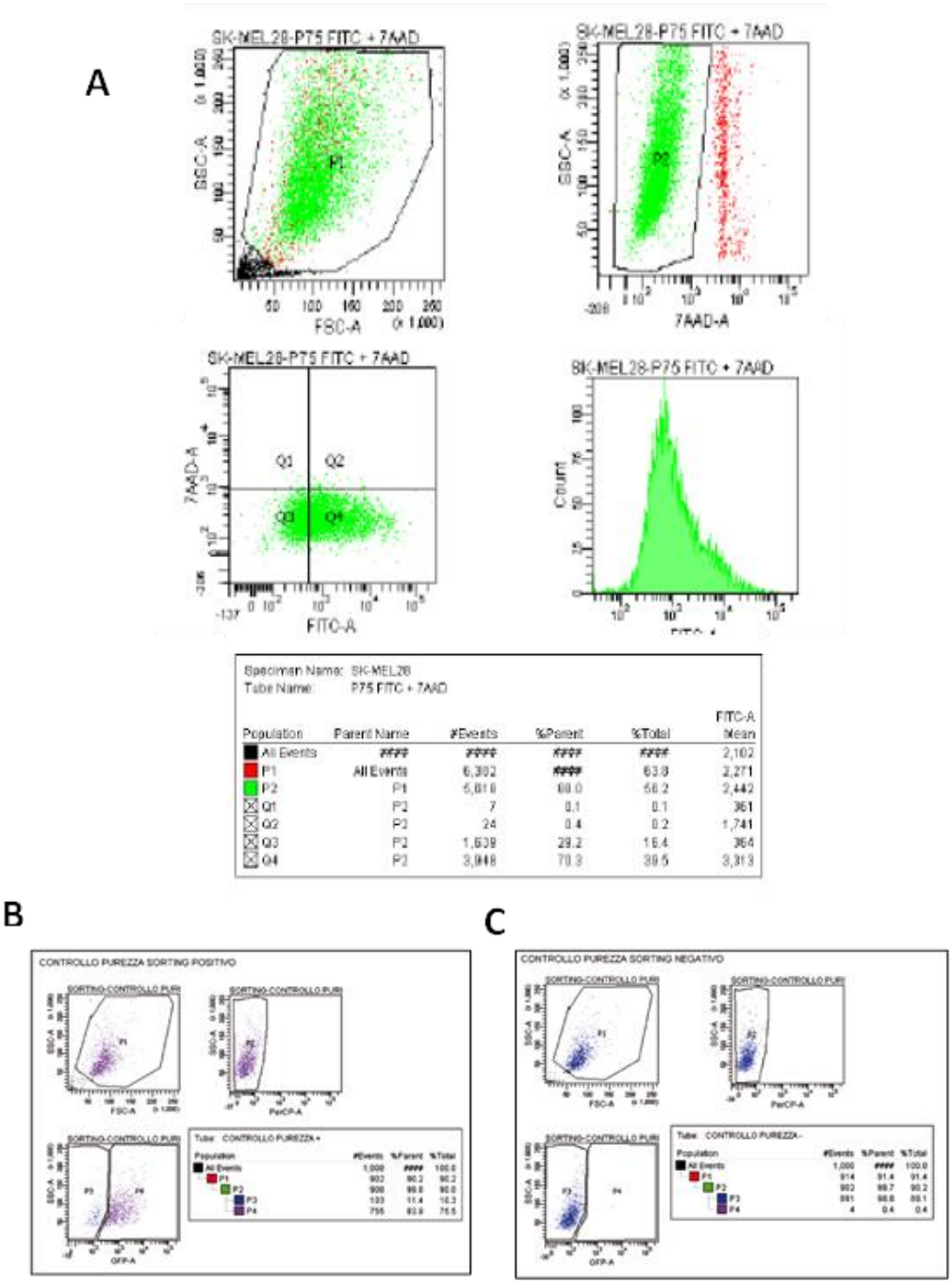

Figure 4.10: Sorting of SkMel28 cell line

A) *SKMEL28 cells were sorted for p75NTR expression by using the instrument FACS ARIA III, as described in M&M, thus obtaining p75NTR dim cells and p75NTR bright cells* ***B)*** *The purity control of p75NTRdim and* ***C)*** *bright cells was evaluated.*

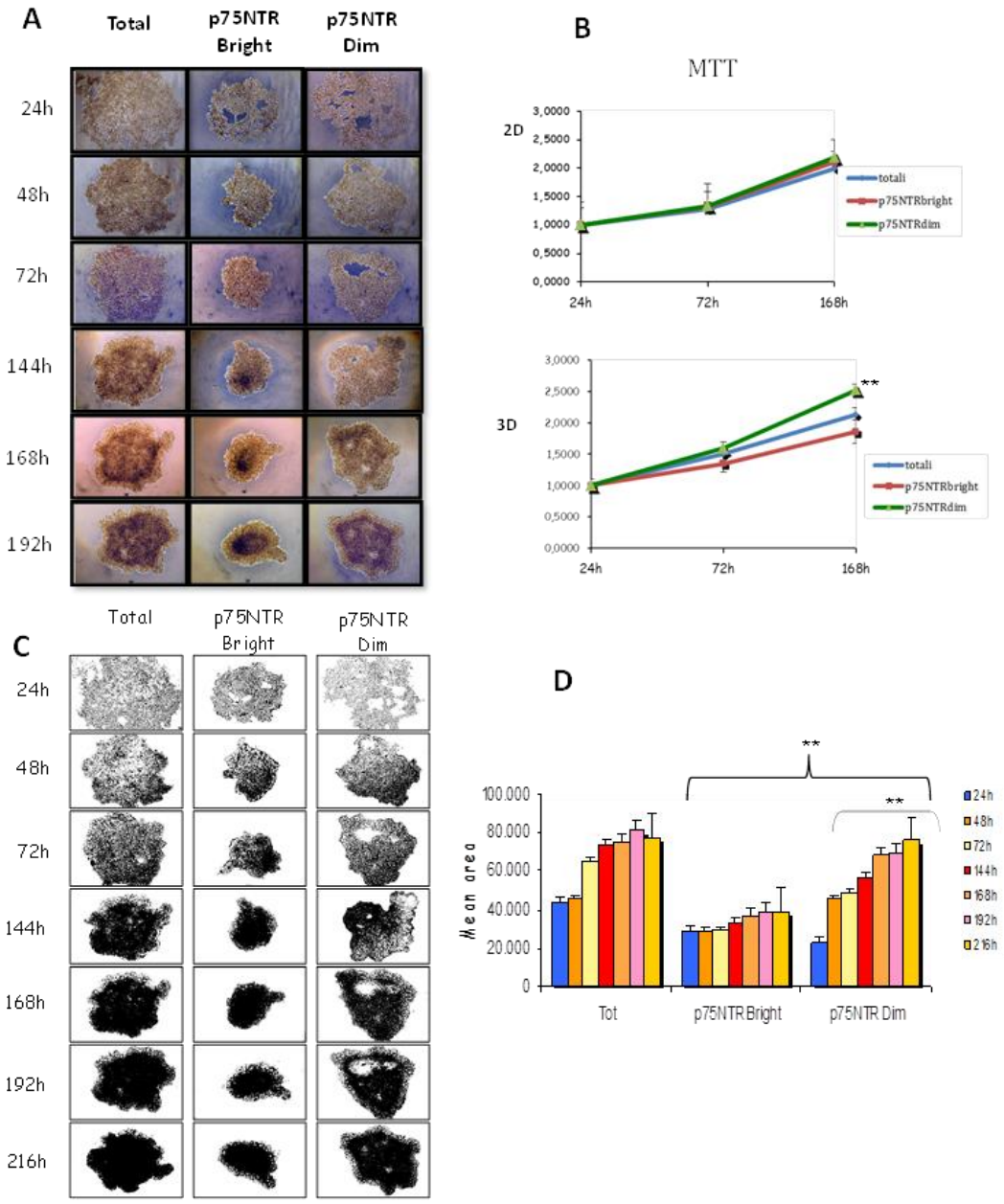

Figure 4.11 ***Proliferation analysis of SKmel28 P75NTR dim and p75NTRbright spheroids.***
A) *Skmel28 p75NTRdim and p75NTRbright cells were seeded in a pre-coated 96multiwell to form spheroids, the total population was used as control. They were photographed at different time (24, 48, 72, 144, 168, 192 hours)* ***B)*** *The proliferative capacity of the two subpopulations was evaluated in 2D and 3D by MTT assay, as described in M&M. The values obtained were subtracted from the values of the background. Data represent the mean of triplicate determinations and T-Student was used for statistical analysis.* ***C)*** *Pictures were converted to 300 pixels / inch and Image J was used to obtain 8 bits images* ***D)*** *Pixel analysis of the photos previously converted was performed with Image J, as indicated in M&M. In the graph are reported the areas obtained from SKMEL28 dim, bright and total spheroids. Data represent the mean ± S.D. of triplicate determinations and T-Student was used for statistical analysis.*

SKMEL28 p75NTR dim spheroids invade more than SKMEL28 p75NTR bright spheroids

The invasive potential of SKMEL28 sorted subpopulations was analyzed to understand the phenotype acquired by p75NTR bright and dim spheroids in terms of invasion abilities.

To this purpose, spheroids were implanted into a matrix of collagen I and photographs were taken at 72, 96, and 120 hours (Figure 4.12A).

SKMEL28 p75NTRdim spheroids were able to invade collagen I to a greater extent, thus indicating a more aggressive behavior than p75NTR bright ones. The most evident differences between the two subpopulations were particularly noticeable at 120 hours.

To quantify their invasion abilities we analyzed the total area occupied by spheroids considering also the invading cells (Figure 4.12B). The pixel analysis demonstrated that p75NTR dim spheroids occupy a greater area in comparison to p75NTR bright spheroids (p value <0,01), with a remarkable increase at 120h (Figure 4.12C).

The number of invading cells was counted by Image J (Figure 4.12D). Results further strengthened previous data showing that the number of invading cells was much higher in p75NTR dim spheroids in comparison to p75NTR bright ones and differences were already appreciable at 96 hours from seeding.

Factor shape and percentage of fragmentation were also calculated confirming that p75NTR dim spheroids have greater invasion abilities (Figure 4.12B).

Finally, the calculation of the average distance reached by the cells in collagen (Figure 4.12E) demonstrated that p75NTR dim spheroids are able to achieve greater distances than p75NTR bright ones (p value <0,01) indicating a more aggressive behavior and predisposition to metastatize.

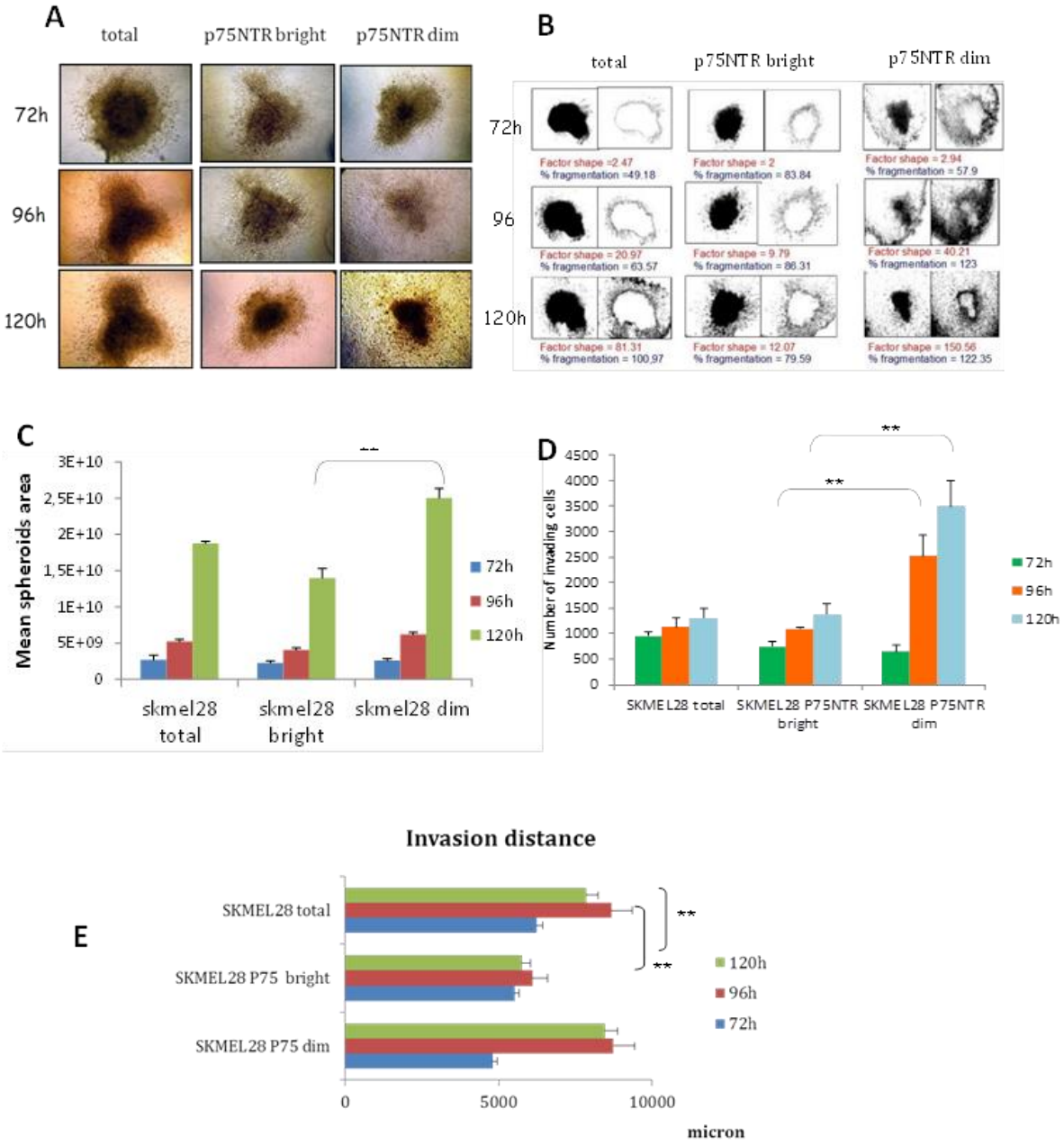

Figure 4.12: Invasive abilities of p75NTRdim and p75NTRbright cells.
A) *SKMEL28 p75NTRdim and bright spheroids were implanted into a matrix of collagen I and they were photographed from 72 to 120 hours. B) Pixel analysis of the pictures was performed with ImageJ, as described in M&M section and the factor shape, percentage of fragmentation and* ***C)*** *total area occupied by spheroids was calculated. The area data were represented as mean ± S.D. of triplicate determinations and T-Student was used for Statistacal analysis.* ***D)*** *The total number of invading cells were counted by using "Cell Counter" application (ImageJ), as described in M&M. Data represent the mean ± S.D. of triplicate determinations and T-Student was used for statistacal analysis.* ***E)*** *The distances reached by the cells in collagen I was evaluated, by using Photoshop, considering the cells migrated in the directions of the four cardinal points. The average distance was calculated and the number of pixel were converted into micron. Data represent the mean of triplicate determinations and T-Student was used for statistacal analysis.*

WM115 acquire a more aggressive phenotype after p75NTR silencing

To further investigate whether p75NTR has a crucial role in melanoma progression and confirm our previous observations according to which its expression is inversely correlated with melanoma aggressiveness, we silenced its expression by p75NTR siRNA transfection in WM115, the least aggressive melanoma cell line that express 98% of this receptor.

After having checked the actual silencing of p75NTR in transfected cells by Western Blotting (Figure 4.13A), spheroids were obtained and monitored up to 120 hours (Figure 4.13B). We then analyzed the area occupied by the spheres (figure 4.13C) and we observed that, although it was not visible an increase in time, the area occupied by p75NTR siRNA spheroids was significantly higher compared to the area of spheroids obtained by mock treated cells ($p<0,01$), as shown in Figure 4.13D.

We also observed that WM115 siRNA transfected spheroids presented a less compact and regular structure in comparison to mock spheroids, as usually occurs in more aggressive cell lines.

To better characterize the phenotype of transfected cells, spheroids obtained from both p75NTR siRNA and mock treated cells were implanted into a matrix of collagen I and their invasion ability was studied. Spheroids were photographed at 24, 48, and 72 hours (Figure 4.14A). Pictures were processed by ImageJ program and the area occupied by spheroids, factor shape and the percentage of fragmentation were calculated.

Spheroids obtained by p75NTR-siRNA treated cells occupied a greater area (Figure 4.14C) and presented higher values of factor shape and percentage of fragmentation (17,2 for mock and 141,5 for siRNA- transfected cells at 72 hours), as shown in Figure 4.14B.

The total number of invading cells was also calculated revealing greater invasion abilities and higher invading cells in p75NTR siRNA spheroids than mock generated spheroids ($p<0,01$) (Figure 4.14D).

Finally, the average invasion distance reached by cells was calculated by Photoshop (Figure 4.14E) and revealed that p75NTR-siRNA transfected cells were able to reach larger distances in collagen I if compared to mock transfected cells, with an increase already appreciable at 48 hours ($p<0,01$).

These data suggest that p75NTR silenced WM115 melanoma cells acquire a more aggressive phenotype with greater proliferative capacities and enhanced invasion abilities.

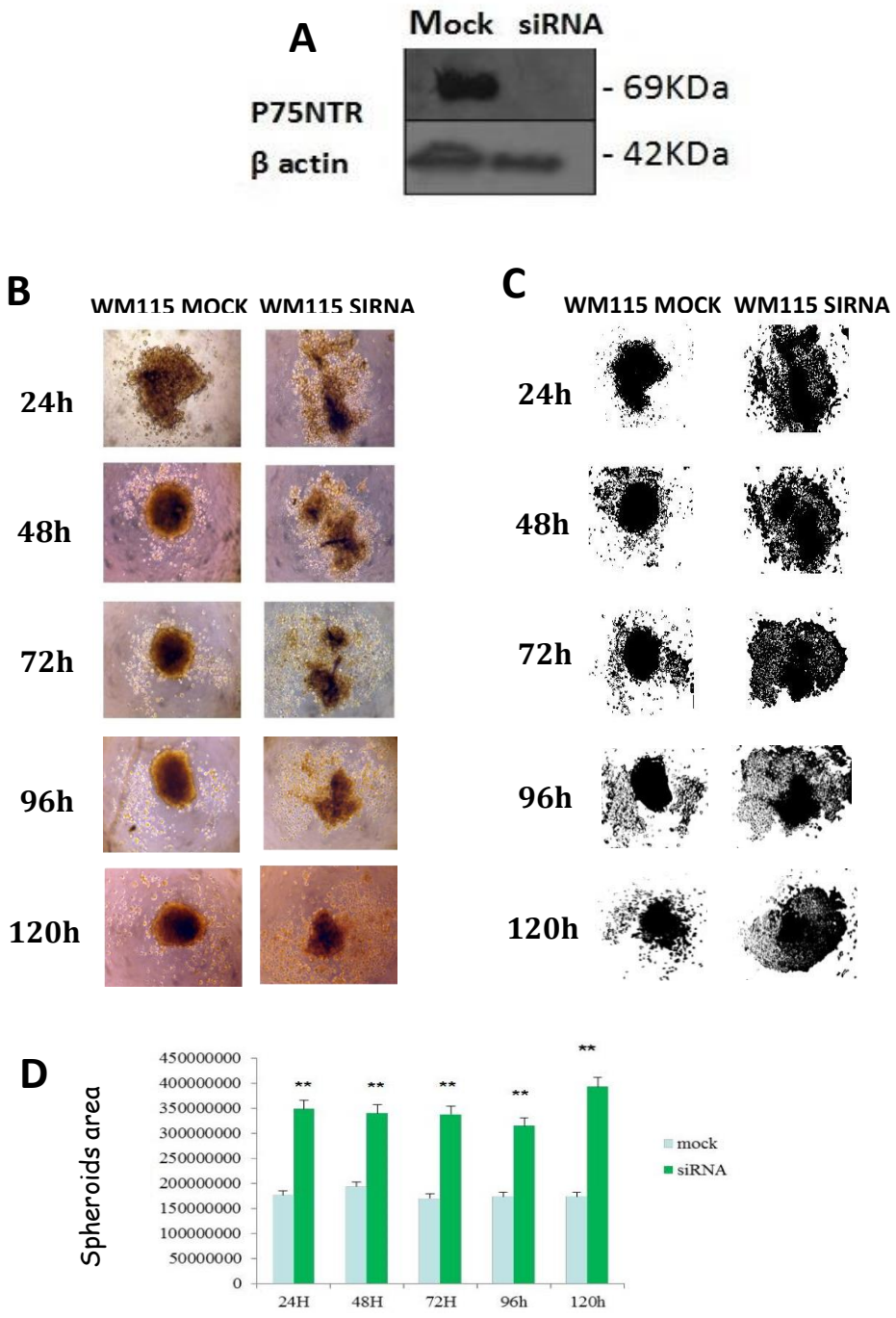

Figure 4.13 ***Proliferation analysis of WM115 spheroids trasfected with p75NTR-siRNA.***
A) *WM115 were transfected with 100nM p75NTR siRNA or scramble siRNA, as control (Mock), as described in M&M. Western Blotting was performed for the analysis of p75NTR expression and beta-actin was used as internal control.* ***B)*** *Transfected cells were seeded in a pre-coated 96multiwell to form spheroids and they were photographed in time (24, 48, 7, 96 and 120 hours).* ***C)*** *Pictures were processed by Image J and* ***D)*** *pixel analysis was performed, as indicated in M&M. Data represent the mean ± S.D. of triplicate determinations and T-Student was used for statistacal analysis.*

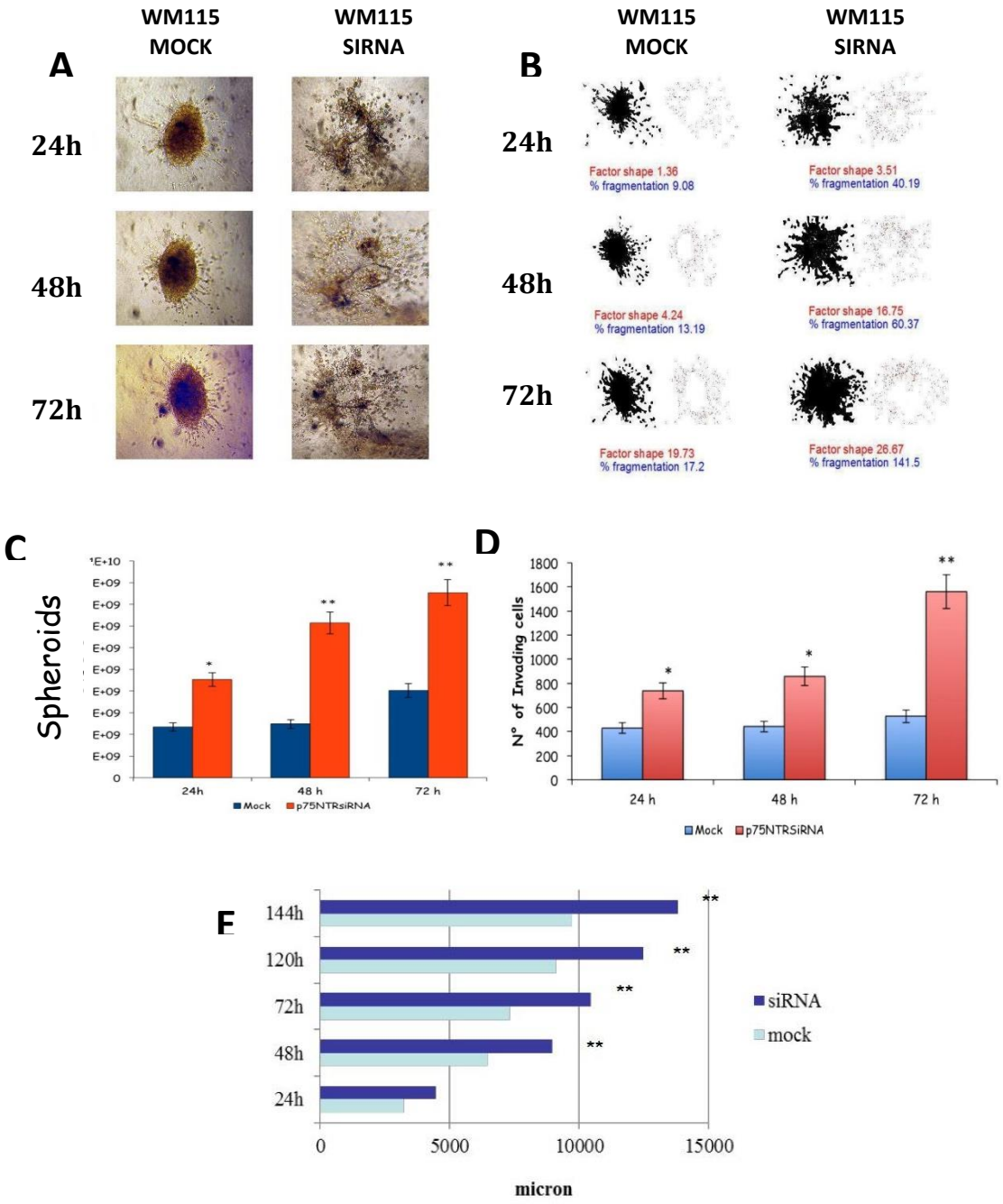

Figure 4.14: Invasive abilities of WM115 spheroids transfected with p75NTR-siRNA
A) *p75NTRsiRNA and scramble transfected spheroids were immersed in a matrix of collagen I and they were photographed at 24, 48 and 72 hours.* ***B)*** *Pictures were analyzed by Image J program and factor shape, the percentage of fragmentation and* ***C)*** *the area occupied by spheroids were calculated, as indicated in M&M.* ***D)*** *The total number of invading cells were counted by using "Cell Counter" application (Image J), as described in M&M.* ***E)*** *The distances reached by the cells in collagen I was evaluated (Photoshop) considering the cells migrated in the directions of the four cardinal points, as indicated in M&M. The average distance was calculated and the number of pixel were converted into micron. All data represent the mean ± S.D. of triplicate determinations and T-Student was used for statistical analysis.*

1205LU p75NTR overexpressing spheroids decrease their size in comparison to mock spheroids

To confirm previous results and demonstrate the role of p75NTR in melanoma progression, we decided to evaluate the effects of its overexpression in 1205Lu cells, the most aggressive cells line that express the lowest level of this receptor (approximately 27%) .

To this purpose, 1205Lu cells were infected with p75NTR viral vector or with empty vector (mock) and infection was validated by Western blotting (Figure 4.15A). Spheroids obtained from 1205Lu infected cells were followed up to 72 hours. Firstly we noticed that p75NTR infected spheroids acquired a more compact morphological structure in comparison to mock spheroids assuming a phenotype quite similar to cell lines that normally express high levels of p75NTR (Figure 4.15B).

Pictures were taken and processed by ImageJ program (Figure 4.15C) and the pixels analysis revealed that spheroids obtained by mock infected cells occupied a greater area in comparison to p75NTR overexpressing spheroids, which, in turn, appeared to decrease up to 72 hours ($p<0,01$) (Figure 4.15D).

From these observations we speculated that the over-expression of p75NTR in 1205Lu cells could lead to cell death. However, this observation should be verified.

Preliminary tests have been done to evaluate the invasive behavior of 1205Lu p75NTR overexpressing spheroids. However, despite the reduced area previously noticed, we didn’t observed significant differences in the invasive capacity between mock and p75NTR overexpressing spheroids. Collagen I invasion assay should be repeated to confirm this data.

In addition, further tests will be needed to assess apoptosis and their proliferation abilities.

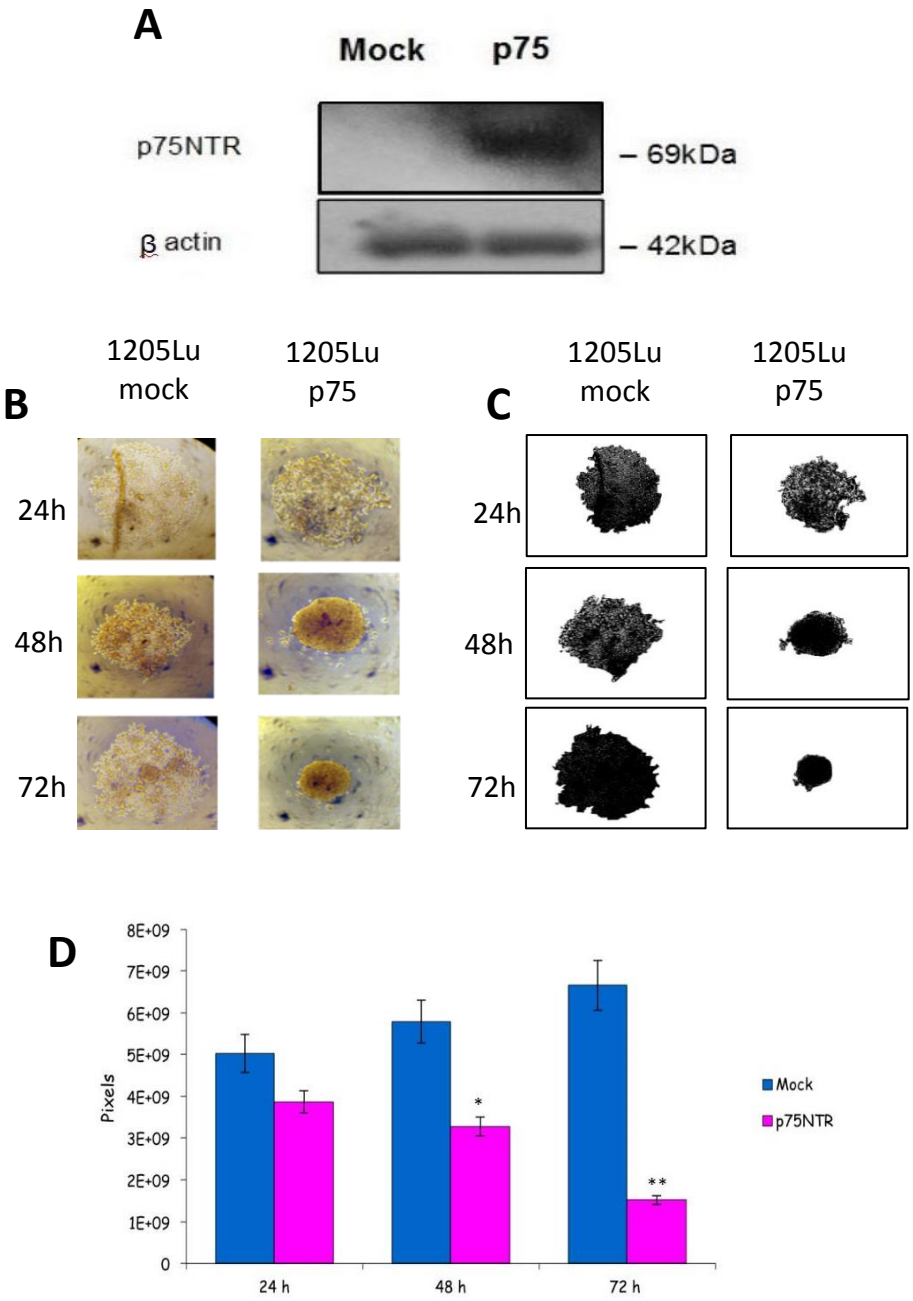

Figure 4.15*: Analysis of areas occupied by 1205Lu p75NTR overexpressing spheroids*
A) *1205Lu cells were infected with p75NTR viral vector or with empty vector for control (Mock), as described in M&M. Western Blotting was performed for the analysis of p75NTR expression, beta-actin was used as internal control.* ***B)*** *Infected cells were seeded in a pre-coated 96multiwell to form spheroids and they were photographed at 24, 48 and 72 hours.* ***C)*** *Pictures were processed by Image J and* ***D)*** *pixel analysis was performed, as indicated in M&M. Data represent the mean ± S.D. of triplicate determinations and T-Student was used for statistical analysis.*

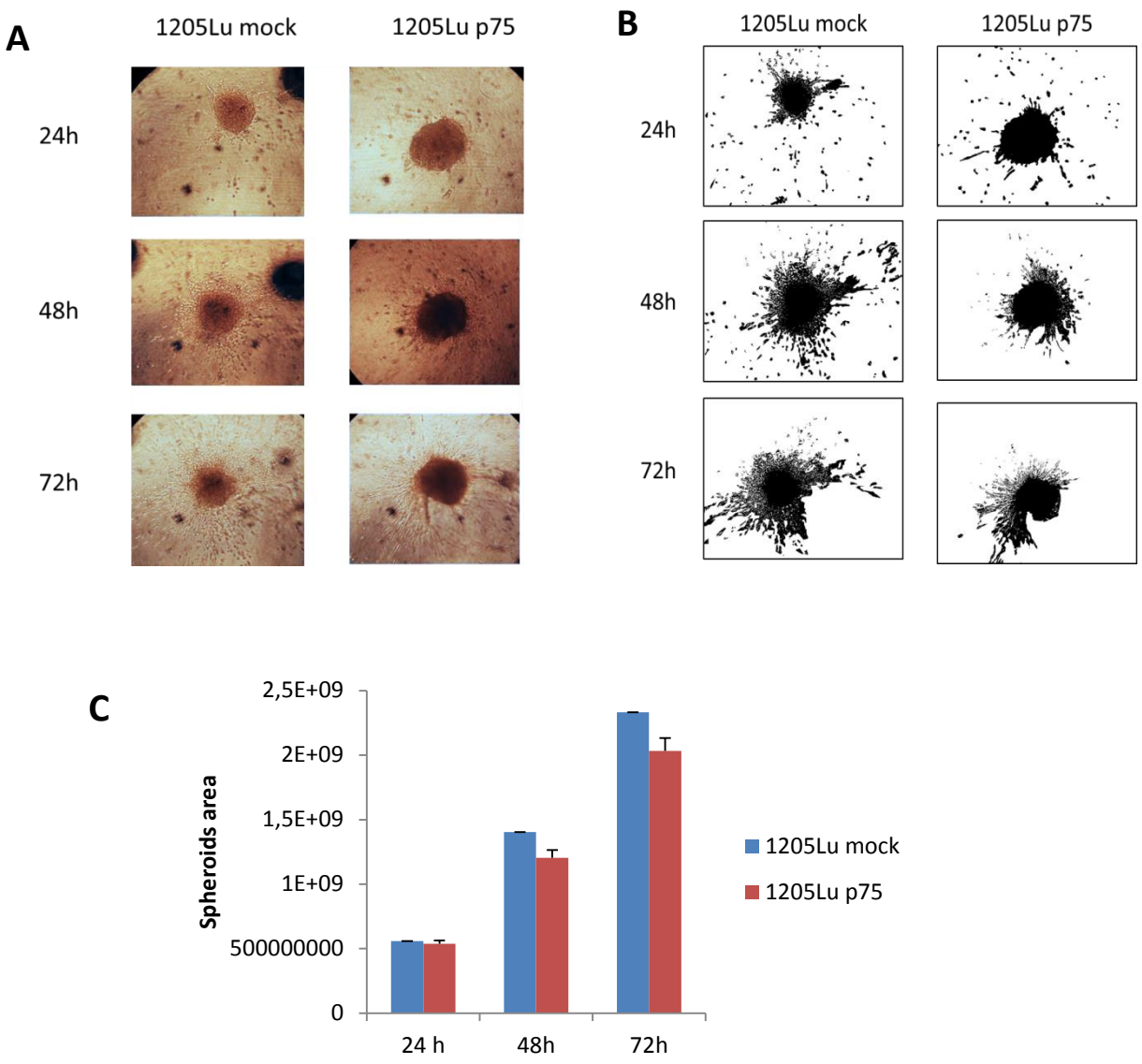

Figure 4.16: ***Evaluation of the invasion abilities in 1205Lu p75NTR overexpressing spheroids***
A) *1205Lu cells were infected with p75NTR viral vector or with empty vector for control (Mock) and spheroids were implanted into a matrix of collagen I* ***B)*** *Spheroids were then photographed at 24, 48 and 72 hours.* ***C)*** *Pictures were processed by Image J pixel analysis was performed, as indicated in M&M. Data represent the mean ± S.D. of triplicate determinations and T-Student was used for statistical analysis.*

5. Discussion

Melanoma is the most aggressive and deadliest type of skin cancer (Greay-Shopfer., 2007a) and its high mortality is closely correlated to metastatic disease. Melanoma is extremely heterogeneous from patient to patient and for this reason therapies are not always effective (Kiran R et al., 2011).

The understanding of the mechanisms of tumor progression and in particular of the pathways that are switched off or switched on during transition from superficial radial growth phase (RGP) to vertical growth phase (VGP) tumor and finally to metastasis represent a major milestone for the development of new therapeutic protocols. In particular, the discovery of the molecular mechanisms that confer a selective advantage in a subpopulation of the primary tumor to invade secondary sites is crucial to treat metastatic melanomas. In fact, while early melanomas can be cured by surgical excision, metastatic melanomas are generally fatal due to its resistance to current treatments (Koh et al., 1998).

For many years, our laboratory has studied the complex network of neurotrophins (NTs) and their receptors (p75NTR and Trks) in healthy and diseased skin. In particular, we have shown that autocrine NTs are responsible for melanoma cell proliferation and migration in 2D cultures (Truzzi et al., 2008). However, the role of p75NTR in melanoma is not yet entirely clear, and many controversial data have been published.

In this study, we employed three-dimensional (3D) melanoma models such as spheroids and skin equivalents to study the role of p75NTR in tumor progression. Given that cell survival and apoptosis strongly depend on cell adhesion and the extracellular matrix (Grassian A.R. et al., 2011), 3D models represent the ideal substrate for studying the mechanisms of invasion, progression, metastasis and resistance to chemotherapy. Five melanoma cell lines of different stages and degree of aggressiveness were maintained in 3D cultures. Spheroids derived from poorly aggressive primary (WM115) and metastatic (WM266-4) radial growth phase cell lines or from primary (WM793B) vertical growth phase cell line slightly grew in time. Conversely, spheroids derived from more aggressive tumors such as primary (SKMEL28) and metastatic (1205Lu) vertical growth phase cell lines displayed considerable proliferation abilities. Therefore, melanoma spheroids showed a trend of growth that mirrors the behavior of the tumor from which cell lines are derived. These results were demonstrated by MTT assay, calculation of the proliferative

index and measurement of the area occupied by spheroids in time. By contrast, 2D model, used as a term of comparison, failed to reproduce growth behavior of the tumor. Several laboratories demonstrated that spheroids mimic the tumor heterogeneity seen in vivo and recreates the oxygen/nutrient gradient. Furthermore, spheroid model faithfully recapitulates the behavior of tumors in vivo, reflecting the original stage of aggressiveness (Desoize and Jardillier, 2000).

The 3D model was further validated by assessing whether it was able to reproduce melanoma invasion ability and response to common chemotherapy. The assessment of response to chemotherapy showed that spheroids derived from WM266-4 metastatic cell line were more resistant to apoptosis than those derived from primary WM115 tumor. Consistently with our results, 3D spheroids are considered a useful tool to prescreen single agents drugs and drug combinations allowing the researcher to narrow down the experiments that need to be done in animals with both ethical and economical advantages (Kimberley AB et al., 2014). In addition, VGP spheroids displayed greater invasion abilities than RGP spheroids and metastatic cell lines were more invasive than their primary tumors.

The more aggressive tumor (1205Lu) showed the greater invasive capacity while the least aggressive cell line (WM115) showed a reduced ability to invade the microenvironment.

There is an increasing interest in how tumor microenvironment can regulate behavior of cancer cells. In fact, microenvironment may influence a cancer cell response or resistance to treatment (Kenny C. et al., 2013). Consistently with our results, 3D melanoma spheroids implanted into a collagen gel matrix mirror the in vivo tumor architecture and invasion of microenvironment (Santiago W. et al., 2009; Smalley K S. et al., 2008; Smalley K S et al., 2006). Given that VGP spheroids were less compact than RGP ones, we hypothesized that a reduced expression of cell-cell adhesion molecules could promote the detachment of some cells from the primary tumor resulting in a greater predisposition to invade the microenvironment and metastatize.

The study of p75NTR in spheroids obtained from all melanoma cell lines revealed a reduced expression in the more aggressive SKMEL28 and 1205Lu cell lines (45% and 27% respectively), while the less aggressive WM115, WM266-4 and WM793B cell lines displayed a higher expression (82,3%, 73,3% and 80,7% respectively). The data were

confirmed in Western blot, flow cytometry and confocal microscopy. Previous studies, carried out in our laboratory on melanoma biopsies with different degrees of aggressiveness, showed that p75NTR is inversely correlated with tumor aggressiveness (manuscript in preparation). To further strengthen our analysis, the same results were obtained in 3D skin equivalents. p75NTR was found highly expressed in WM115 derived reconstructs, while it was almost absent in 1205Lu skin equivalent. To further understand the relationship between invasive capacity of melanoma spheroids and p75NTR expression, p75NTR was evaluated by immunohistochemistry on multicellular spheroids assessing whether the labeled cells were invasive or localized within the sphere. The analysis showed that the expression of p75NTR is inversely related to melanoma invasion abilities. In fact, the majority of the invading cells were p75NTR negative, indicating a greater predisposition to invade the microenvironment.

This result could indicate that, within the heterogeneous population of the tumor, a subpopulation of cells need to turn off p75NTR expression to acquire the ability to invade. It remains to be confirmed whether p75NTR pro-apoptotic effects (Selimovic et al, 2012) could account for the result. Alternatively, p75NTR could play a role in cell-cell adhesion. In contrast with our observations, other authors reported that p75NTR is frequently overexpressed in aggressive melanoma (Brocker et al., 1991; Herraman et al., 1993; Mattei et al., 1994) and that it can play a direct and active role in NT signalling to promote invasion of melanoma cells (Marchetti et al., 1998). These conflicting results may be due to the culture model used. To demonstrate that p75NTR levels are influenced by the culture method, we evaluated its expression in 2D and 3D-models and in cells derived from spheroids reseeded as 2D cultures. Results obtained clearly showed differences between the two models revealing that the previously highlighted correlation between p75NTR and aggressiveness of the tumor, was not appreciable in 2D cultures. Several data in literature confirm this assumption. Noteworthy, comparative gene expression profile studies revealed that several genes associated with proliferation, differentiation and resistance to therapy are differentially expressed in cells maintained as 3D multicellular spheroids in comparison with 2D cultures, suggesting the preferential expression of specific constellations of genes in well-defined and structured architectures (Sourach Ghosh et al., 2005; Cody et al., 2008). A recent genomic array hybridization

study showed that the genomic profile of human malignant glioma is preserved in spheroids but not in primary monolayer cultures (De Witt Hamer et al., 2009). Given our results, we postulate that the reduced expression of p75NTR could be responsible for the acquisition of a more aggressive phenotype. To further investigate this aspect, we decided to: 1) isolate p75NTRdim and p75NTRbright subpopulations from SKMEL28 cell line, which expresses approximately 50% of the receptor, 2) silence p75NTR expression in the least aggressive WM115 cell line which is not sortable since it expresses more than 80% of the receptor, and 3) finally obtain p75NTR overexpression in the most aggressive metastatic 1205Lu cell line, that expresses only 20% of the receptor. The goals were respectively to: verify the phenotype of SKMEL28 cell subpopulations, evaluate whether silencing of p75NTR induced the acquisition in WM115 of a more aggressive phenotype and finally trying to reduce 1205Lu aggressive behavior in terms of growth and invasion abilities, to eventually make it more sensitive to treatment. SKMEL28 dim p75NTR spheroids demonstrated to be more aggressive than p75NTRbright ones, revealing greater proliferative and invasive capacities. Numerous studies have been reported on melanoma p75NTR dim and bright subpopulations, mostly aimed to understand its role in tumorigenesis, in particular as melanoma stem cell marker. Yet, results are still conflicting. Boiko and co-workers showed that p75NTR expression characterizes a population of melanoma cells with tumor initiating properties (Boiko et al., 2010). On the contrary, Quintana et al., demonstrated that cell isolation through p75NTR does not enrich for melanoma stem cells (Quintanaet al., 2010; Civenni et al., 2011). These studies are often carried out on spheroids maintained in a stem cell medium that could select a subpopulation of the tumor. Our results show that melanoma cell lines expressing higher levels of p75NTR are more quiescent and tend to grow slowly. However, a such high expression level may exclude a role of p75NTR in stemness.

Results obtained in WM115 confirmed that p75NTR silencing is responsible for the acquisition of a more aggressive phenotype, as p75NTR siRNA spheroids displayed significantly increased proliferative and invasion abilities. Moreover, overexpression of p75NTR in 1205Lu caused a reduction of the area occupied by spheroids. Interestingly, we noticed that p75NTR overexpressing spheroids acquire a more compact morphological structure in comparison to mock spheroids, getting closer to that observed

in the less aggressive melanoma cell lines. The reduced area measured could be explained with a reduction in proliferation or could suggest that p75NTR lead to melanoma cell death. Indeed, melanoma is characterized by alteration in the apoptotic signal which in turn accounts for its chemoresistance (Reed and Pellecchia, 2005). Several molecules involved in the regulation and execution of apoptosis have been shown to be either up- or down-regulated (Eberle et al., 2008). p75NTR, upon binding to a specific ligand, induces apoptosis via its own transduction pathway and by interacting with a number of downstream molecules (Blochl and Bloch, 2007). Moreover, p75NTR can interact with sortilin to mediate cell death (Dobrowsky et al, 1998, Skeldal et al., 2012). Transfecting psoriatic keratinocytes, that are normally resistant to apoptosis, with p75NTR, restores β-amyloid-induced cell death (Truzzi et al, 2011). Moreover, p75NTR activation mediates apoptosis in bladder and prostate cancer (Khwaja et al, 2004). Finally, Selimovic et al. (2012) demonstrated that apoptosis related protein-1 (APR-1) triggers melanoma cell death via interaction with the juxtamembrane region of p75NTR. In substance, the level of p75NTR seems to determine the rate of apoptosis in cancer and its absence is associated with more invasive phenotypes. Consistently, we present evidence that, in vitro, p75NTR expression is dowregulated as a function of the aggressiveness of melanoma cells.

Preliminary tests have also been done to evaluate the invasive behavior of 1205Lu p75NTR overexpressing spheroids. However, despite a reduction in the area occupied, we failed to observe significant differences in the invasive capacity between mock and p75NTR infected spheroids. Collagen I invasion assay should be repeated to confirm this preliminary data. Two hypotheses have been proposed to explain this result. The first hypothesis is that, being 1205Lu a metastatic tumor, its cells are in at advanced stage. Thus, they could have acquired modifications able to confer a selective advantage and neutralize the effects related to the addition of exogenous p75NTR, not allowing to observe a reduced aggressiveness. Alternatively, one could postulate that p75NTR overexpression does not necessarily lead to the activation of the apoptotic cascade, but it might also mediate survival signals. Finally, 1205Lu is not directly derived from a human tumor, as it was obtained by injecting cells of the primary tumor (WM793B) in a nude

mouse. Recent studies (cercare ref) have shown that 50% of 1205Lu is composed of murine cells. Same assays on the highly aggressive SKMEL28T cell line, which is directly derived from a primary human tumor would possibly solve the issue. In addition we should analyze proliferation and apoptosis of p75NTR overexpressing spheroids by MTT and Annexin/Pi assays .

We conclude that p75NTR plays an important role in melanoma progression. Further studies are necessary to identify the signaling pathways involved. We intend to confirm p75NTR activity in melanoma in an *in vivo* model. If the correlation between reduced p75NTR expression and increased tumor aggressiveness will be further confirmed, we should envisage a prognostic role of p75NTR in melanoma.

6. References

- Abbott, A. Cell culture: biology of new dimension. (2003) Nature 424, 87072.
- Al-Hajj M, Wicha MS, Benito-Hernandez A, Morrison SJ, Clarke MF. Prospective identification of tumorigenic breast cancer cells. Proc Natl Acad Sci U S A 2003;100:3983–8.
- Alonso, S.R., Ortiz, P., Pollan, M. et al. (2004). Progression in cutaneous malignant melanoma is associated with distinct expression profiles: a tissue microarray-based study. Am. J. Pathol. 164, 193–203.
- Alonso, S.R., Tracey, L., Ortiz, P. et al. (2007). A high-throughput study in melanoma identifies epithelial-mesenchymal transition as a major determinant of metastasis. Cancer Res. 67, 3450–3460.
- Anaka M, C. Freyer, C. Gedye, O. Caballero, I.D. Davis, A. Behren, J. Cebon, Stem cell media culture of melanoma results in the induction of a nonrepresentative neural expression profile, Stem Cells 30 (2012) 336–343.
- Andre F, N. Berrada, C. Desmedt, Implication of tumor microenvironment in the resistance to chemotherapy in breast cancer patients, Curr. Opin. Oncol. 22 (2010) 547–551.
- Archambault M, Yaar M, Gilchrest BA: Keratinocytes and fibroblasts in a human skin equivalent model enhance melanocyte survival and melanin synthesis after ultraviolet irradiation. (1995) J *Invest Dermatol* 104:85967
- Balch CM, Soong S, Ross MI, Urist MM, Karakousis CP, Temple WJ, et al: Long-term results of a multi-institutional randomized trial comparing prognostic factors and surgical results for intermediate thickness melanomas (1.0 to 4.0 mm). Intergroup Melanoma Surgical Trial. (2000) Ann Surg Oncol. 7:87-97
- Balint, K., Xiao, M., Pinnix, C.C., Soma, A., Veres, I., Juhasz, I., Brown, E.J., Capobianco, A.J., Herlyn, M., and Liu, Z.J. Activation of Notch1 signaling is required for beta-catenin-mediated human primary melanoma progression. (2005) J. Clin. Invest. 115:3166176.
- Bandarchi B., Ma l., Navab R., Seth A. and Rasty G. From melanocyte to metastatic malignant melanoma. (2010) Dermatology Researche and Practice.
- Barbacid M. Nerve growth factor: A tale of two receptors. Oncogene (1993) 8: 2033-2042.

- Batsakis J. G. and Suarez P. Mucosal melanomas: a review. (2000) Advanced in Anatomic
  Pathology 7:167-180.
- Bechetoille N., Haflek M., Staquet M.J., Cochran A.J., Schmitt D. and Berthier-Vergnes.
  Penetration of human metastatic melanoma cells through an authentic dermal-epidermal junction is associated with dissolution of native collagen types IV and VII. (2000) Melanoma Res. 10,427-434.
- Belicchi M, Pisati F, Lopa R, et al. Human skin-derived stem cells migrate throughout forebrain and differentiate into astrocytes after injection into adult mouse brain. J Neurosci Res 2004;77: 475-86.
- Berking C and Herlyn M. Human skin reconstruct models: A new application dor studies of
  melanocyte and melanoma biology. (2001) Histol. Histopathol., 16, 669674.
- Bilbo PR, Nolte CJM, Oleson MA, Mason VS, Parenteau NL: Skin in complex culture: the
  transition from culture phenotype to organotypic phenotype. (1993) *J Toxicol-Cutaneous Ocular Toxicol* 12:183196
- Bittner, M., Meltzer, P., Chen, Y. et al. (2000). Molecular classification of cutaneous malignant melanoma by gene expression profiling. Nature 406, 536–540.
- Boiko, A.D.; Razorenova, O.V.; van de Rijn, M.; Swetter, S.M.; Johnson, D.L.; Ly, D.P.; Butler, P.D.; Yang, G.P.; Joshua, B.; Kaplan, M.J.; Longaker, M.T. & Weissman, I.L. (2010). Human melanoma-initiating cells express neural crest nerve growth factor receptor CD271. Nature. 470;424.
- Brooks, P.C., Stromblad, S., Sanders, L.C., von Schalscha, T.L., Aimes, R.T., Stetler-Stevenson, W.G., Quigley, J.P., and Cheresh, D.A. Localization of matrix metalloproteinase MMP-2 to the surface of invasive cells by interaction with integrin alpha v beta 3. (1996) Cell 85:68393
- Bredel-Geissler A, U. Karbach, S. Walenta, L. Vollrath, W. Mueller-Klieser, Proliferation-associated oxygen consumption and morphology of tumor cells in

monolayer and spheroid culture, J. Cell. Physiol. 153 (1992) 44–52.

- Brocker E.B., Magiera H., Herlyn M. Nerve growth and expression of receptors for nerve growth factor in tumors of melanocyte origin. J. Invest Dermatol. (1991) 96: 662-665.
- Brohem C.A. et al. Artificial skin in prospective: Concepts and applications Pigment Cell

  melanoma Res. (2011) 24(1): 35-50.
- Bullani RR, Huard B, Viard-Leveugle I, Byers HR, Irmler M, Saurat JH et al. Selective expression of FLIP in malignant melanocytic skin lesions. (2001) J Invest Dermatol 117(2): 360-364
- Bustelo, X.R. (2012). Intratumoral stages of metastatic cells: a synthesis of ontogeny, Rho/Rac GTPases, epithelial-mesenchymal transitions, and more. BioEssays 34, 748–759.
- Carlson J. A., MD, FRCP, Slominski A., MD, PhD, Linette G. P. et al. Malignat melanoma 2003. Predisposition, diagnosis, parognosis, and staging. *(*2003) *Pathology Patterns Review. Am J Clin Pathol.*
- Chang, T.T., Hughes-Fulford, M.. Monolayer and spheroid culture of human liver hepatocellular carcinoma cell line cells demonstrate distinct global gene expression patterns and functional phenotypes. (2009) Tissue Eng. Part A 15, 55967.
- Chao M.V,. Neurotrophin receptor: A window into neuronal differentiation. Neuron (1992) 9: 583-595.
- Chao MV and Bothwell M (2002) Neurotrophins: to cleave or not to cleave. *Neuron* 33:9-12
- Chin, L., Garraway, L.A., and Fisher, D.E. (2006). Malignant melanoma: genetics and therapeutics in the genomic era. Genes Dev. 20, 2149–2182
- Civenni, G.; Walter, A.; Kobert, N.; Mihic-Probst, D.; Zipser, M.; Belloni, B.; Seifert, B.; Moch, H.; Dummer, R.; van den Broek, M. & Sommer, L. (2011). Human CD271-Positive Melanoma Stem Cells Associated with Metastasis Establish Tumor Heterogeneity and Long-Term Growth. Cancer Res. Epub ahead of print

- Clary D.O., & Reichardt L.F., An alternatively spliced form of the nerve growth factor receptor TrkA confers an enhanced response to neurotrophin 3. Proc. Natl Acad. Sci. USA (1994) 91: 11133-11137.
- Clark, W.H. Jr (1991). Human cutaneous malignant melanoma as a model for cancer. Cancer Metastasis Rev. 10, 83–88.
- Clark, W.H. Jr, Elder, D.E., Guerry, D.T., Epstein, M.N., Greene, M. H., and Van Horn, M. (1984). A study of tumor progression: the precursor lesions of superficial spreading and nodular melanoma. Hum. Pathol. 15, 1147–1165.
- Clark, E.A., Golub, T.R., Lander, E.S., and Hynes, R.O. (2000). Genomic analysis of metastasis reveals an essential role for RhoC. Nature 406, 532–535.
- Clarke MF, Dicks JE, Dirks PB, et al. Cancer stem cells—perspectives on current status and future directions: AACR Workshop on cancer stem cells. Cancer Res 2006;66:9339–44.
- Cody, N.A., Zietarska, M., Filali-Mouhim, A., Provencher, D.M., Mes-Masson, A.M., Tonin, P.N. Influence of monolayer, spheroid, and tumor growth conditions on chromosome 3 gene expression in tumorigenic epithelial ovarian cancer cell lines. (2008) *BMC Med. Genomics* 1, 34.
- Cohen L.M. Lentigo maligna and lentigo maligna melanoma. (1995) Journal of the American Academy of Dermatology, 33-6:923-939.
- Collins AT, Berry PA, Hyde C, Stower MJ, Maitland NJ. Prospective identification of tumorigenic prostate cancer stem cells. Cancer Res 2005;65:10946-51.
- Coppola V, Kucera J, Palko ME, Martinez-De Velasco J, Lyons WE, Fritzsch B & Tessarollo L (2001) Dissection of NT3 functions in vivo by gene replacement strategy. *Development* 128:4315–4327
- Dang, D., Bamburg, J.R., and Ramos, D.M. (2006). Alphavbeta3 integrin and cofilin modulate K1735 melanoma cell invasion. Exp. Cell Res. 312, 468–477.
- Davies, H., Bignell, G.R., Cox, C. et al. (2002). Mutations of the BRAF gene in human cancer. Nature 417, 949–954.
- Degen, W.G., van Kempen, L.C., Gijzen, E.G., van Groningen, J.J., van Kooyk, Y., Bloemers, H.P., and Swart, G.W. MEMD, a new cell adhesion molecule in

metastasizing human melanoma cell lines, is identical to ALCAM (activated leukocyte cell adhesion molecule). (1998) Am. J. Pathol. 152:80513.

- Demitsu T., Nagato H., Nishimaki K., et al. Melanoma in situ of the penis. (2000) *Journal of the American Academy of Dermatology*, 42:386-388.
- Dick JE. Stem cell concepts renew cancer research. Blood 2008;112: 4793-807.
- Di Chiara T. Ph.D. Clark level and Breslow Thickness: What Do These Measures Mean? About.com Skin Cancer. Clark level and Breslow thickness for melanoma staging and prognosis. 2013.
- Di Marco, E.; Mathor, M.; Bondanza, S.; Cutuli, N.; Marchisio, P.C.; Cancedda, R. & De Luca, M. (1993). Nerve growth factor binds to normal human keratinocytes through high and low affinity receptors and stimulates their growth by a novel autocrine loop. *J Biol Chem*, Vol.268, pp. 22838-22846.
- Donovan MJ, Lin MI, Wiegn P, Ringstedt T, Kraemer R, Hahn R *et al.* (2000) Brain derived neurotrophic factor is an endothelial cell survival factor required for intramyocardial vessel stabilization. *Development* 127: 4531–4540
- Egan MF, Kojima M, Callicott JH, Goldberg TE, Kolachana BS, Bertolino A, Zaitsev E, et al. (2003) The BDNF val66met polymorphism affects activity-dependent secretion of BDNF and human memory and hippocampal function. Cell 112:257–269
- Eskens FA, Dumez H, Hoekstra R, et al. Phase I and pharmacokinetic study of continuous twice weekly intravenous administration of Cilengitide (EMD 121974), a novel inhibitor of the integrins alphavbeta3 and alphavbeta5 in patients with advanced solid tumours. (2003) Eur J Cancer; 39(7): 917926.
- Fang D, Y.J. Kim, C.N. Lee, S. Aggarwal, K. McKinnon, D. Mesmer, J. Norton, C.E. Birse, T. He, S.M. Ruben, P.A. Moore, Expansion of CD133(+) colon cancer cultures retaining stem cell properties to enable cancer stem cell target discovery, Br. J. Cancer 102 (2010) 1265–1275.
- Fang D, Nguyen TK, Leishear K, et al. A tumorigenic subpopulation with stem cell properties in melanomas. Cancer Res 2005;65: 9328-37.
- Fecher, L.A., Cummings, S.D., Keefe, M.J., and Alani, R.M. (2007). Toward a molecular classification of melanoma. J. Clin. Oncol. 25, 1606–1620.

- Folkman J. Angiogenesis. (2006) Annu.Rev. Med. 57:18
- Frade J.M., & Barde Y.A. Nerve growth factor: two receptors, multiple functions. Bioessay (1998) 20: 137-145.
- Frago LM, Leon Y, de la Rosa EJ, Gomez-Munoz A and Varela-Nieto I (1998) Nerve growth factor and ceramides modulate cell death in the early developing inner ear. J. Cell Sci. 111:549–556
- Frank, N.Y., Margaryan, A., Huang, Y., Schatton, T., Waaga-Gasser, A.M., Gasser, M., Sayegh, M.H., Sadee, W., and Frank, M.H. ABCB5-mediated doxorubicin transport and chemoresistance in human malignant melanoma. (2005) Cancer Res. 65:43204333.
- Friedrich J, R. Ebner, L.A. Kunz-Schughart, Experimental anti-tumor therapy in 3-D: spheroids—old hat or new challenge? Int. J. Radiat. Biol. 83 (2007) 849–871.
- Friedman RJ., Rigel DS., Silverman MK. Et al. Malignant melanoma in the 1990s: the continued importance of early detection and the role of phisycian examination and self-examination of the skin. (1991) *CA Cancer J Clin.* 41:201-226.
- Fukuda, A. Khademhosseini, Y. Yeo, X. Yang, J. Yeh, G. Eng, J. Blumling, C.F. Wang, D.S. Kohane, R. Langer, Micromolding of photocrosslinkable chitosan hydrogel for spheroid microarray and co-cultures, Biomaterials 27 (2006) 5259–5267.
- Gaedtke, L., Thoenes, L., Culmsee, C., Mayer, B., Wagner, E.. Proteomic analysis reveals
  differences in protein expression in spheroid versus monolayer cultures of low-passage colon carcinoma cells. (2007) J. Proteome Res. 6, 4111118.
- Gaggioli, C., and Sahai, E. (2007). Melanoma invasion – current knowledge and future directions. Pigment Cell Res. 20, 161–172.
- Garraway L.A., Widlund H.R., Rubin M.A. Et al. Integrative genomic analyses identify MITF as a lineage survival oncogene amplified in malignant melanoma. (2005) *Nature* 436:117-122.
- Gassmann M, J. Fandrey, S. Bichet, M. Wartenberg, H.H. Marti, C. Bauer, R.H. Wenger, H. Acker, Oxygen supply and oxygen-dependent gene expression in

differentiating embryonic stem cells, Proc. Natl. Acad. Sci. U. S. A. 93 (1996) 2867–2872

- Gray-Schopfer, V.C., Da Rocha Dias, S., and Marais, R. (2005). The role of B-RAF in melanoma. Cancer Metastasis Rev. 24, 165–183.
- Gray-Schopfer, V., Wellbrock, C., and Marais, R. (2007a). Melanoma biology and new targeted therapy. Nature 445, 851–857.
- Griffith L.G. And Swarz M.A. Capturing complex 3D tissue physiology in vitro. Nat Rev. Mol.Cell Biol (2006) 7: 211-224.
- Grossman D and Altieri DC. Drug resistance in melanoma: mechanisms, apoptosis, and new potential therapeutic target. (2001) Cancer Metast. Rev. 20:31.
- Guitera P, Menzies SW, Longo C, Cesinaro AM, Scolyer RA and Pellacani G In vivo confocal microscopy for diagnosis of melanoma and basal cell carcinoma using a two-step method: analysis of 710 consecutive clinically equivocal cases. Journal of Investigative Dermatology (2012) 132,2386-2394
- Guitera P, Pellacani G, Longo C *et al*. (2009) *In vivo* reflectance confocal microscopy enhances secondary evaluation of melanocytic lesions. *J Invest Dermatol* 129:131–138
- Haass, N.K., Smalley, K.S., and Herlyn, M. (2004). The role of altered cell–cell communication in melanoma progression. J. Mol. Histol. 35, 309–318.
- He X.L., & Garcia K.C. Structure of nerve growth factor complexed wiyh the shared neurotrophin receptor p75. Sciente (2004) 304: 870-875.
- Held, M.A.; Curley, D.P.; Dankort, D.; McMahon, M.; Muthusamy, V. & Bosenberg, M.W. (2010). Characterization of melanoma cells capable of propagating tumors from a single cell. Cancer Res, 70:388-397.
- Hendrix, M.J., Seftor, E.A., Hess, A.R., and Seftor, R.E. Vasculogenic mimicry and tumour-cell plasticity: lessons from melanoma. (2003) Nat. Rev. Cancer 3:41121.
- Herraman J.L., Menter D.G., Hamanda J., Marchetti D., et al. Madiation of NGF-stimulated extracellular matrix invasion by the human melanoma low-affinity p75 neurotrphin receptor: Melanoma p74 functions independently of TrkA. Mol Biol Cell (1993) 4: 1205-1216

- Hynes R.O. The emergence of integrins: a personal and historical perspective. (2004) Matrix Biol. 23 (6):33340.
- Hoek, K.S., Schlegel, N.C., Brafford, P. et al. (2006). Metastatic potential of melanomas defined by specific gene expression profiles with no BRAF signature. Pigment Cell Res. 19, 290–302.
- Holzmann, B., Gosslar, U., and Bittner, M. Alpha 4 integrins and tumor metastasis. (1998) Curr. Top. Microbiol. Immunol. 231:125141.
- Hsu, M.Y., Shih, D.T., Meier, F.E., Van Belle, P., Hsu, J.Y., Elder, D.E., Buck, C.A., and Herlyn, M. (1998). Adenoviral gene transfer of beta3 integrin subunit induces conversion from radial to vertical growth phase in primary human melanoma. Am. J. Pathol. 153, 1435–1442.
- Huntington, J.T., Shields, J.M., Der, C.J., Wyatt, C.A., Benbow, U., Slingluff, C.L. Jr, and Brinckerhoff, C.E. (2004). Overexpression of collagenase 1 (MMP-1) is mediated by the ERK pathway in invasive melanoma cells: role of BRAF mutation and fibroblast growth factor signaling. J. Biol. Chem. 279, 33168–33176
- Itoh, M., Murata, T., Suzuki, T., Shindoh, M., Nakajima, K., Imai, K., and Yoshida, K. Requirement of STAT3 activation for maximal collagenase-1 (MMP-1) induction by epidermal growth factor and malignant characteristics in T24 bladder cancer cells. (2006) Oncogene 25, 1195204.
- James, William D.; Berger, Timothy G.; et al. (2006). Andrews'Diseased of the Skin: clinical dermatology. Saunders Elsevier. Pp.694-9
- Jemal A, Siegel R, Xu J, Ward E (2010) Cancer statistics, 2010. CA Cancer J Clin 60: 277–300.
- Kaplan D.R & Miller F.D. Neurobiology: a move to sort life from death. Nature (2004) 427- 798-799.
- Kiene P., Petres-Dunsche & Folster-Holst R. Pigmented pedunculated malignant melanoma. A rare variant of nodular melanoma. (1995) British Journal of Dermatology, 133:300-302.
- Kim S.H, H.J. Kuh, C.R. Dass, The reciprocal interaction: chemotherapy and tumor microenvironment, Curr. Drug Discov. Technol. 8 (2011) 102–106.
- Kelly P, Dakic A, Adams J, Nutt S, Strasser A. Tumor growth need not be driven

by rare cancer stem cells. Science 2007; 318:1722.

- Kelm J.M, M. Fussenegger, Scaffold-free cell delivery for use in regenerative medicine, Adv. Drug Deliv. Rev. 62 (2010) 753–764
- Klein WM, Wu BP, Zhao S, Wu H, Klein-Szanto AJ, Tahan SR. Increased expression of stem cell markers in malignant melanoma. Mod Pathol 2007;20:102-7.
- Korff T, H.G. Augustin, Integration of endothelial cells in multicellular spheroids prevents apoptosis and induces differentiation, J. Cell Biol. 143 (1998) 1341–1352.
- Kortylewski, M., Jove, R., and Yu, H. Targeting STAT3 affects melanoma on multiple fronts. (2005). Cancer Metastasis Rev. 24, 31527.
- Krohn A, Y.H. Song, F. Muehlberg, L. Droll, C. Beckmann, E. Alt, CXCR4 receptor positive spheroid forming cells are responsible for tumor invasion in vitro, Cancer Lett. 280 (2009) 65–71.
- Kruttgen, A.; Schneider, I. & Weis, J. (2006). The dark side of the NGF family: neurotrophins in neoplasias. *Brain Pathol*, Vol.16, No.4, pp. 304-310.
- Kunz-Schughart LA, K. Groebe, W. Mueller-Klieser, Three-dimensional cell culture induces novel proliferative and metabolic alterations associated with oncogenic transformation, Int. J. Cancer 66 (1996) 578–586.
- Kunz-Schughart LA, J.P. Freyer, F. Hofstaedter, R. Ebner, The use of 3-D cultures for high-throughput screening: the multicellular spheroid model, J. Biomol. Screen. 9 (2004) 273–285.
- Kuphal, S., Bauer, R., and Bosserhoff, A.K. (2005a). Integrin signaling in malignant melanoma. Cancer Metastasis Rev. 24, 195–222.
- Kuratomi, Y., Nomizu, M., Nielsen, P.K., Tanaka, K., Song, S.Y., Kleinman, H.K., and Yamada, Y. (1999). Identification of metastasis-promoting sequences in the mouse laminin alpha 1 chain. Exp. Cell Res. 249, 386–395.
- Kuroyanagi Y, Shiraishi A, Tanaka M, Kageyama H, Ootage N, Shioya N: Cytotoxicity tests for antimicrobial agents using cultured skin substitutes fixed at interface of air and culture medium. (1996) *J Biomater Sci Polym Ed.* 7:1005015
- Haass, N.K., Smalley, K.S.M. & Herlyn, M. The role of altered cell-cell

comunication in
melanoma progression. (2004) J.Mol.Histol. 35:309-318.

- Hazan RB, PhillipsGR, Qiao RF, Norton L and Aaronson SA. (2000). J. Cell Biol., 148, 77990.
- Hegerfeldt, Y., Tusch, M., Brocker, E.B., and Friedl, P. Collective cell movement in primary melanoma explants: plasticity of cell-cell interaction, beta1-integrin function, and migration strategies. (2002) Cancer Res. 62:2125130.
- Hirschberg, H., Sun, C.H., Krasieva, T., Madsen, S.J. Effects of ALA-mediated photodynamic therapy on the invasiveness of human glioma cells. (2006) Lasers Surg. Med. 38, 93945.
- Hirschhaeuser F, H. Menne, C. Dittfeld, J. West, W. Mueller-Klieser, L.A. Kunz-Schughart, Multicellular tumor spheroids: an underestimated tool is catching up again, J. Biotechnol. 148 (2010) 3–15.
- Huang GS, L.G. Dai, B.L. Yen, S.H. Hsu, Spheroid formation of mesenchymal stem cells on chitosan and chitosan–hyaluronan membranes, Biomaterials 32 (2011) 6929–6945.
- Huang EJ and Reichardt LF (2003) Trk receptors: roles in neuronal signal transduction. *Annu Rev Biochem* 72:609-42
- Huttenbach, Y.; Prieto, V.G. & Reed, J.A. (2002). Desmoplastic and spindle cell melanomas
  express protein markers of the neural crest but not of later committed stages of Schwann cell differentiation. *J Cutan Pathos.* 29:562-568.
- Iwamoto, S.; Burrows, R.C.; Agoff, S.N.; Piepkorn, M.; Bothwell, M. & Schmidt, R. (2001). The p75 neurotrophin receptor, relative to other Schwann cell and melanoma markers, is abundantly Expressed in spindled melanomas. *Am J Dermatopathol.* 23:288-294.
- Indo Y (2001) Molecular basis of congenital insensitivity to pain with anhidrosis (CIPA): mutations and polymorphisms in TRKA (NTRK1) gene encoding the receptor tyrosine kinase for nerve growth factor. Hum. Mutat. 18:462–471.
- Ingram M, G.B. Techy, R. Saroufeem, O. Yazan, K.S. Narayan, T.J. Goodwin, G.F. Spaulding, Three-dimensional growth patterns of various human tumor cell

lines in simulated microgravity of a NASA bioreactor, In Vitro Cell. Dev. Biol. Anim. 33 (1997) 459–466.

- Jacobson MD, Weil,M & Raff MC (1997) Programmed cell death in animal development. *Cell* 88:347–354.
- Johnson, J.P., Rummel, M.M., Rothbacher, U., and Sers, C. MUC18: A cell adhesion molecule with a potential role in tumor growth and tumor cell dissemination. (1996) Curr. Top. Microbiol. Immunol. 213:9505.
- Lambert, B., De, R.L., De, V.F., Slegers, G., De, G.V., Van De, W.C., Thierens, H.. Assessment of supra-additive effects of cytotoxic drugs and low dose rate irradiation in an in vitro model for hepatocellular carcinoma. (2006) Can. J. Physiol. Pharmacol. 84, 1021028.
- Langley RG, Walsh N, Sutherland AE et al. (2007) The diagnostic accuracy of in vivo confocal scanning laser microscopy compared to dermoscopy of benign and malignant melanocytic lesions: a prospective study. Dermatology 215:365–372
- Lapidot T, Sirard C, Vormoor J, et al. A cell initiating human acute myeloid leukaemia after transplantation into SCID mice. Nature 1994;367:645–8.
- Lee, J.T.; Li,L.; Brafford , P.A; van den Eijnden, M.; Halloran, M.B.; Sproesser, K.; Haas, N.K.; Smalley, K.S.; Tsai, J.; Bollag, G.; et al. PLX4023, a potent inhibitor of the B-Raf V600E oncogene, selectively inhibits V600E-positive melanomas. Pigment Cell melanoma Res. 2010, 23, 820-827
- Lens MB, Dawes M (2004) Global perspectives of contemporary epidemiological trends of cutaneous malignant melanoma. Br J Dermatol 150: 179–185.
- Levi-Montalcini, R. (1987) The nerve growth factor 35 years later. *Science* 237, 1154–1162.
- Levy C., Khaled M. & Fisher D.E. MITF: master regulator of melanocyte development and melanoma oncogene. (2006) *Trends Mol. Med.* 12:406-414.
- Li G., Satyamoorthy K., Herlyn M. Dynamics of cell interactions and comunications during
  melanoma development. (2002) Crit Rev Oral Biol Med 13(1):62-70.
- Li F, Ambrosini G, Chu EY, Plescia J, Tognin S, Marchisio PC, et al. Control of apoptosis and mitotic spindle checkpoint by survivin. (1998) Nature.

10;396(6711):580-4.

- Liang, S., Sharma, A., Peng, H.H., Robertson, G., and Dong, C. (2007). Targeting mutant (V600E) B-Raf in melanoma interrupts immunoediting of leukocyte functions and melanoma extravasation. Cancer Res. 67, 5814–5820.
- Limat A, Mauri D, Hunziker T: Successful treatment of chronic leg ulcers with epidermal

  equivalents generated from cultured autologous outer root sheath cells. (1996) J Invest Dermatol 107:12835.
- Lin MI, Das I, Schwartz GM, Tsoulfas P, Mikawa T & Hempstead BL (2000) Trk C receptor signaling regulates cardiac myocyte proliferation during early heart development in vivo. Dev. Biol. 226: 180–191
- Lin R.Z, H.Y. Chang, Recent advances in three-dimensional multicellular spheroid culture for biomedical research, Biotechnol. J. 3 (2008) 1172–1184.
- Linggi MS, Burke TL, Williams BB, Harrington A, Kraemer R, Hempstead BL, Yoon SO and Carter BD (2005) Neurotrophin receptor interacting factor (NRIF) is an essential mediator of signaling by the p75 neurotrophin receptor. *J. Biol.Chem.* 280: 13 801–13 808
- Lomuto, M., Calabrese, P., and Giuliani, A. (2004). Prognostic signs in melanoma: state of the art. J. Eur. Acad. Dermatol. Venereol. 18, 291–300
- Lotze MT: Melanoma. In: DeVita VT Jr, Hellman S, Rosenberg SA, eds.: Cancer: Principles and Practice of Oncology. 6th ed. Philadelphia, Pa: Lippincott Williams & Wilkins. (2001) 2022-2028.
- Luberg K., Wong J., Weickert C.S. & Timmusk T. Human TrkB gene: novel alternative transcripts, protein isoforms and expression pattern in the prefrontal cerebral cortex during postnatal development. J. Neurochem. (2010) 113: 952-964.
- Madhunapantula, S.V., and Robertson, G.P. (2009). The PTEN-AKT3 signaling cascade as a therapeutic target in melanoma. Pigment Cell Melanoma Res. 22, 400–419.
- Makabe, T., Saiki, I., Murata, J., Ohdate, Y., Kawase, Y., Taguchi, Y., Shimojo, T., Kimizuka, F., Kato, I., and Azuma, I. (1990). Modulation of haptotactic

migration of metastatic melanoma cells by the interaction between heparin and heparin-binding domain of fibronectin. J. Biol. Chem. 265, 14270–14276

- Marchetti D., Menter D, Jin L., Nakajima M., Nicolson G.L. Nerve growth factor effects on human and mause melanoma cell invasion and heparanase production. Int J Cancer (1993) 55: 692-699.
- Marchetti D, Parikh N, Sudol M, Gallick GE. 1998. Stimulation of the protein tyrosine kinase c-Yes but not c-Src by neurotrophins in human brain-metastatic melanoma cells. Oncogene 16:3253260.
- Marchetti D, Nicolson GL. 2001. Human heparanase: A molecular determinant of brain metastasis.Adv Enz Reg 41:34359.
- Marchetti, D.; Denkins, Y.; Reiland, J.; Greiter-Wilke, A.; Galjour, J.; Murry, B.; Blust, J. & Roy, M. (2003). Brain-metastatic melanoma: a neurotrophic perspective. Pathol Oncol Res. 9: 14758
- Marconi, A.; Vaschieri, C.; Zanoli, S.; Giannetti, A. & Pincelli, C. (1999). Nerve growth factor protects human keratinocytes from ultraviolet-B-induced apoptosis. *J Invest Dermatol*, Vol.113, pp. 920-927.
- Marconi A., Terracina M., Fila C., Franchi J., BontF., Romagnoli G., Maurelli R., Failla C.M., Dumas M., & Pincelli C. Expression and function of neurotrophins and their receptors in cultured human keratinocytes. J. Invest Dermatol (2003) 121: 1515-21. Erratum in: J. Invest Dermatol 2004; 123-803.
- Marconi A., Panza M.c:, Bonnet-DFuquennoy M., Lazou K., Kurfurst R., Truzzi F., Lotti R., De Santis G., Dumas M., BontF & Pincelli C. Espression and function of neurotrophins and their receptors in human melanocytes. Int J Cosmet Sci (2006) 28: 255-261.
- Marks R., The changing incidence and mortallity of melanoma in Australia (2002) Recent Result Cancer Res. 160:113-21.
- Mattei S, Colombo MP, Melani C, Silvani A, Parmiani G, Herlyn M. 1994. Expression of

  cytokine/growth factors and their receptors in human melanoma and melanocytes. Int J Cancer 56:85357.
- Meakin S.O., Suter U. Drinkwater C.C, Welcher A.A.& Shooter E.M. The rat trk

prooncogene product exhibits proprietes characteristic of the slow nerve growth factor receptor. Proc. Natl Acad. Sci. USA. (1992) 89: 2374-2378.

- Meier F, Satyamoorthy K, Nesbit M, Hsu MY, Schittek B, Garbe C, et al. Molecular events in melanoma development and progression. (1998) Front Biosci 3:1005-1010.
- Melchiori, A., Mortarini, R., Carlone, S., Marchisio, P.C., Anichini, A., Noonan, D.M., and Albini, A. (1995). The alpha 3 beta 1 integrin is involved in melanoma cell migration and invasion. Exp. Cell Res. 219, 233–242.
- Miller, A.J., and Mihm, M.C. Jr (2006). Melanoma. N. Engl. J. Med. 355, 51–65.
- Monzani E, Facchetti F, Galmozzi E, et al. Melanoma contains CD133 and ABCG2 positive cells with enhanced tumourigenic potential. Eur J Cancer 2007;43:935-46.
- Mueller-Klieser, W.. Tumor biology and experimental therapeutics. (2000) *Crit. Rev. Hematol. Oncol.* 36, 12339.
- Murray S.S., Perez P., Lee R., Hempstead B.L. & Chao M.V. A nover p75 neurotrophin receptorrelated protein, NRH2, regulates nerve growth factor binding to the TrkA receptor. J Neurosi (2004) 24: 2742-2749.
- Nakazawa K, Nakazawa H, Sahuc F, Lepavec A, Collombel C, Damour O: Pigmented human skin equivalent: new method of reconstitution by grafting an epithelial sheet onto a non-contractile dermal equivalent. (1997) *Pigment Cell Res* 10:38290.
- Niu G., Wright K.L., Huang M., et al. Constitutive Stat3 activity up-regulates VEGF expression and tumor angiogenesis. (2002) *Oncogene* 21, 2000-2008.
- Nykajaer A., Lee R., Teng K.K et al. Sortilin is essential for pro-NGF-induced neuronal cell deadth. Nature (2004) 427: No.6977 pp. 843-848.
- O'Brien CA, Pollett A, Gallinger S, Dick JE. A human colon cancer cell capable of initiating tumor growth in immunodeficient mice. Nature 2007;445:106–10.
- Olive P.L, R.E. Durand, Detection of hypoxic cells in a murine tumor with the use of the comet assay, J. Natl. Cancer Inst. 84 (1992) 707–711
- Omholt K., Krockel D., Ringborg U. & Hansson J. Mutation of PIK3CA are rare in cutaneous melanoma. (2006) *Melanoma Res.* 16:197-200.

- Ong S.M, C.Zhang,Y.C. Toh, S.H. Kim, H.L.Foo,C.H. Tan,D.van Noort, S. Park,H.Yu, A gel-free 3D microfluidic cell culture system, Biomaterials 29 (2008) 3237–3244.
- Orgaz, J.L., and Sanz-Moreno, V. (2013). Emerging molecular targets in melanoma invasion and metastasis. Pigment Cell Melanoma Res. 26, 39–57.
- Oloumi A., W. Lam, J.P. Banath, P.L. Olive, Identification of genes differentially expressed in V79 cells grown as multicell spheroids, Int. J. Radiat. Biol. 78 (2002) 483–492.
- Papatsoris, A.G.; Liolitsa, D. & Deliveliotis, C. (2007). Manipulation of the nerve growth factor network in prostate cancer. *Expert Opin Investig Drugs.* 16:303-309.
- Peacocke, M.; Yaar, M.; Mansur, C.P.; Chao, M.V. & Gilchrest, B.A. (1988). Induction of nerve growth factor receptor on cultured human melanocytes. *Proc Natl Acad Sci USA*, Vol.85, pp. 5282-5286.
- Pellacani G, Cesinaro AM, Seidenari S (2005) Reflectance-mode confocal microscopy of pigmented skin lesions—improvement in melanoma diagnostic specificity. *J Am Acad Dermatol* 53:979–985
- Pellacani G, Guitera P, Longo C *et al*. (2007) The impact of *in vivo*reflectance confocal microscopy for the diagnostic accuracy of melanoma and equivocal melanocytic lesions. *J Invest Dermatol* 127:2759–2765
- Pincelli, C.; Fantini, F. & Giannetti, A. (1994). Nerve growth factor and the skin. Int J Fermato, Vol.33, pp. 308-312.
- Pincelli, C.; Haake, A.R.; Benassi, L.; Grassilli, E.; Magnoni, C.; Ottani, D.; Polakowska, R.; Franceschi, C. & Giannetti, A. (1997). Autocrine nerve growth factor protects human keratinocytes from apoptosis through its high affinity receptor (TRK): a role for BCL-2. J Invest Dermatol, 109:757-764.
- Pincelli C. & Yaar M. Nerve growth factor: its significance in cutaneous biology. (1997) J. Investing Dermatol Symp Proc 2:31-6.
- Plotnick H., Rachmaninoff N., and VandenBerg Jr. H. J. Polypoid melanoma: a virulent variant of nodular melanoma. (1990) Journal of the American Academy od dermatology, 23:880-884.

- Pollock, P.M., Harper, U.L., Hansen, K.S. et al. (2003). High frequency of BRAF mutations in nevi. Nat. Genet. 33, 19–20.
- Ponec M, Kempenaar J: The use of human skin recombinants as an in vitro model for testing the irritation potential of cutaneous irritants. (1995) *Skin Pharmacol.* 8:499
- Q. Zhang, A.L. Nguyen, S. Shi, C. Hill, P. Wilder-Smith, T.B. Krasieva, A.D. Le, Three-dimensional spheroid culture of human gingiva-derived mesenchymal stem cells enhances mitigation of chemotherapy-induced oral mucositis, Stem Cells Dev. 21 (2012) 937–947
- Quatresooz P., Pierard G.E., Pierard-Franchimont C. et al. Molecular pathways supporting the proliferation staging of malignant melanoma. (2009) International Journal of Molecular Medicine. 24:29501.
- Quintana E, Shackleton M, Sabel MS, Fullen DR, Johnson TM, Morrison SJ. Efficient tumor formation by single human melanoma cells. Nature 2008;456:593–8.
- Quintana E, Shackleton M, Foster HR, et al. Phenotypic heterogeneity among tumorigenic melanoma cells from patients that is reversible and not hierarchically organized. Cancer Cell 2010;18:510-23.
- Ramakrishnan V, Bhaskar V, Law DA, et al. Preclinical evaluation of an anti-alpha5beta1 integrin antibody as a novel anti-angiogenic agent. (2006) J Exp Ther Oncol. 5(4):27386
- Rangarajan A., Hong S.J. Gifford A. and Weinberg R.A. Species.and cell-type-specific requirements for cellular trasformation. Cancer Cell (2004) 6: 171-183.
- Rappa G, Fodstad O, Lorico A. The stem cell-associated antigen CD133 (Prominin-1) is a molecular therapeutic target for metastatic melanoma. Stem Cells 2008;26:3008-17.
- Reed R. J. Acral lentiginous melanoma. (1976) New concepts in surgical pathology of the skin, 89-90.
- Reichardt L.F. Neurotrophin-regulated signalling pathways. Philos Trans R Soc Lond B Biol Sci (2006) 2: 1545-1564.
- Rennekampff H.O, Kiessig V, Hansbrough J.F: Current concepts in the

development of cultured skin replacements. (1996) *J Surg Res.* 62: 28895

- Ricci-Vitiani L, Lombardi DG, Pilozzi E, et al. Identification and expansion of human colon-cancer-initiating cells. Nature 2007;445: 111-5.
- Roesch A, Fukunaga-Kalabis M, Schmidt EC, et al. A temporarily distinct subpopulation of slow-cycling melanoma cells is required for continuous tumor growth. Cell 2010;141:583-94.
- Ronan S. G., Eng A. M., Briele H. A., Walker M. J. and Das Gupta T. K. Malignant melanoma of the female genitalia. (1990) Journal of the American Academy of Dermatology, 22:428-435.
- Rothhammer, T., Bataille, F., Spruss, T., Eissner, G., and Bosserhoff, A.K. Functional implication of BMP4 expression on angiogenesis in malignant melanoma. (2007) Oncogene 26:4158170.
- Sabolinski ML, Alvarez O, Auletta M, Mulder G, Parenteau NL: Cultured skin as a smart material for healing wounds: experience in venous ulcers. (1996) *Biomaterials.* 17:31120
- Sahai, E., and Marshall, C.J. (2002). RHO-GTPases and cancer. Nat. Rev. *Cancer* 2, 13342.
- Saltier A.R. And Decker S.J. Cellular mechanisms of signal trasduction for neurotrophins. Bioessays (1994) 16: 405-411.
- Sariola H. The neurotrophic factors in nonneuronal tissues. Cell Mol Life Sci (2001) 58: 1061-6.
- Satyamoorthy K, Chehab NH, Waterman MJ, Lien MC, El-Deiry WS, Herlyn M and Halazonetis TD. (2000a). Cell Growth Differ. 11:46774.
- Seftor, R.E., Seftor, E.A., and Hendrix, M.J. (1999). Molecular role(s) for integrins in human melanoma invasion. Cancer Metastasis Rev. 18, 359–375.
- Seftor, E.A., Brown, K.M., Chin, L. et al. (2005). Epigenetic transdifferentiation of normal melanocytes by a metastatic melanoma microenvironment. Cancer Res. 65, 10164–10169.
- Schmitt CA, Fridman JS, Yang M, Baranov E, Hoffman RM and Lowe SW. (2002a). Cancer Cell, 1, 28998.
- Schmitt CA, Fridman JS, Yang M, Lee S, Baranov E, Hoffman RM and Lowe

SW. (2002b). Cell, 109, 33546.

- Shaw, R.J., and Cantley, L.C. (2006). Ras, PI(3)K and mTOR signalling controls tumour cell growth. Nature 441, 424–430.
- Shekhar M.P, Drug resistance: challenges to effective therapy, Curr. Cancer Drug Targets 11 (2011) 613–623.
- Shimada, M., Yamashita, Y., Tanaka, S., Shirabe, K., Nakazawa, K., Ijima, H., Sakiyama, R., Fukuda, J., Funatsu, K., Sugimachi, K.. Characteristic gene expression induced by polyurethane foam/spheroid culture of hepatoma cell line, Hep G2 as a promising cell source for bioartificial liver. (2007) Hepatogastroenterology 54, 81420.
- Shmelkov SV, St Clair R, Lyden D, Rafii S. AC133/CD133/Prominin-1. Int J Biochem Cell Biol 2005;37:715-9.
- Shonukan, O.; Bagayogo, I.; McCrea, P.; Chao, M. & Hempstead, B. (2003). Neurotrophininduced melanoma cell migration is mediated through the actin-bundling protein fascin. *Oncogene.* 22:3616-3623.
- Schor NF (2005) The p75 neurotrophin receptor in human development and disease. Prog. Neurobiol. 77: 201–214
- Siegel R, Naishadham D, Jemal A. Cancer statistics, 2013. CA Cancer J Clin (2013) 63(1):11-30. doi:10.3322/caac.21166
- Simonetti O, Hoogstrate JA, Bialik W, Kempenaar JA, Schrijvers AHGJ, Bodde HE, Ponec M: Visualisation of diffusion pathways across the stratum corneum of native and in vitro reconstructed epidermis by confocal laser scanning microscopy. (1995) *Arch Dermatol Res.* 287:46573
- Simpson, A.J., Caballero, O.L., Jungbluth, A., Chen, Y.T., and Old, L.J. Cancer / testis antigens, gametogenesis and cancer. (2005) Nat. Rev. Cancer 5:61525.
- Singh SK, Clarke ID, Terasaki M, et al. Identification of a cancer stem cell in human brain tumors. Cancer Res 2003;63:5821–8.
- Slominski, A., Tobin, D.J., Shibahara, S., and Wortsman, J. (2004). Melanin pigmentation in mammalian skin and its hormonal regulation. Physiol. Rev. 84, 1155–1228.

- Sodunke T.R, K.K. Turner, S.A. Caldwell, K.W. McBride, M.J. Reginato, H.M. Noh, Micropatterns of matrigel for three-dimensional epithelial cultures, Biomaterials 28 (2007) 4006–4016
- Soengas M.S & Lowe S.W. Apoptosis and melanoma chemoresistence. (2003) Oncogene 22:3138-3151.
- Stahl, J.M., Sharma, A., Cheung, M., Zimmerman, M., Cheng, J.Q., Bosenberg, M.W., Kester, M., Sandirasegarane, L., and Robertson, G.P. (2004). Deregulated Akt3 activity promotes development of malignant melanoma. Cancer Res. 64, 7002–7010.
- Stemple D.L., Anderson D.J. Isolation of a ste cell for neurons and glia from the mammalial neural crest. Cell (1992) 71: 973-85.
- Strohmaier C., Carter B.D., Urfer R., Barde Y.A. & Dechant G. A splice variant of the neurotrophin receptor TrkB with increased specificity for brian-derived neurotrophic factor. EMBO J. (1996) 15: 3332-3337.
- Sumimoto, H., Miyagishi, M., Miyoshi, H., Yamagata, S., Shimizu, A., Taira, K., and Kawakami, Y. (2004). Inhibition of growth and invasive ability of melanoma by inactivation of mutated BRAF with lentivirus-mediated RNA interference. Oncogene 23, 6031–6039.
- Sutherland RM, Cell and environment interactions in tumor microregions: the multicell spheroid model, Science 240 (1988) 177–184.
- Tarhini A.A, & Agarwala S.S. Cutaneous melnaoma: available therapy for metastatic disease (2006) Dermathol. Ther. 19, 19.25.
- Tauszing-Delamasure S., Yu L.Y., Cabrera J.R. Et al. The TrkC receptor induces apoptosis when the dependence receptor notion meets the neurotrophin paradigm. Proc natl Acad Sci USA (2007)14: 104 13361-13366.
- Teng K.K., & Hempstead B.L. Neurotrophins and their receptors: Signalling trios in complex biological system. Cell Mol Life Sci (2004) 61: 35-48.
- Thiele, C.J.; Li, Z. & McKee, A.E. (2009). On Trk--the TrkB signal transduction pathway is an increasingly important target in cancer biology. Clin Cancer Res, 15:5962-5967.
- Thies, A., Schachner, M., Moll, I., Berger, J., Schulze, H.J., Brunner, G., and

Schumacher, U. Overexpression of the cell adhesion molecule L1 is associated with metastasis in cutaneous malignant melanoma. (2002b) Eur. J. Cancer 38:1708716.

- Thoenen H & Barde Y A (1980) Physiology of nerve growth factor. *Physiol. Rev*. 60:1284–1335.
- Thomas L, Tranchand P, Berard F, et al. Semiological value of ABCDE criteria in the diagnoses of cutaneous pigmentes tumors. (1998) Dermatology. 197:11-17
- Tiberio, R.; Marconi, A.; Fila, C.; Fumelli, C.; Pignatta, M.; Krajewski, S.; Giannetti, A.; Reed, J.C. & Pincelli, C. (2002). Keratinocytes enriched for stem cells are protected from anoikis via an integrin signaling pathway in a Bcl-2 dependent manner. FEBS Lett, Vol.524, pp. 139-144.
- Timmins, N.E., Dietmair, S., Nielsen, L.K.. Hanging-drop multicellular spheroids as a model of tumour angiogenesis. (2004) Angiogenesis 7, 9703.
- Tschopp J, Irmler M and Thom M. Inhibition of fas death signals by FLIPs. (1998) Curr. Opin. Immunol. 10: 552-558
- Torisawa Y.S, B.H. Chueh, D. Huh, P. Ramamurthy, T.M. Roth, K.F. Barald, S. Takayama, Efficient formation of uniform-sized embryoid bodies using a compartmentalized microchannel device, Lab. Chip 7 (2007) 770–776
- Torisawa Y.S, A. Takagi, H. Shiku, T. Yasukawa, T. Matsue, A multicellular spheroid-based drug sensitivity test by scanning electrochemical microscopy, Oncol. Rep. 13 (2005) 1107–1112.
- Truzzi, F.; Marconi, A.; Lotti, R.; Dallaglio, K.; French, L.E. & Hempstead, B.L. & Pincelli, C. (2008). Neurotrophins and their receptors stimulate melanoma cell proliferation and migration. J Invest Dermatol. 128:2031-2040.
- Truzzi, F.; Marconi, A.; Atzei, P.; Panza, M.C.; Lotti, R.; Dallaglio, K.; Tiberio, R.; Palazzo, E.; Vaschieri C. & Pincelli, C. p75 neurotrophin receptor mediates apoptosis in transit-amplifying cells and its overexpression restores cell death in psoriatic keratinocytes. Cell Death Differ. (2011) 18:948-958.
- Tsai, J; Lee, J T ; Wang, W; Zhang, J.; Cho, H.; Mamo, S.; Bremer, R.; Gilette, S.; Kong, J.; Haass, N.K; et al. Discovery of a selective inhibitor of oncogenic B-Raf kinase with potent antimelanoma activity. Proc. Natl. Acad Sci. USA 2008,

105, 3041-3046

- Tsukamoto E, Hashimoto Y, Kanekura K, Niikura T, Aiso S and Nishimoto I (2003) Characterization of the toxic mechanism triggered by Alzheimer's amyloid-b peptides via p75 neurotrophin receptor in neuronal hybrid cells. *J. Neurosci. Res*. 73: 627–636
- Ungrin M.D, C. Joshi, A. Nica, C. Bauwens, P.W. Zandstra, Reproducible, ultra high-throughput formation of multicellular organization from single cell suspension-derived human embryonic stem cell aggregates, PLoS One 3 (2008) e1565
- Ugurel S, Seiter S, Rappl G, Stark A, Tilgen W, Reinhold U. Heterogenous susceptibility to CD95-induced apoptosis in melanoma cells correlates with bcl-2 and bcl-x expression and is sensitive to modulation by interferon-gamma. (1999) Int J Cancer. 82(5):727-36.
- Ultsch M.H.; Weismann C., Simmons L.C., Henrich J., Yang M., Reilly D., Bass S.H., & de Vos A.M. Crystal structure of the neurotrophin-binding domain of TrkA, TrkB and TrkC. J Mol Biol. (1999) 290: 149-159.
- Valastyan, S., and Weinberg, R.A. (2011). Tumor metastasis: molecular insights and evolving paradigms. Cell 147, 275–292.
- Van Belle, P.A., Elenitsas, R., Satyamoorthy, K. et al. (1999). Progression-related expression of beta3 integrin in melanomas and nevi. Hum. Pathol. 30, 562–567.
- Van Kempen, L.C., Van Den Oord, J.J., Van Muijen, G.N., Weidle, U.H., Bloemers, H.P., and Swart, G.W. Activated leukocyte cell adhesion molecule / CD166, a marker of tumor progression in primary malignant melanoma of the skin. (2000) Am. J. Pathol. 156:76974.
- Vega, F.M., and Ridley, A.J. (2008). Rho GTPases in cancer cell biology. FEBS Lett. 582:2093101.
- Valyi-Nagy I.T., Murphy G.F., Mancianti M.L., Whitaker D. and Herlyn M**.** Phenotypes and

  interactions of human melanocytes and keratinocytes in an epidermal rewnstniction model. (1990) *Lab. Invest.* 62, 31 4-324.
- Villanueva, J., and Herlyn, M. (2009). Melanoma. In Encyclopedia of Life

Sciences (ELS), (Chichester: John Wiley & Sons, Ltd), pp. 1–9.

- Visvader JE, Lindeman GJ. Cancer stem cells in solid tumors: accumulating, evidence and unresolved questions. Nat Rev Cancer 2008; 8:755–68.
- Vucic D, Stennicke HR, Pisabarro MT, Salvesen GS, Dixit VM ML-IAP, a novel inhibitor of apoptosis that is preferentially expressed in human melanomas. (2000) Curr Biol 10(21):1359- 1366.
- Walch, E.T.; Albino, A.P. & Marchetti, D. (1999). Correlation of overexpression of the lowaffinity p75 neurotrophin receptor with augmented invasion and heparanase production in human malignant melanoma cells. *Int J Cancer*, Vol.82, pp. 11220.
- Wanebo HJ, Argiris A, Bergsland E, et al. Targeting growth factors and angiogenesis; using small molecules in malignancy. (2006) Cancer Metastasis Rev. 25(2):27992.
- Wang J.J., Tapinat A., Ethell D.W et al. Phosphorylation of the common neurotrophin receptor p75 by p38beta2 kinase NF-kappaB and AP-1 activities. J. Mol Neurosci (2000) 15: 19-29.
- Wartenberg M, F. Donmez, F.C. Ling, H. Acker, J. Hescheler, H. Sauer, Tumor-induced angiogenesis studied in confrontation cultures of multicellular tumor spheroids and embryoid bodies grown from pluripotent embryonic stem cells, FASEB J. 15 (2001) 995–1005.
- Weeraratna, A.T., Jiang, Y., Hostetter, G., Rosenblatt, K., Duray, P., Bittner, M., and Trent, J.M. Wnt5a signaling directly affects cell motility and invasion of metastatic melanoma. (2002) Cancer Cell 1:27988.
- Wellbrock, C., and Marais, R. (2005). Elevated expression of MITF counteracts B-RAF-stimulated melanocyte and melanoma cell proliferation. J. Cell Biol. 170, 703–708.
- Wellbrock, C., Ogilvie, L., Hedley, D., Karasarides, M., Martin, J., Niculescu-Duvaz, D., Springer, C.J., and Marais, R. (2004). V599EB-RAF is an oncogene in melanocytes. Cancer Res. 64, 2338–2342.
- Woods, D., Cherwinski, H., Venetsanakos, E., Bhat, A., Gysin, S.,Humbert, M., Bray, P.F., Saylor, V.L., and Mcmahon, M. (2001). Induction of beta3-integrin

gene expression by sustained activation of the Ras-regulated Raf-MEK-extracellular signal-regulated kinase signaling pathway. Mol. Cell. Biol. 21, 3192–3205.

- Wu, H., Goel, V., and Haluska, F.G. (2003). PTEN signaling pathways in melanoma. Oncogene 22, 3113–3122.
- Wu L.Y, D. Di Carlo, L.P. Lee, Microfluidic self-assembly of tumor spheroids for anticancer drug discovery, Biomed. Microdevices 10 (2008) 197–202
- Wurm EM, Soyer HP. (2010), Scanning for melanoma. Australian prescribers(33): 150-5
- Zietarska, M., Maugard, C.M., Filali-Mouhim, A., Am-Fahmy, M., Tonin, P.N., Provencher, D.M., Mes-Masson, A.M. Molecular description of a 3D in vitro model for the study of epithelial ovarian cancer (EOC).(2007) *Mol. Carcinog.* 46, 87285.
- Zettersten E, Shaikh L, Ramirez R, et al. Prognostic factors in primary cutaneous melanoma. (2003) *Surg Clin North Am.* 83:61-75.
- Yaar, M., Eller, M.S.; DiBenedetto, P.; Reenstra, W.R.; Zhai, S.; McQuaid, T.; Archambault, M. & Gilchrest, B.A. (1994). The trk family of receptors mediates nerve growth factor and neurotrophin-3 effects in melanocytes. *J Clin Invest.* 94:1550-1562.
- Yamashita, Y., Shimada, M., Harimoto, N., Tanaka, S., Shirabe, K., Ijima, H., Nakazawa, K., Fukuda, J., Funatsu, K., Maehara, Y.. cDNA microarray analysis in hepatocyte differentiation in Huh 7 cells. (2004) Cell Transplant. 13, 79399.
- Yeiser EC, Rutkoski NJ, Naito A, Inoue J and Carter BD (2004) Neurotrophin signaling through the p75 receptor is deficient in traf6-/- mice. *J. Neurosci*. 24, 10 521–10 529.
- Yu, H., Pardoll, D., and Jove, R. STATs in cancer inflammation and immunity: a leading role for STAT3. (2009) Nat. Rev. Cancer 9:79809.
- You MJ, Castrillon DH, Bastian BC, O'agan RC, Bosenberg MW, Parsons R, Chin L and DePinho RA. (2002). Proc. Natl. Acad. Sci. USA, 99, 1455460.

7. Ringraziamenti

Vorrei ringraziare tutte le persone che in questi tre anni di dottorato mi sono state vicine e mi hanno supportato e spronato a migliorarmi sempre.

In particolare vorrei ringraziare i miei genitori che mi hanno insegnato a non abbattermi mai di fronte alle difficoltà.. perché senza di loro non avrei raggiunto questo traguardo.

Un ringraziamento speciale va a Marco che ha sopportato con pazienza i miei momenti di stress e mi ha aiutato a superarli. Grazie per tutto quello fai ogni giorno per me.

Vorrei inoltre ringraziare il Prof. Pincelli e Alessandra per avermi dato l'opportunità di fare il tirocinio di dottorato in laboratorio, per la fiducia che mi avete dato e per ogni aiuto e consiglio prezioso. Un ringraziamento anche allo speciale gruppo di laboratorio in particolare a Francesca, Tiziana, Roberta, Paolo per il vostro aiuto, per le vostre opinioni, il vostro supporto e per avermi insegnato cosa significa essere un gruppo!

Infine un ringraziamento ai miei amici Grazia, Gaia, Daria, Marika, Ivana per le risate e l'affetto che mi avete sempre dimostrato.

Annalisa